

10 January 2020

Biogeosciences Editorial Office

Manuscript ID: bg-2019-322

Dear Prof. Abril,

Thank you for taking into consideration our manuscript for publication in *Biogeosciences*. We are grateful for the granted extension of the submission deadline of our revised manuscript. This has allowed us to improve the depth of the discussion and the scientific significance of the work. We attach our responses to the reviewer's comments, as well as a revised version of the manuscript and supplementary material in which the edits have been highlighted.

We have made several important changes to the manuscript. Foremost, we have changed the manuscript title and improved the structure of the discussion, as per the suggestions of yourself and Referee #2. We have also increased the relevance of the manuscript to other researchers working on trace gas emissions from lakes by expanding the discussion with a detailed analysis of between-lake differences in the drivers of emissions, which include the effects of atmospheric stability and sheltering on the gas transfer velocity. Contextualizing in this way, we have illustrated which flux-driving mechanisms may be important in different lake types, such as those that are shallow and exposed to wind, deeper and more sheltered, or lakes that are fed by a stream. Minor changes include improved model estimates of lake CH₄ emissions by using lake-specific scaling parameters – the analyses for which are provided in the updated supplement.

We hope that these revisions have made our manuscript suitable for publication in *Biogeosciences*. We will be pleased to answer any additional questions or make any further changes that you or the reviewers recommend. Thank you for your kind support.

On behalf of the co-authors,

Joachim Jansen

Response to reviewer 1:

L 33: Statement “A significant portion of sediment-produced CH₄ reaches the atmosphere by turbulence-driven diffusion-limited gas exchange” is misleading and term “significant” is conveniently vague. The synthesis of CH₄ fluxes from inland waters given by Bastviken et al (2011) and cited by the authors provides a total diffusive flux of CH₄ of 9.9 TgCH₄/yr that is much smaller than the total flux of 103.3 TgCH₄/yr. I suggest that authors be more specific and introduce quantitatively the importance of diffusive CH₄ fluxes from inland waters.

Author’s response: we have changed the introductory paragraph to include the estimated contribution of open water diffusive CH₄ emissions from three regional and global budget studies. We note that the Bastviken et al. (2011) study separates ‘diffusive’ and ‘storage’ emissions. Because the latter is defined as the ‘flux when CH₄ stored in the water column is emitted upon lake overturn’, and occurs via the diffusion-limited pathway, we counted storage fluxes as diffusive fluxes. We thus computed the contribution of diffusion from the pathway specific budgets in Table 1 of Bastviken et al. (2011) as follows: (‘diffusive’ + ‘storage’)/(‘plant flux’ + ‘ebullition’ + ‘diffusive’ + ‘storage’) = 34.8%. This is within the range of values computed from diffusive and ebullitive flux estimates in DelSontro et al. (2018) (21-24%) and Wik et al. (2016b) (46%).

L36: Chambers also “traditionally” capture CH₄ ebullition fluxes in addition to diffusive fluxes.

Author’s response: as described in the method section (L. 124-125) our chambers were equipped with plastic shields to prevent bubbles from entering the chamber headspace.

L44: DelSontro et al. (2018) estimated global (and not regional as stated) CH₄ emissions based on a statistical (and not “process-based” as stated) approach.

Author’s response: we have removed the reference to DelSontro et al. (2018).

L 52: the formulation of equation (1) was given by Liss and Slater (1974) well before Wanninkhof (1992).

Author’s response: the reference has been changed.

I have the impression that methane oxidation is the main process “that dissociate[s] production from emission rates”, it’s odd this is not mentioned in section L69-83.

Author’s response: we have included oxidation as one of the dissociating factors.

L141-143: Can you please elaborate this section? It’s unclear how the effect of artificial enhancement of turbulence was discarded, and how the citation of the Ribas-Ribas et al. paper is relevant in this context, since this technical paper describes an apparatus to measure fluxes with chambers.

Author’s response: we included a more detailed description of the analysis of the cited paper: “Ribas-Ribas et al. (2018) compared acoustic Doppler velocimeter measurements inside and outside the perimeter of a chamber of similar design, size and flotation depth as those used in this study, and, based on a comparison of measured TKE dissipation rates and computed gas transfer velocities, concluded that the chambers did not cause artificial turbulence.”

L164: It's strange that only one standard was used to calibrate the GC-FID (a multipoint calibration curve is recommended, Wilson et al. 2018), and the value of standard is so low compared to the sample values, as pCH₄ in the headspace was » 2 ppm, as shown in Figure 2.

Authors should provide an accuracy and precision of the CH₄ measurements and propagate this into an error analysis of the CH₄ fluxes, as well as for the computed k₆₀₀ values.

Author's response: detector FID's with N₂ carriers are known to be linear over several orders of magnitude (e.g. Colson, 1986). The linearity of the detector is better than the uncertainty in the gas mixtures.

The instrument precision is discussed in Section 2.4 of the paper. 10 standard measurements before and after each run were used to assess instrument precision and drift. The precision – defined as the relative standard deviation of the 10 standard measurements - was generally <0.25%. This converts to negligible deviations in the surface concentration and derived fluxes, and would not affect any of the binned or multi-year mean values or functional relationships discussed in the paper. For example, relative standard deviations of the air-water concentration difference binned by time, temperature and wind speed (Fig. 4e-g) are generally >30%. Thus, uncertainty in this study is dominated by the spatiotemporal variability of the fluxes and surface concentrations rather than uncertainty in the concentration measurements.

L168: Could be useful to explain here how z_{mix} was estimated from the temperature profiles.

Author's response: the mixing depth was estimated from a density gradient threshold, as described at L. 431. We have now written a few sentences about water density calculations and mixing depth in section 2.5. Here is the revised text:

“Water density was computed from temperature and salinity (Chen and Millero, 1977), using lake-averaged specific conductivity and a salinity factor [$\text{mS cm}^{-1} / \text{g kg}^{-1}$] of 0.57. The salinity factor was based on a linear regression of simultaneous measurements of conductivity and dissolved solids ($R^2 = 0.99$, $n = 7$) in five lakes in the Torneträsk catchment (Miljödata-MVM, 2017). We defined the diel mixing depth (z_{mix}) at a density gradient threshold ($d\rho/dz$) of $0.03 \text{ kg m}^{-3} \text{ m}^{-1}$ (Rueda et al., 2007).”

L206: This equation assumes that C_{aq} remains unchanged during the 24h chamber deployment which seems unrealistic. Please clarify what does C_{aq} correspond to. Was C_{aq} measured each time C_h was measured?

Author's response: C_{aq} is defined at L. 51 and corresponds to the measured CH₄ concentration in the surface water. When we compute gas transfer velocities from chamber fluxes and the air-water concentration difference ($C_{\text{aq}} - C_{\text{air,eq}}$), we only use water samples that were collected simultaneously with, and in close proximity to the floating chamber observations. We took one water sample at each chamber location. Thus when we compute k_{ch} from Eq. 2, we assume that the flux at the time of the concentration measurement was equal to the 24h flux. It is likely that the flux varied over those 24 hours (Fig. 7b,d). However, a quantitative bias assessment would require continuous, 24h observations of the diffusive fluxes and of the surface concentration, which were unavailable for this study.

L207: specify if T is the average during the 24h chamber deployment. In Eq [3] explain how dx/dt was computed. Linear regression over all points? Difference between end and start? Difference between each of the samples?

Author's response: we have now specified how T and dx/dt were computed. That is, the average over the flux integration time (this is the 24h chamber deployment time for most of our analyses) and OLS linear regression of concentrations onto time, respectively. Here is the revised text:

" $\partial x_h/\partial t$ is the headspace mole fraction change [$\text{mol mol}^{-1} \text{d}^{-1}$] computed with an ordinary least squares (OLS) linear regression (Fig. 2), M is the molar mass of CH_4 ($0.016 \text{ mg mol}^{-1}$), P is the air pressure [Pa], T_{air} is the air temperature [K]. Scalar c_1 corrects for accumulation of CH_4 gas in the chamber headspace and increases over the deployment time. Comparing both chamber flux calculation methods we find $c_1 = 1.21$ for 24 hour deployments (OLS, $R^2 = 0.85$, $n = 357$). Chambers were sampled up to 4 times during deployment (at 10 minutes, 1–5 hours and 24 hours) which allowed us to compute fluxes at time intervals of 1 hour and 24 hours. P and T_{air} were averaged over the relevant time interval."

The use of a single value for scalar c_1 is surprising because the accumulation of CH_4 in the chamber should depend on the flux intensity itself, so I would expect this value not to be constant.

Author's response: c_1 is based on a linear regression of fluxes computed with Eq. 3 (simple linear regression in the time vs chamber headspace concentration plot) and Eq. 2, which corrects for the headspace effect. The good linear fit ($R^2 = 0.85$, L. 216) indicates to us that the headspace effect did not change significantly within the range of fluxes observed. If the headspace accumulation effect would increase significantly with the flux, we would expect a highly non-linear correlation.

In equations 2 and 3, the same symbol (T) is used for water temperature and air temperature, when separate symbols should be used for distinct variables.

Author's response: we have specified the symbols in the equations.

L 241: It's odd that both a symbol and an abbreviation are used for turbulent kinetic energy

Author's response: they refer to different quantities. As stated at L. 241, we use TKE as an abbreviation for 'turbulent kinetic energy' and epsilon as the symbol for the dissipation rate of turbulent kinetic energy. Both the abbreviation and the symbol are commonly used in the literature.

L307: Please explain how the residence time of a CH_4 molecule in the lake was estimated.

Author's response: this computation is described in section 2.7 at L198-199. The sentence reads: "We computed the average residence time of a CH_4 molecule by dividing the amount stored by the lake mean surface flux."

In Figure 6 the relation between storage time and water T seems significant for I Harrjon and M Harrsjon.

Author's response: we infer that the reviewer refers to Fig. 6e, which shows an increase of storage with water temperature. We fitted Arrhenius functions, added lines of best fit to the plot and included the following sentence in the figure caption: "Arrhenius-type functions (Eq. 7) adequately described the relation between storage and temperature in each lake ($R^2 \geq 0.70$, $p < 0.001$)."

L637-639: why would damping of turbulence by near-surface stratification affect particularly your lakes but not those reported by Cole & Caraco (1998) and Wanninkhof and Crusius (2003)?

Author's response: we moved the discussion of turbulence damping to a separate paragraph, which now reads: "Damping of turbulence results from near-surface stratification and can reduce the gas transfer velocity (MacIntyre et al., 2010, 2018), however, such strong stratification ($N > 25$ cph) was intermittent in our study (Fig. 5f-h)."

An alternative explanation could be fetch limitation (Wanninkhof 1992) in the very small sampled ponds, and this effect could be more marked at high wind speeds than at low wind speeds.

Author's response: we thank the reviewer for this suggestion.

Figure 9: abbreviations given in the plot should be defined in the figure legend.

Author's response: abbreviations of literature references are now included in the figure caption.

In Figure 9, the binned data value at highest wind correspond to a wind speed that is higher than highest wind speeds of individual Kch measurements. How is this possible? The binned value should be below the highest individual wind speeds measurements.

Author's response: we chose to plot the symbols for binned quantities at the center value of each bin. The center value of the bin may be higher than or lower than the mean value of the datapoints contained in that bin.

L668-670: While I agree with the idea that CH₄ is formed in the sediment, as this seems the most likely process in this type of environments, I do not see why the Arrhenius relation proves this. All biological processes follow Arrhenius-type relations, so the occurrence of this relation only shows that CH₄ might be biologically produced, but does not allow to pin-point it as sedimentary. Please rephrase. Since it's not explained in the text how the residence time was computed it is not clear how this proves or disproves a sedimentary CH₄ production.

Author's response: we explain how the residence time was computed at L. 198-199. Sediment production of CH₄ is well-known in aquatic systems and we do not mean to prove or disprove it with our observations. We restructured the sentence to put more emphasis on redistribution rather than sediment production: "The Arrhenius-type relation of CH₄ fluxes and concentrations (Fig. 4b,f) together with short CH₄ residence times (Fig. 6) suggest that efficient redistribution of dissolved CH₄ strongly coupled emissions from the Stordalen lakes to sediment production."

L671: Why do high CH₄ in the stream suggest this is of "terrestrial" origin? CH₄ is also produced in-stream in sediments. Do you mean that CH₄ comes from soils then to streams? Or that the stream CH₄ production is fueled by terrestrial organic matter? This statement is very vague and confusing, please clarify.

Author's response: we have clarified this sentence as follows: "High CH₄ concentrations in the stream suggest that external inputs of CH₄ — produced in the fens and transported into the stream with surface runoff, or produced in stream sediments — may have elevated emissions in Mellersta Harrsjön (Lundin et al., 2013; Paytan et al., 2015)."

L677-679: or alternatively from dilution with water with low CH₄ from surface runoff and rain?

Author's response: we thank the reviewer for this suggestion.

L723: methane oxidation is also an important removal process that should contribute to imbalances between production and emission.

Author's response: One could argue that because methane oxidation rates tend to change with concentration and temperature, they would influence the flux on timescales similar to those of production (that is, timescales of a week or more). Changes in storage occur within the short residence times of CH₄ gas (1-5 days). This suggests that dissociation occurs on shorter timescales – i.e. those governed by wind speed. However, in this paper we do not present a quantitative assessment of methane oxidation. Following the reviewer's earlier comment we have mentioned oxidation as a process that dissociates production from emission in the introduction.

L730-740: Wave breaking and bubbles also explain why the relation between the gas transfer velocity and wind speed is non-linear in the ocean (e.g. Wanninkhof 1992), while here you report a linear relation between gas transfer velocity and wind speed.

Author's response: the processes obtained in large water bodies are not necessarily operative in small lakes. Moreover, it is not clear from our data whether the wind-k relationship is linear or non-linear. At L. 643-645 we state "Due to the large spread of the chamber-derived gas transfer velocities (small rhombuses, Fig. 9) a power-law exponent to U₁₀ (1.0 (0.0-1.8); exponent and 95% CI) and thus the nature of the wind-k relation could not be determined with confidence."

L763: Is thermocline tilting expected to occur in small ponds?

Yes, wind forcing can cause the thermocline to tilt in small water bodies. The extent of tilt is computed from the Wedderburn number (Imberger and Patterson, 1989). This dimensionless index takes into account stratification, wind speed, and basin dimensions. The lakes in this study are larger than ponds, albeit small, and for the relatively high winds found at these arctic sites, thermocline tilting is expected.

L797-811: Methane oxidation affects CH₄ concentrations, so it's very obscure why methane oxidation should affect the alpha term. This is a scaling between gas transfer velocity that is measured and modelled, and gas transfer velocity depends on physical processes (mainly turbulence)

Author's response: in this study we infer k_{ch} from measurements of the chamber concentration increase and surface concentrations. The formulations of Eq. 1 and Eq. 2 implicitly assume that all CH₄ measured in the water column is emitted to the atmosphere. However, if a fraction of CH₄ is removed by oxidation, this would lead to an overestimation of $\Delta[CH_4]$ and an underestimation of k_{ch} . This in turn affects the alpha term. So oxidation does not impact gas transfer velocities directly, but may bias the gas transfer velocity high if one uses the two-layer model (Eq. 1), as is common. We have added a few sentences to the paragraph to clarify this point.

References

Bastviken, D., Tranvik, L. J., Downing, J. A., Crill, P. M. and Enrich-Prast, A.: Freshwater Methane Emissions Offset the Continental Carbon Sink, *Science* (80-.), 331(6013), 50–50, doi:10.1126/science.1196808, 2011.

Chen, C.-T. and Millero, F. J.: The use and misuse of pure water PVT properties for lake waters, *Nature*,

266(5604), 707–708, doi:10.1038/266707a0, 1977.

Colson, E. R.: Flame ionization detectors and high-end linearity, *Anal. Chem.*, 58(2), 337–344, doi:10.1021/ac00293a017, 1986.

Imberger, J. and Patterson, J. C.: Physical Limnology, in *Advances in Applied Mechanics*, vol. 27, pp. 303–475., 1989.

Lundin, E. J., Giesler, R., Persson, A., Thompson, M. S. and Karlsson, J.: Integrating carbon emissions from lakes and streams in a subarctic catchment, *J. Geophys. Res. Biogeosciences*, 118(3), 1200–1207, doi:10.1002/jgrg.20092, 2013.

MacIntyre, S., Jonsson, A., Jansson, M., Aberg, J., Turney, D. E. and Miller, S. D.: Buoyancy flux, turbulence, and the gas transfer coefficient in a stratified lake, *Geophys. Res. Lett.*, 37(24), n/a-n/a, doi:10.1029/2010GL044164, 2010.

MacIntyre, S., Crowe, A. T., Cortés, A. and Arneborg, L.: Turbulence in a small arctic pond, *Limnol. Oceanogr.*, 63(6), 2337–2358, doi:10.1002/lno.10941, 2018.

Miljödata-MVM. Swedish University of Agricultural Sciences (SLU). National data host for lakes and watercourses, and national data host for agricultural land, <http://miljodata.slu.se/mvm/> [07-10-2017].

Paytan, A., Lecher, A. L., Dimova, N., Sparrow, K. J., Kodovska, F. G.-T., Murray, J., Tulaczyk, S. and Kessler, J. D.: Methane transport from the active layer to lakes in the Arctic using Toolik Lake, Alaska, as a case study, *Proc. Natl. Acad. Sci.*, 112(12), 201417392, doi:10.1073/pnas.1417392112, 2015.

Ribas-Ribas, M., Kilcher, L. F. and Wurl, O.: *Sniffle*: a step forward to measure *in situ* CO₂ fluxes with the floating chamber technique, *Elem Sci Anth*, 6(1), 14, doi:10.1525/elementa.275, 2018.

Rueda, F., Moreno-Ostos, E. and Cruz-Pizarro, L.: Spatial and temporal scales of transport during the cooling phase of the ice-free period in a small high-mountain lake, *Aquat. Sci.*, 69(1), 115–128, doi:10.1007/s00027-006-0823-8, 2007.

Response to reviewer 2:

The authors wish to thank the reviewer for their thoughtful comments and detailed suggestions, which helped improve the paper and clarify the narrative.

RC2: This manuscript documents almost a decade of weekly-monthly resolution methane concentration and flux data from 3 sub-Arctic lakes. They found Arrhenius-type temperature relationships with flux and concentration, which has been found before and suggests a strong coupling to methane production rates. They also found that wind shear drove the gas transfer velocity, but on timescales of less than a month while temperature was a driver on timescales longer than a month. They also found that stratification only played a small role in storage/accumulation and emissions in general from their systems. The methods are sound and the results are well-detailed, perhaps a bit on the long side. The dataset is quite unique as it is so long. The authors need to use the length of their dataset to substantiate their results more. They find a temperature relationship that has been shown before in quite a few other datasets, but perhaps ones not as long as theirs. Also, they find that convection does not play as large of a role in surface turbulence as has been found in other lakes. How do those datasets compare to theirs? I also strongly suggest the authors structure the discussion to highlight the main takeaway messages from this work.

Author's response: The concerns raised in the reviewer's initial statement have been addressed in our response to individual comments below.

General comments:

RC2: 1. The title seems broad as if you are referring to all lakes, but you actually point out in the manuscript many differences between your findings and those of other lakes, for example, in terms of convection contribution to k . I suggest you narrow down your title slightly. You could even highlight more in the title the amount of data that you have. This multi-year dataset is quite unique.

Author's response: We have changed the title to "Drivers of diffusive CH₄ emissions from shallow subarctic lakes on daily to multi-year time scales." However, we chose specify the length of the dataset in the abstract. The basic physics that control diffusion-limited emissions from water surfaces are common to all lakes though, of course, specifics such as depth and geomorphological setting will be unique to each. We feel that this is a contribution that is broadly useful.

RC2: 2. I think the discussion could do with some restructuring and more concisely define the main points of your findings. The subheadings closely follow the results structure, but this doesn't help the reader easily identify your main points. I like the way you summarized your findings in the first paragraph of the last section (summary and conclusions). I would suggest laying out the discussion with subheadings similar to the structure in that paragraph, at least to start and then edit from there. You also may not need all the information in the discussion if you find it does not highlight one of your main points.

Author's response: We believe the dataset and the variety of the analyses merits a detailed and thorough discussion. We hope the sections and subheadings as they are currently structured would allow for easy navigation to topical discussions of interest. Noting your point, we added summarizing sentences to some of the paragraphs, restructured Section 4.2 and removed section 4.7 as it does not add to the discussion. Thank you for having us revisit the organization.

Specific comments:

RC2: Line 50- should read ‘, of which the upper boundary..’

Author’s response: We changed the sentence in accordance with the reviewer’s suggestion.

RC2: Line 72 – did you not include Aben et al. 2017 because it is about ebullition? You don’t specifically mention diffusive only in this sentence.

Author’s response: Yes, correct. We considered the Aben et al. paper to not be directly relevant to the diffusion–limited emissions focus of our paper.

RC2: Line 101 – ‘stochastic tools’ sounds too vague here

Author’s response: Thanks for pointing this out. We changed line 101 to “We then estimate the importance of these and other flux controls on different timescales.”

RC2: Line 129 – I would say ‘During the 24 hr period...’ to avoid confusion. But why 2-4 samplings? What resolution and why?

Author’s response: This information is detailed in section 2.8, where we write: “Chambers were sampled up to 4 times during deployment (at 10 minutes, 1–5 hours and 24 hours) which allowed us to compute fluxes at time intervals of 1 hour and 24 hours.” Also the use of a short and longer time sampling provided information on those manual fluxes that might have been more episodic (i.e. affected by sub-daily changes in the gas transfer velocity) than the more regular increases that we might expect given our assumptions about diffusion-limited emissions.

RC2: Line 135-136 – you need to define $F_{ch,unsh}$ and $F_{ch,sh}$ here in this sentence (i.e., place the variables after ‘shielded’ and ‘unshielded’)

Author’s response: Thanks for noting the confusion. We removed $F_{ch,unch}$ - $F_{ch,sh}$ from the equation, as we clearly state that we talk about the difference.

RC2: Section 2.2 – Do you flush the chambers between samplings or leave them the entire 24 hrs?

Author’s response: This is clarified in section 2.8. We use the accumulation rate of gas in the chamber headspace to compute the flux, so we don’t flush the chamber within the 24 hour deployment period.

RC2: Section 2.3 – Do you flush or mix the 4m long tube before sampling?

Author’s response: Yes we do and we clarified this point in the text as follows: “the tubes were flushed by extracting a sample volume equal to the tube’s volume at each location and depth.”

RC2: Line 196 – do you mean ‘offshore’ instead of ‘nearshore’ here since you are differentiating between the littoral zone and another zone?

Author’s response: Yes, we consider the shallow littoral zone to be near-shore, and the deeper, pelagic or profundal zone to be offshore.

RC2: Line 198 – make sure the year is correct on the reference

Author’s response: Thanks, we have corrected the year.

RC2: Line 205 – define and give units for 'kch'

Author's response: k_{ch} is now defined and units given.

RC2: Line 211-212 – why were there some water measurements not taken and which ones and how many?

Author's response: The design of the initial water sampling program was not intended to facilitate computation of gas transfer velocities. Simultaneous and co-located sampling was introduced in years 2016 and 2017.

RC2: Line 239 – should be 'kmod' specifically in this sentence, no?

Author's response: In our usage here, k refers to the gas transfer velocity in general.

RC2: Line 245 – why do you need to do this qualitative comparison? Why is it important?

Author's response: We added a note of explanation with the following sentence: "In this way, we can assess whether the flux relations with wind speed and temperature are reproduced by the model."

RC2: Line 338 – definite 'σinit'

Author's response: This term has now been defined in the text as follows: "To allow for comparison between variables we normalized each σ -series by its initial, smallest-bin value: $\sigma_{norm} = \sigma/\sigma_{init}$."

RC2: Line 420 – include in the caption the panel letters for the histograms in parentheses too

Author's response: Yes that will help our explanation, panel letters have been added.

RC2: Figure 4 caption – you need to describe the squares, triangles, and diamonds in the caption itself – all the variables that you are presenting here.

Author's response: Thanks for noting our oversight, symbol descriptions have been added to the figure caption.

RC2: Figure 5 caption – what are the curves you speak of in line 500? Are you sure that e and f are the right panels when you discuss the white lines on line 499? What is the resolution in panels c and d?

Author's response: Thanks for catching this; the white mixing depth lines are indeed displayed in panel f-h, not e-f. We replaced the word 'curves' with 'lines' at line 500. The resolution of the chamber flux and water concentration measurements was approximately weekly. We hope this is evident when looking at the monthly tick mark intervals.

RC2: Table 3 title – need to describe N here

Author's response: The table title has been adjusted to reflect all variables.

RC2: Figure 6 caption – add '(a-c)' after 'residence time' and '(d-f)' after 'storage'. You mention the regressions for residence time but not for storage. Also, it looks as if there could be a trend between temperature and storage (panel e) for at least 2 of the lakes. Was there not?

Author's response: We have included the panel indicators, and fit storage quantities to Arrhenius-type exponential functions in panel e, which describe the data reasonably well ($R^2 \geq 0.70$, $p < 0.001$).

RC2: Line 560-561 – the sentence starting with ‘On diel timescales..’ needs rewording. I don’t understand it.

Author’s response: Thanks, we rewrote the sentence as follows: “On diel timescales $\Delta[\text{CH}_4]$ and k_{mod} were out of phase; $\Delta[\text{CH}_4]$ peaked just before noon, when k_{mod} reached its maximum value (Fig. 7b,d).”

RC2: Figure 7 – put a complete legend in panels a and c and state that they apply to panels b and d.

Author’s response: We preferred to keep the legend as is to avoid crowding in the left panels, but we changed the symbol colour of the 1-hour fluxes to improve the clarity of the figure.

RC2: Line 612 – what is ‘T_{water/ice}’?

Author’s response: Our surface temperature sensors were frozen in the ice in winter. Because we use the whole-year temperature timeseries in our spectral analysis, we specify that this variable reflects both summer and winter variability. In the caption, we now specify “temperature of the surface water and ice”.

RC2: Section 4.1 – The subheading ‘Magnitude’ doesn’t explain much. Magnitude of what?

Author’s response: We have changed the section title to ‘Magnitudes of fluxes and gas transfer velocities’.

RC2: Line 632 – you obtained lower k-values by nearly a factor of 2 compared to what?

Author’s response: This is in comparison to literature models. This has now been specified in the text.

RC2: Line 636 – who had the offset at 0 wind speed? You or the literature? Be specific as this sentence is a bit confusing.

Author’s response: Thanks for pointing out this omission. We meant that several models in the literature have a default offset at 0 wind speed. We have amended the text as follows: “Part of the difference with the models of Vachon and Prairie (2013), Cole and Caraco (1998) and Soumis et al. (2008) was caused by the offset at 0 wind speed.”

RC2: Line 637 – ‘Another explanation’ for what?

Author’s response: Thanks for noting our oversight. This refers to the other explanation for the low k-values found in our study. We changed the sentence to specify this.

RC2: Line 639-640 – how was the atmosphere stable?

Author’s response: We consider a stable atmosphere to be those periods when the tropospheric boundary layer being stably stratified, i.e. when the air temperature exceeds the surface water temperature.

RC2: Line 644-645 – I am confused because you have an equation in Figure 9 caption that has an exponent for u_{10} with 95% Cis.

Author’s response: The equation in the caption was a linear equation, while we discussed a power-law equation in the text. We’ve now changed the equation in the caption to the power-law equation of Table S1.

RC2: Section 4.2 – delete ‘the’ in the subheading

Author’s response: Thanks for noting this. ‘Drivers of flux’ sounds better.

RC2: Section 4.2 – this is a very important part of the discussion but I feel it needs a little more work to really bring out your main points. It reads a bit like a bunch of ideas thrown into a paragraph but without linking them all together nor highlighting why these ideas matter. For example, the first sentence states that the temperature relationship with flux and concentration suggests a strong coupling to sediment [methane] production (need that word ‘methane’ in there). I agree with this statement and it’s an important one because you did find some nice relationships there. But the next sentence talks about stream inputs (from your own data, correct?) and then the following sentence is back to how sediment methane production could be enhanced. They seem out of order. Then the last thought about the decrease in CH₄ after cold rain events is actually still in line with the temperature relationship you saw but you start this sentence off attempting to state that that shouldn’t be the case if there was runoff from fens. This fens part goes more along with the streams sentence from above.

Author’s response: We have revisited the organization and added two introductory sentences to the paragraph to add context to the discussion: “Methane emitted from lakes in wetland environments can be produced in situ, or be transported in from the surrounding landscape (Paytan et al., 2015). The distinction is important because some controls on terrestrial methane production, such as water table depth (Brown et al., 2014), are irrelevant in lakes.”. We also replaced “cold and rainy” in the final sentence of the paragraph with “rainy”, to emphasize that we are discussing horizontal transport processes here. We removed the sentence about terrestrial inputs of nutrients.

RC2: I feel the same for the second paragraph of the section. I think you clarify your point about the difference between your results and those of Read et al. I am actually not sure who had lake in the warmer, lower humidity regions – you or them? Also need to put the 50 W/m² value in context. At the end, I wouldn’t use the word ‘expect’ because I think you showed this. And I believe in this whole section you should already allude to the fact that these drivers work on different timescales.

Author’s response: We have rewritten this section. Read et al. (2012) did not consider Monin-Obukhov similarity scaling in their analysis. When computing dissipation rates with it, wind shear is raised to the 3rd power and divided by depth whereas the contribution from buoyancy flux is only to the first power. With that constraint, buoyancy flux only drives near-surface turbulence when winds have ceased. Figure 4k shows this for our model. Thus, differences in the meteorology between temperate and arctic lakes are not relevant here. On average, the 50 W/m² represents the value of the net long wave radiation (L_{win} - L_{Wout}) we’ve computed during the ice-free season in the Toolik area. We normally measured L_{win} and computed L_{Wout} as a function of the surface water temperature. For reference, in our arctic work at other sites, net long wave radiation applies to periods with cloudy conditions, as often occur in the Stordalen Mire.

RC2: Line 716-728 – The first sentence of this paragraph reads more like a summary sentence. It’s confusing to hear about the feedback before you describe how you got to that point. I would try restructuring this paragraph a bit. I would start with the second sentence and state it like so: ‘Higher temperatures led to elevated CH₄ concentrations, which in turn increased emission rates, but high wind speed was correlated with high emission rates and low concentrations. In this way,...’

Author's response: We agree and we rewrote the paragraph as suggested by the reviewer: "Higher temperatures led to elevated CH₄ concentrations (Fig. 4f) which in turn increased emission rates (Eq. 1, Fig. 4b) but high wind speed was correlated with high emission rates and low concentrations (Fig. 4c,g). Degassing prevented an unlimited increase of the emission rate with the gas transfer velocity. In this way, Δ[CH₄] acted as a negative feedback that maintained a quasi steady state between CH₄ production and removal processes throughout the ice-free season."

RC2: Line 744 – add the range of binned means in those parentheses of 0 – 10

Author's response: The ranges have been included.

RC2: Line 784-791 – This is actually one very long sentence. Consider splitting it.

Author's response: Thank you, the sentence has been split per the reviewer's suggestion.

RC2: Line 798-799 – missing a word or something here '....but can limit surface exchange could be responsible...'

Author's response: We have split the sentence to clarify its meaning: "The observed variability in α' could be explained by chemical or biological factors that limit surface exchange. Such processes do not affect turbulence in the actively mixed layer, and are thus not accounted for in k_{mod} ."

RC2: Line 834-837 – So you don't completely degas the lake, despite shallowness and frequent mixing, but you also don't have storage/accumulation of methane. I am finding a hard time reconciling those two results. I feel this needs more explanation here but also in the discussion where you mention it.

Author's response: Of course there are dynamics in the water column methane concentrations as a result of variability in the loss and input terms. Accumulation is transient – it changes on a timescale of days – and is the result of an imbalance between production and emission rates. Storage increases during long periods of stratification are not due not only due to the reduction in turbulence-driven emissions but also, in the ice-free seasons especially, to higher production rates as a result of elevated water temperatures. We rewrote section 4.3 to provide a more intuitive explanation of these processes.

1 **Drivers of diffusive ~~lake~~ CH₄ emissions from shallow subarctic lakes on daily to**
2 **multi-year time scales**

3 Joachim Jansen^{1,2}, Brett F. Thornton^{1,2}, Alicia ~~Cortes~~³Cortés³, Jo Snöäl⁴, Martin Wik^{1,2}, Sally
4 MacIntyre³ and Patrick M. Crill^{1,2}

5
6
7

8 ¹Department of Geological Sciences, Stockholm University, Stockholm, Sweden

9 ²Bolin Centre for Climate Research, Stockholm, Sweden

10 ³Marine Science Institute, University of California at Santa Barbara, Santa Barbara, USA

11 ⁴Department of Geography, University of Exeter, Exeter, UK

12

13 Corresponding author: Joachim Jansen (joachim.jansen@geo.su.se)

14 **Abstract**

15 Lakes and reservoirs ~~are important emitters~~ contribute to regional carbon budgets via significant emissions
16 of climate forcing trace gases. ~~Various environmental drivers of the flux, such as temperature and wind~~
17 ~~speed, have been identified, but their relative importance remains poorly understood.~~ Here, ~~for improved~~
18 ~~modelling,~~ we use ~~an extensive field dataset to disentangle physical and biogeochemical controls on the~~
19 ~~turbulence-driven diffusive flux of methane (CH₄) on daily to multi-year timescales.~~ We compare 8 years
20 of floating chamber ~~fluxes~~ measurements from three small, shallow subarctic lakes (2010–2017, $n = 1306$)
21 ~~with fluxes computed using~~ to separate the contribution of physical and biogeochemical processes to the
22 turbulence-driven, diffusion-limited flux of methane (CH₄) on daily to multi-year timescales. Correlative
23 data include 9 years of surface water concentration measurements (2009–2017, $n = 606$) and ~~a small-eddy~~
24 ~~surface renewal model informed by~~ in situ meteorological observations. We used the latter to compute
25 near surface turbulence based on similarity scaling and then applied the surface renewal model to
26 compute gas transfer velocities. Chamber fluxes averaged $6.9 \pm 0.3 \text{ mg m}^{-2} \text{ d}^{-1}$ and gas transfer velocities
27 (k_{600}) ~~from the chamber-calibrated surface renewal model~~ averaged $4.0 \pm 0.1 \text{ cm h}^{-1}$. ~~We find robust ($R^2 \geq$~~
28 ~~$0.93, p < 0.01$) Arrhenius-type temperature functions of the CH₄ flux ($E_a' = 0.90 \pm 0.14 \text{ eV}$) and of the surface~~
29 ~~CH₄ concentration ($E_a' = 0.88 \pm 0.09 \text{ eV}$).~~ Chamber-derived gas transfer velocities tracked the power-law
30 ~~wind speed relation of the model ($k \propto u^{3/4}$).~~ While the flux increased with wind speed, during storm events
31 ~~($U_{10} \geq 6.5 \text{ m s}^{-1}$) emissions were reduced by rapid water column degassing.~~ Spectral analysis
32 ~~revealed~~ indicated that on timescales shorter than a month, emissions were driven by wind shear, ~~but~~
33 ~~whereas~~ on longer timescales variations in water temperature governed the flux, ~~suggesting.~~ Chamber
34 ~~derived gas transfer velocities tracked the power-law wind speed relation of the model.~~ Coefficients for
35 ~~the model and dissipation rates depended on shear production of turbulence, atmospheric stability, and~~
36 ~~exposure to wind.~~ Fluxes increased with wind speed until they exceeded 6.5 m s^{-1} , at which point emissions
37 ~~were suppressed due to rapid water column degassing reducing the water-air concentration gradient.~~
38 Arrhenius-type temperature functions of the CH₄ flux ($E_a' = 0.90 \pm 0.14 \text{ eV}$) were robust ($R^2 \geq 0.93, p < 0.01$)
39 and also applied to the surface CH₄ concentration ($E_a' = 0.88 \pm 0.09 \text{ eV}$). These results indicate that
40 emissions were strongly coupled to production ~~and supply to the water column.~~ Our findings ~~suggest~~ show
41 that accurate short- and long-term projections of lake CH₄ emissions can be based on distinct weather-
42 and climate controlled drivers ~~of the flux.~~

43 1. Introduction

44 Inland waters are an important source of the radiatively active trace gas methane (CH₄) to the atmosphere
45 (~~Bastviken et al., 2011; Cole et al., 2007~~). A significant portion of sediment-produced CH₄ reaches the
46 atmosphere by turbulence-driven diffusion-limited gas exchange (~~Bastviken et al., 2004; Wik et al., 2016b~~)
47 (~~hereafter abbreviated to ‘diffusive fluxes’~~). Traditionally, ~~diffusive fluxes are measured with floating~~
48 ~~chambers (Bastviken et al., 2004) but gas exchange models are increasingly used, for example to estimate~~
49 ~~annual emissions on regional scales (Holgerson and Raymond, 2016; Weyhenmeyer et al., 2015). Fluxes~~
50 ~~computed with modelled gas transfer velocities agree to a certain extent with floating chambers and the~~
51 ~~eddy covariance technique in short-term intercomparison campaigns (Bartosiewicz et al., 2015; Crill et al.,~~
52 ~~1988; Erkkilä et al., 2018). However, long-term comparisons are needed to test the validity of flux-driver~~
53 ~~relations on which models are based across a wider range of meteorological conditions, and to identify~~
54 ~~weather- and climate related controls on the flux that are appropriate for seasonal assessments.~~
55 ~~Considering the increased use of process-based approaches in regional emission estimates (DelSontro et~~
56 ~~al., 2018; Tan and Zhuang, 2015), understanding the mechanisms that drive the components of the~~
57 ~~diffusive flux is imperative to improving emission budgets(Bastviken et al., 2011; Cole et al., 2007). On~~
58 ~~regional to global scales, an estimated 21–46% of ice-free season CH₄ emissions from lakes, ponds and~~
59 ~~reservoirs occur via turbulence-driven diffusion-limited gas exchange (Bastviken et al., 2011; DelSontro et~~
60 ~~al., 2018; Wik et al., 2016b) (hereafter abbreviated to ‘diffusive fluxes’). Diffusive fluxes are often~~
61 ~~measured with floating chambers (Bastviken et al., 2004) but gas transfer models are increasingly used,~~
62 ~~for example in regional emission budgets (Holgerson and Raymond, 2016; Weyhenmeyer et al., 2015).~~
63 ~~Fluxes computed with modelled gas transfer velocities agree to a certain extent with floating chambers~~
64 ~~and the eddy covariance technique in short-term intercomparison campaigns (Bartosiewicz et al., 2015;~~
65 ~~Crill et al., 1988; Erkkilä et al., 2018). However, long-term comparisons are needed to identify weather-~~
66 ~~and climate related controls on the flux that are appropriate for seasonal assessments. Considering the~~
67 ~~increased use of process-based approaches in regional emission estimates (Tan and Zhuang, 2015),~~
68 ~~understanding the mechanisms that drive the components of the diffusive flux is imperative for improving~~
69 ~~emission estimates.~~

70

71 1.1 Drivers of diffusive CH₄ emissions

72 ~~Diffusive fluxes at the air-water interface can be modelled as:~~

73 ~~Diffusive fluxes at the air-water interface are estimated with a two-layer model (Liss and Slater, 1974):~~

$$F = k(C_{aq} - C_{air,eq}) \quad [1]$$

74 ~~The flux F [$\text{mg m}^{-2} \text{d}^{-1}$] depends on the concentration difference across a thin layer immediately below~~
75 ~~the air-water interface ($\Delta[\text{CH}_4]$ in mg m^{-3}), which upper boundary is in equilibrium with the atmosphere~~
76 ~~($C_{air,eq}$) and base represents the bulk liquid (C_{aq}), and is limited by the gas transfer velocity k [m d^{-1}]~~
77 ~~(Wanninkhof, 1992). k has been conceptualized as characterizing transfer across the diffusive boundary~~
78 ~~layer, although other models envision a surface renewal approach in which parcels of water~~
79 ~~intermittently are in contact with the atmosphere and k depends on the frequency of these renewal~~
80 ~~events (Csanady, 2001; Lamont and Scott, 1970).~~

81

82 The gas transfer coefficient depends on turbulence caused by wind shear and convection and on the
83 molecular diffusivity of the dissolved gas (see MacIntyre et al., 1995 for an overview of the
84 thermodynamic and kinetic drivers of k). In a stratified water column the force of buoyancy counteracts
85 that of wind shear, and gases may accumulate below a shallow upper mixing layer (MacIntyre et al.,
86 2010). Conversely, thermal convection as a result of surface cooling can deepen the mixed layer and
87 transfer stored gas to the surface (Crill et al., 1988; Eugster et al., 2003), and enhance emissions at night
88 when the surface cools despite low wind speeds (Heiskanen et al., 2014; Podgrajsek et al., 2014b;
89 Poindexter et al., 2016). While progress has been made in understanding how the components of k vary
90 as a function of turbulence (Tedford et al., 2014) and other factors, such as lake morphology and
91 distance to the shoreline (Read et al., 2012; Schilder et al., 2013; Vachon and Prairie, 2013), the temporal
92 variability and drivers of $\Delta[\text{CH}_4]$ remain poorly resolved (Loken et al., 2019; Natchimuthu et al., 2016).

94 CH_4 emissions to the atmosphere also depend on the rates of methane metabolism regulated by
95 substrate availability and temperature dependent shifts in enzyme activity and microbial community
96 structure (Borrel et al., 2011; McCalley et al., 2014; Tveit et al., 2015). Arrhenius-type relationships of
97 CH_4 fluxes have emerged from field studies (DelSontro et al., 2018; Natchimuthu et al., 2016; Wik et al.,
98 2014) and across latitudes and aquatic ecosystem types in synthesis reports (Rasilo et al., 2015; Yvon-
99 Durocher et al., 2014). However, the temperature sensitivity is modulated by biogeochemical factors
100 that differ between lake ecosystems, such as nutrient content (Davidson et al., 2018; Sepulveda-Jauregui
101 et al., 2015), methanotrophic activity (Duc et al., 2010; Lofton et al., 2014), predominant emission
102 pathway (DelSontro et al., 2016; Jansen et al., 2019) and warming history (Yvon-Durocher et al., 2017). In
103 lakes, the air-water concentration difference driving the flux (Eq. 1) is further impacted by abiotic factors
104 that dissociate production from emission rates, such as hydrologic inputs of terrestrially produced CH_4
105 (Miettinen et al., 2015; Murase et al., 2003; Paytan et al., 2015), redistribution of dissolved gas in the
106 water column (DelSontro et al., 2017; Hofmann, 2013) and storage and release cycles associated with
107 transient stratification (Czikowsky et al., 2018; Jammot et al., 2017; Vachon et al., 2019). From these
108 interacting functional dependencies emerge complex responses of the flux to biotic and abiotic factors.

110 Disentangling the physical and biogeochemical drivers of the diffusive CH_4 flux remains a challenge. They
111 respond differently to slow and fast changes in meteorological covariates (Baldocchi et al., 2001;
112 Koebisch et al., 2015) such that different mechanisms may explain the diel and seasonal variability of the
113 flux. For example, temperature affects emissions through convective mixing on short timescales and
114 through the rate of sediment methanogenesis on longer timescales; the diurnal cycle of insolation may
115 have a limited effect on production because the heat capacity of the water buffers the temperature
116 signal (Fang and Stefan, 1996). Similar phase lags and amplifications may lead to hysteretic flux patterns,
117 such as cold season emission peaks due to hypolimnetic storage in dimictic lakes (Encinas Fernández et
118 al., 2014; López Bellido et al., 2009) or thermal inertia of lake sediments (Zimov et al., 1997). Spectral
119 analysis of the flux and its components can improve our understanding of the flux variability by
120 quantifying how much power is associated with key periodicities (Baldocchi et al., 2001).

121
122 The flux F [$\text{mg m}^{-2} \text{d}^{-1}$] depends on the concentration difference across a thin layer immediately below
123 the air-water interface ($\Delta[\text{CH}_4]$ in mg m^{-3}), of which the upper boundary is in equilibrium with the

124 atmosphere ($C_{air,eq}$) and the base represents the bulk liquid (C_{aq}), and is limited by the gas transfer
125 velocity k [$m\ d^{-1}$]. k has been conceptualized as characterizing transfer across the diffusive boundary layer.
126 Other models envision exchange as driven by parcels of water intermittently in contact with the
127 atmosphere. In these surface renewal models, k depends on the frequency of the renewal events
128 (Csanady, 2001; Lamont and Scott, 1970). The resulting calculation for k is based on the Kolmogorov
129 velocity scale, $u_0 = (\epsilon\nu)^{1/4}$ where ϵ is dissipation rate of turbulent kinetic energy (TKE) and ν is kinematic
130 viscosity (Tennekes and Lumley, 1972). Progress has been made in understanding how to compute ϵ and
131 gas transfer rates as a function of wind speed and the heating and cooling at the lake's surface (Tedford
132 et al., 2014). Comparisons between models and other flux estimation methods, such as eddy covariance,
133 illustrate the improved accuracy when computing gas transfer velocities using a turbulence-based as
134 opposed to wind based models (Czikowsky et al., 2018; Heiskanen et al., 2014; Mammarella et al., 2015).

135
136 A key control on emissions is the periodicity at which dissolved gases are brought to the air-water
137 interface. During stratification, the density gradient makes it difficult for wind driven mixing to bring gases
138 to the surface, and they may accumulate in the stratified regions. Conversely, thermal convection
139 associated with surface cooling can deepen the mixed layer and transfer stored gas to the surface (Crill et
140 al. 1988; Eugster et al. 2003). Nighttime emissions can be enhanced when the surface cools despite low
141 wind speeds (Podgrajsek et al., 2015; Poindexter et al., 2016). Temporal patterns of stratification and
142 mixing contribute to variability in diffusive CH_4 fluxes (López Bellido et al., 2009; Podgrajsek et al., 2016)
143 and concentrations (Loken et al., 2019; Natchimuthu et al., 2016). Periodic emissions from storage at depth
144 have been particularly difficult to resolve in lake emission budgets (Bastviken et al., 2004; Wik et al.,
145 2016b).

146
147 CH_4 emissions to the atmosphere also depend on the rates of methane metabolism regulated by substrate
148 availability and temperature-dependent shifts in enzyme activity and microbial community structure
149 (Borrel et al., 2011; McCalley et al., 2014; Tveit et al., 2015). Arrhenius-type relationships of CH_4 fluxes
150 have emerged from field studies (DelSontro et al., 2018; Natchimuthu et al., 2016; Wik et al., 2014) and
151 across latitudes and aquatic ecosystem types in synthesis reports (Rasilo et al., 2015; Yvon-Durocher et al.,
152 2014). However, the temperature sensitivity is modulated by biogeochemical factors that differ between
153 lake ecosystems, such as nutrient content (Davidson et al., 2018; Sepulveda-Jauregui et al., 2015),
154 methanotrophic activity (Duc et al., 2010; Lofton et al., 2014), predominant emission pathway (DelSontro
155 et al., 2016; Jansen et al., 2019) and warming history (Yvon-Durocher et al., 2017). In lakes, the air-water
156 concentration difference driving the flux (Eq. 1) is further affected by factors that dissociate production
157 from emission rates. These include biotic factors, such as aerobic and anaerobic methanotrophy, and
158 abiotic factors such as hydrologic inputs of terrestrially produced CH_4 (Miettinen et al., 2015; Paytan et al.,
159 2015) and storage-and-release cycles associated with transient stratification (Czikowsky et al., 2018;
160 Jammet et al., 2017; Vachon et al., 2019). Given these interacting functional dependencies, the magnitude
161 of fluxes has complex patterns of temporal variability.

162
163 Disentangling the physical and biogeochemical drivers of the diffusive CH_4 flux remains a challenge. The
164 component drivers respond differently to slow and fast changes in meteorological covariates (Baldocchi
165 et al., 2001; Koebisch et al., 2015) such that different mechanisms may explain the diel and seasonal

166 variability of the flux. For example, temperature affects emissions through convective mixing on short
167 timescales and through the rate of sediment methanogenesis on longer timescales; the diurnal cycle of
168 insolation may have a limited effect on production because the heat capacity of the water buffers the
169 temperature signal (Fang and Stefan, 1996). Similar phase lags and amplifications may lead to hysteretic
170 flux patterns, such as cold season emission peaks due to release of gases from the hypolimnion in dimictic
171 lakes (Encinas Fernández et al., 2014; López Bellido et al., 2009) or thermal inertia of lake sediments (Zimov
172 et al., 1997). Spectral analysis of the flux and its components can improve our understanding of the flux
173 variability by quantifying how much power is associated with key periodicities (Baldocchi et al., 2001).

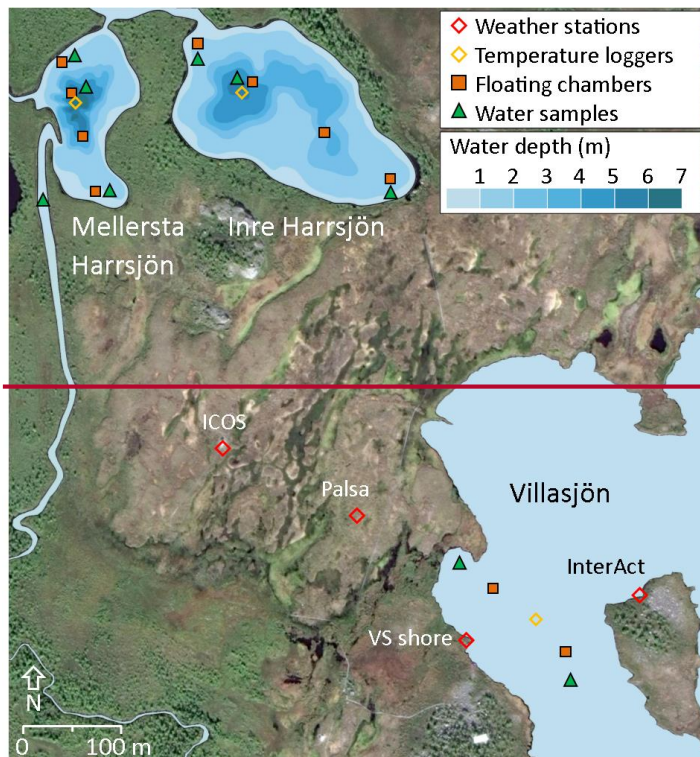
174
175 Here we present a high-resolution, long-term dataset (2010–2017) of ~~turbulence-driven diffusion-~~
176 ~~limited~~diffusive CH₄ fluxes from three subarctic lakes estimated with floating chambers ($n = 1306$), and a
177 ~~gas exchange model informed~~fluxes obtained by modelling using in situ meteorological observations and
178 surface water concentrations ($n = 535$). ~~We use a~~The surface renewal model and is used to compute gas
179 transfer velocities. Arrhenius relationships of $\Delta[\text{CH}_4]$ to disentangle the and fluxes of CH₄ are also
180 calculated. Using spectral analysis of our time series data, we distinguish the temporal dependency of
181 abiotic and biotic controls on the flux. The effects of temperature on the flux. We then use stochastic tools
182 to estimate the importance of these and other flux controls on lake size and wind exposure are illustrated
183 by comparing results from the 3 different timescales lakes.

184 **2. Materials and Methods**

185 **2.1 Field site**

186 We monitored CH₄ emissions from three subarctic lakes of post-glacial origin (Kokfelt et al., 2010),
187 located on the Stordalen Mire in northern Sweden (68°21' N, 19°02' E, Fig. 1), a peatland underlain by
188 discontinuous permafrost (Malmer et al., 2005). The mire (350 m a.s.l.) is part of a catchment that
189 connects Mt. Vuoskoåiveh (920 m a.s.l.) in the south to Lake Torneträsk (341 m a.s.l.) in the north
190 (Lundin et al., 2016; Olefeldt and Roulet, 2012). Villasjön is the largest and shallowest of the lakes (0.17
191 km², 1.3 m max. depth) and drains through water-logged fens into a stream feeding Mellersta Harrsjön
192 and Inre Harrsjön, which are 0.011 and 0.022 km² in size and have maximum depths of 6.7 m and 5.2 m,
193 respectively (Wik et al., 2011). The lakes are normally ice-free from the beginning of May through the
194 end of October. Manual observations were generally conducted between mid-June and the end of
195 September. Diffusion accounts for 17%, 52% and 34% of the ice-free CH₄ flux in Villasjön, Inre and
196 Mellersta Harrsjön, respectively, with the remainder being emitted via ebullition (2010–2017; Jansen et
197 al., 2019).

198



199

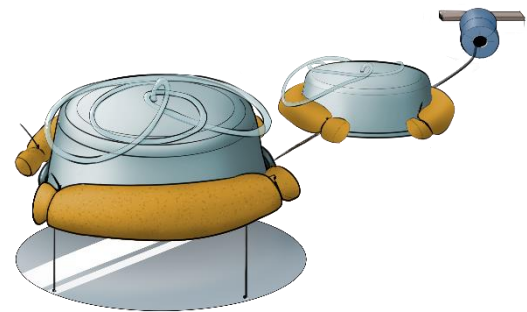
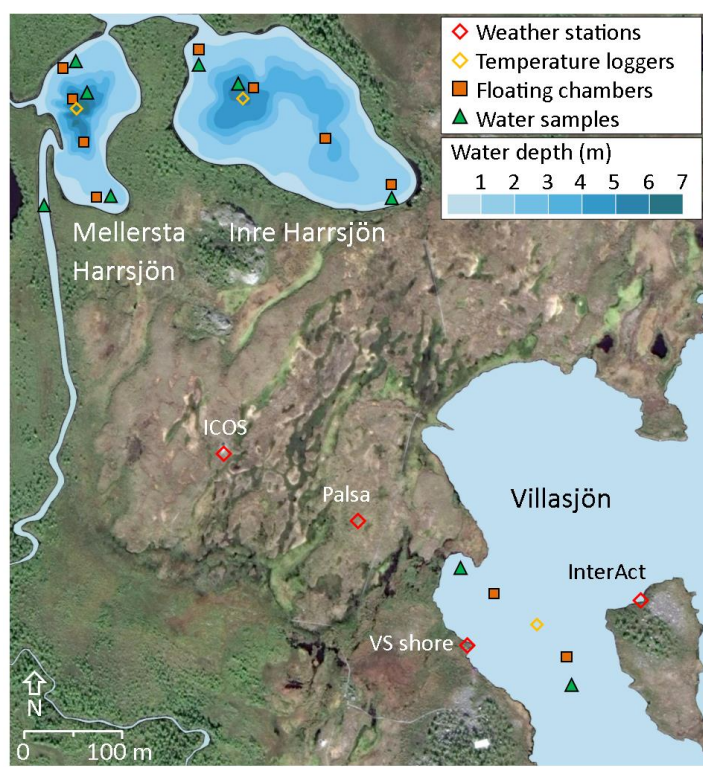


Figure 1—Map of the Stordalen Mire field site (left). Chamber and sampling locations are shown as they were in 2015–2017. A schematic of the floating chamber pairs is shown to the right. Lake bathymetry from Wik et al. (2011). Satellite imagery: Google, DigitalGlobe, 2017.

200 [CH₄ emissions were measured from three subarctic lakes of post-glacial origin \(Kokfelt et al., 2010\), located](#)
201 [around the Stordalen Mire in northern Sweden \(68°21' N, 19°02' E, Fig. 1\), a palsa mire complex underlain](#)
202 [by discontinuous permafrost \(Malmer et al., 2005\). The Mire \(350 m a.s.l.\) is part of a catchment that](#)
203 [connects Mt. Vuoskoåiveh \(920 m a.s.l.\) in the south to Lake Torneträsk \(341 m a.s.l.\) in the north \(Lundin](#)
204 [et al., 2016; Olefeldt and Roulet, 2012\). Villasjön is the largest and shallowest of the lakes \(0.17 km², 1.3](#)
205 [m max. depth\) and drains through fens into a stream feeding Mellersta Harrsjön and Inre Harrsjön, which](#)
206 [are 0.011 and 0.022 km² in size and have maximum depths of 6.7 m and 5.2 m, respectively \(Wik et al.,](#)
207 [2011\). The lakes are normally ice-free from the beginning of May through the end of October. Manual](#)
208 [observations were generally conducted between mid-June and the end of September. Diffusion accounts](#)
209 [for 17%, 52% and 34% of the ice-free CH₄ flux in Villasjön, Inre and Mellersta Harrsjön, respectively, with](#)
210 [the remainder emitted via ebullition \(2010–2017; Jansen et al., 2019\).](#)
211



212

Figure 1 – Map of the Stordalen Mire field site (left). Chamber and sampling locations are shown as they were in 2015–2017. A schematic of the floating chamber pairs is shown to the right. Lake bathymetry from Wik et al. (2011). Satellite imagery: Google, DigitalGlobe, 2017.

2.2 Floating chambers

We used floating chambers to directly measure the turbulence-driven diffusive CH₄ flux across the air-water interface (Fig. 1). They consisted of plastic tubs covered with aluminium tape to reflect incoming radiation and were equipped with polyurethane floaters/floats and flexible sampling tubes capped at one end with 3-way stopcocks (Bastviken et al., 2004) (Bastviken et al., 2004). Depending on flotation depth, each chamber covered an area between 610 and 660 cm² and contained a headspace of 4 to 5 litres. Chambers were deployed in pairs with a plastic shield was mounted underneath 30 cm below one chamber of each pair to deflect methane bubbles rising from the sediment. Every 1–2 weeks during the ice-free seasons of 2010 to 2017, 2–4 chamber pairs were deployed in Villasjön and 4–7 chamber pairs in Inre and Mellersta Harrsjön in different depth zones (Fig. 1). The number of chambers and deployment intervals exceeded the minimum needed to resolve the spatiotemporal variability of the flux (Wik et al., 2016a) (Wik et al., 2016a). Over a 24 hour period, 2–4 60 mL headspace samples were collected from each chamber using polypropylene syringes and the flotation depth and air temperature were noted in order to calculate the headspace volume. The 24-hour deployment period was chosen to compute fluxes over timescales which integrate/integrates diel variations in the gas transfer velocity (Bastviken et al., 2004) (Bastviken et al., 2004).

~~The fluxes reported here are from the shielded chambers only. To check that the shields were not reducing fluxes from turbulent processes such as convection, we compared fluxes from shielded and unshielded chambers on days when the lake mean bubble flux was <1% of the lake mean diffusive flux (bubble traps, 2009–2017; Jansen et al., 2019; Wik et al., 2013). Averaged over the three lakes, the difference was statistically significant ($F_{ch,unsh} - F_{ch,sh} = 0.20 \pm 0.16 \text{ mg m}^{-2} \text{ d}^{-1}$ ($n = 58$) (mean \pm 95% CI)) but only a 6% difference from mean fluxes. Conversely, some types of floating chambers can enhance gas transfer by creating artificial turbulence when dragging through the water (Matthews et al., 2003; Vachon et al., 2010; Wang et al., 2015). The effect appears to be negligible for chambers of the design, size and flotation depth used in this study (acoustic Doppler velocimeter measurements, Ribas-Ribas et al., 2018).~~

The fluxes reported here are from the shielded chambers only. To check that the shields were not reducing fluxes from turbulent processes such as convection, we compared fluxes from shielded and unshielded chambers on days when the lake mean bubble flux was <1% of the lake mean diffusive flux (bubble traps, 2009–2017; Jansen et al., 2019; Wik et al., 2013). Averaged over the three lakes, the difference was statistically significant ($0.20 \pm 0.16 \text{ mg m}^{-2} \text{ d}^{-1}$ ($n = 58$) (mean \pm 95% CI)), but small in relative terms (6% of the mean flux). Conversely, some types of floating chambers can enhance gas transfer by creating artificial turbulence when dragging through the water (Matthews et al., 2003; Vachon et al., 2010; Wang et al., 2015). Ribas-Ribas et al. (2018) compared acoustic Doppler velocimeter measurements inside and outside the perimeter of a chamber of similar design, size and flotation depth as those used in this study, and, based on a comparison of measured TKE dissipation rates and computed gas transfer velocities, concluded that the chambers did not cause artificial turbulence.

2.3 Water samples

254 Surface water samples were collected ~~at a depth of~~ 0.2–0.4 m below the surface at 2–3 different locations
255 in each lake ~~(Fig. 1)~~, at one to two-week intervals from June to October ~~(Fig. 1)~~. Samples were collected
256 from shore with a 4 m Tygon tube attached to a ~~float~~ float to avoid disturbing the sediments (2009–
257 2014), and from a ~~rowing boat~~ rowboat over the deepest points of Inre and Mellersta Harrsjön (2010–
258 2017) and at shallows (<1 m water depth) on either end of the lakes (2015–2017) using a 1.2 m L x 3.2 mm
259 ID Tygon tube. In addition, water samples were collected at the deepest point of Inre and Mellersta
260 Harrsjön at 1 m intervals down to 0.1 m from the sediment surface with a 7.5 m L x 6.4 mm ID fluorinated
261 ethylene propylene (FEP) tube. Subsequently, 60 mL polypropylene syringes were rinsed thrice with
262 sample water before duplicate bubble-free samples were collected, and were capped with airtight 3-way
263 stopcocks. 30 mL samples were equilibrated with 30 mL headspace and shaken vigorously by hand for 2
264 minutes (2009–2014) or on a mechanical shaker at 300 rpm for 10 minutes (2015–2017). Prior to 2015,
265 ~~lab~~ outside air – with a ~~predetermined~~ measured CH₄ content – was used as headspace. From 2015 on we
266 used an N₂ 5.0 headspace (Air Liquide). Water sample conductivity was measured over the ice-free season
267 of 2017 ($n = 323$) (S230, Mettler-Toledo), and converted to specific conductance using a temperature-
268 based approach.

269 **2.4 Concentration measurements**

270 Gas samples were analysed within 24 hours after collection at the Abisko Scientific Research Station, 10
271 km from the Stordalen Mire. Sample CH₄ contents were measured on a Shimadzu GC-2014 gas
272 chromatograph which was equipped with a flame ionization detector (GC-FID) and a 2.0 m long, 3 mm ID
273 stainless steel column packed with 80/100 mesh HayeSep Q and used N₂ >5.0 as a carrier gas (Air Liquide).
274 For calibration we used standards of 2.059 ppm CH₄ in N₂ (Air Liquide). 10 standard measurements were
275 made before and after each run. After removing the highest and lowest values, relative standard
276 deviations of the standard runs were generally less than 0.25%.

277

278 **2.5 Water temperature ~~and~~, pressure ~~loggers~~, density and mixed layer depth**

279 Water temperature was measured every 15 minutes from 2009 to 2018 with temperature loggers (HOBO
280 Water Temp Pro v2, Onset Computer) in Villasjön and at the deepest locations within Inre and Mellersta
281 Harrsjön. Sensors ~~monitored the surface water in all lakes were deployed~~ at 0.1, 0.3, 0.5, 1.0 m depth, ~~and~~
282 further in all lakes, with additional sensors at 3.0, 5.0 m (IH and MH) and at 6.7 m (MH) ~~at the deep points.~~.
283 Sensors were intercalibrated prior to deployment in a well-mixed water tank, and by comparing readouts
284 just before and during ice-on when the water column was isothermal. In this way a precision of <0.05 °C
285 was achieved. The bottom sensors were buried in the surface sediment and were excluded from in situ
286 intercalibration. Water pressure was measured in Mellersta Harrsjön (5.5 m) with a HOBO U20 Water Level
287 logger (Onset Computer). Water density was computed from temperature and salinity (Chen and Millero,
288 1977), using lake-averaged specific conductivity and a salinity factor [mS cm⁻¹ / g kg⁻¹] of 0.57. The salinity
289 factor was based on a linear regression of simultaneous measurements of conductivity and dissolved solids
290 (R² = 0.99, n = 7) in five lakes in the Torneträsk catchment (Miljödata-MVM, 2017). We defined the depth
291 of the surface mixing layer (z_{mix}) at a density gradient threshold (dp/dz) of 0.03 kg m⁻³ m⁻¹ (Rueda et al.,
292 2007).

293

294 **2.6 Meteorology**

295 Meteorological data was collected from four different masts on the Mire ~~(Fig. 1)~~, and collectively covered
296 a period from June 2009 to October 2017 with half-hourly measurements of wind speed, air temperature,
297 relative humidity, air pressure and irradiance (Fig. 1, Table 1). Wind speed was measured with 3D sonic
298 anemometers at the Palsa tower (z = 2.0 m), the Villasjön shore tower (z = 2.9 m), at the InterAct Lake
299 tower (z = 2.0 m) and at the Integrated Carbon Observation System (ICOS) site (z = 4.0 m). Air temperature
300 and relative humidity were measured at the Palsa tower, at the Villasjön shore tower (Rotronic MP100a
301 (2012–2015) / Vaisala HMP155 (2015–2017)) and at the InterAct lake tower. Incoming and outgoing
302 shortwave and long wave radiation were monitored with net radiometers at the Palsa tower (Kipp & Zonen
303 CNR1) and at the InterAct lake tower (Kipp & Zonen CNR4). Precipitation data was collected with a
304 WeatherHawk 500 at the ICOS site. Overlapping measurements were cross-validated and averaged to form
305 a single timeseries.

306

307 **Table 1** – Location and instrumentation of meteorological observations on the Stordalen Mire, 2009–2018.

Identifier	Period	Location	Wind	Air temp. and humidity	Radiation	Ref.
Palsa tower	2009-11	68°21'19.68"N 19° 2'52.44"E	C-SAT 3 <i>Campbell Scientific</i>	HMP-45C <i>Campbell Scientific</i>	CNR-1 <i>Kipp & Zonen</i>	Olefeldt et al., 2012 Olefeldt et al., 2012
Villasjön shore tower	2012-18	68°21'14.58"N 19° 3'1.07"E	R3-50 <i>Gill</i>	MP100a, <i>Rotronic</i> HMP155, <i>Vaisala</i>	REBS Q7.1 <i>Campbell Sci.</i>	Jammet et al., 2015 Jammet et al., 2015
InterAct Lake tower	2012-18	68°21'16.22"N 19° 3'14.98"E	uSonic 3 Scientific <i>Metek</i>	CS215 <i>Campbell Scientific</i>	CNR-4 <i>Kipp & Zonen</i>	*n/a
ICOS site	2013-18	68°21'20.59"N 19° 2'42.08"E	Weatherhawk 500 <i>Campbell Scientific</i>			*n/a

308

309 **2.7 Computation of CH₄ storage and residence time**

310 The amount of CH₄ stored in the water column [g CH₄ m⁻²] was computed by weighting and then
 311 adding each concentration measurement by the volume of the 1 m depth interval within which it was
 312 collected. For the upper 2 m of the two deeper lakes we separately computed storage in the vegetated
 313 littoral zone from near-shore concentration measurements, as these values could be different from those
 314 further from shore due to outgassing and oxidation during transport (DelSontro et al., 2017): horizontal
 315 transport (DelSontro et al., 2017). We computed the average residence time of a-CH₄ molecule in the lake
 316 by dividing the amount stored by the lake mean surface flux. Residence times computed with this approach
 317 should be considered upper limits, because we implicitly in this calculation we assumed that removal
 318 processes other than surface emissions, such as microbial oxidation, were negligible or took place at the
 319 sediment-water interface with minimal impact effect on water column CH₄.

320

321 **2.8 Flux calculations**

322 In order to calculate the chamber flux with Eq. 1 we estimated k_{ch} from the time dependent equilibrium
 323 chamber headspace concentration $C_{h,eq}(t)$ [mg m⁻³] (Bastviken et al., 2004):

324 In order to calculate the chamber flux with Eq. 1, we estimated the gas transfer velocity, k_{ch} [cm h⁻¹] from
 325 the time-dependent equilibrium chamber headspace concentration $C_{h,eq}(t)$ [mg m⁻³] (Bastviken et al.,
 326 2004):

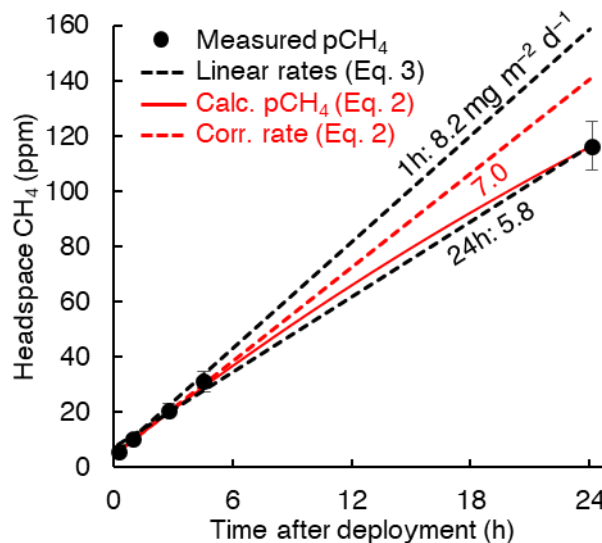
$$\begin{aligned}
 [C_{aq} - C_{h,eq}(t)] &= [C_{aq} - C_{h,eq}(t_0)] e^{-\frac{K_H R T A}{V} k_{ch} t} (C_{aq} - C_{h,eq}(t)) \\
 &= (C_{aq} - C_{h,eq}(t_0)) e^{-\frac{K_H R T_{water} A}{V} k_{ch} t}
 \end{aligned}
 \tag{2}$$

327 where K_H is Henry's law constant for CH₄ [mg m⁻³ Pa⁻¹] (~~Wiesenburg and Guinasso, 1979~~) (Wiesenburg and
 328 Guinasso, 1979), R is the universal gas constant [m³ Pa mg⁻¹ K⁻¹], T_{water} is the surface water temperature
 329 [K] and V and A are the chamber volume [m³] and area [m²], respectively. This method accounts for gas
 330 accumulation in the chamber headspace, which reduces the concentration gradient and limits the flux (Eq.
 331 1) (Fig. 2). For a subset of chamber measurements where simultaneous water concentration
 332 measurements were unavailable ($n = 949$) we computed the flux from the headspace concentrations
 333 alone:

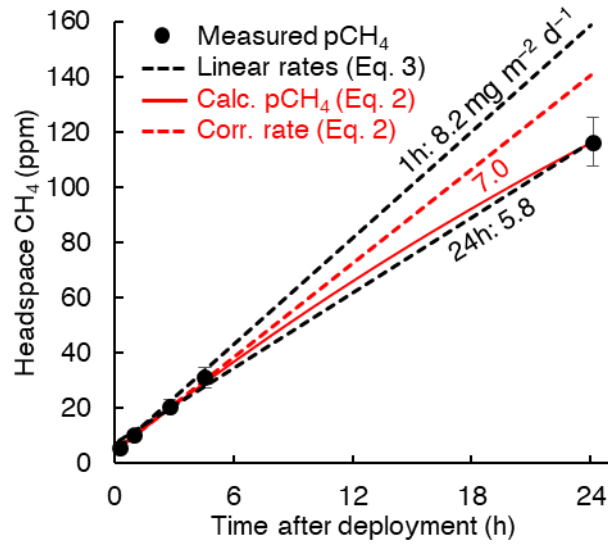
$$F = c_1 M \frac{\partial x_h}{\partial t} \frac{PV}{RT_{air}A} \quad [3]$$

334 where $\partial x_h / \partial t$ is the headspace CH_4 mole fraction change [$10^{-6} \text{ ppm mol mol}^{-1} \text{ d}^{-1}$], computed with ordinary
 335 least squares (OLS) linear regression (Fig. 2), M is the molar mass of CH_4 ($0.016 \text{ mg mol}^{-1}$), P is the air
 336 pressure [Pa], T_{air} is the air temperature [K]. Scalar c_1 corrects for the accumulation of CH_4 gas in the
 337 chamber headspace and increases over the deployment time. Comparing both chamber flux calculation
 338 methods we find $c_1 = 1.21$ for 24 hour deployments (OLS, $R^2 = 0.85$, $n = 357$). Chambers were sampled up
 339 to 4 times during their 24 hour deployment (at 10 minutes, 1–5 hours and 24 hours) which allowed us to
 340 compute fluxes at different time intervals of 1 hour and 24 hours. P and T_{air} were averaged over the
 341 relevant time interval.

343 Figure 2 illustrates the importance of shows that the headspace correction is necessary to avoid
 344 underestimating fluxes. The headspace-corrected flux (dashed red line) equals the initial slope of Eq. 2
 345 (solid red line) and is about 21% higher than the non-corrected flux (lower dashed black line in Fig. 2).
 346 However, both Eq. 2 (solid red line) and Eq. 3 with $c_1 = 1$ (dashed black lines) fit the concentration data (R^2
 347 ≥ 0.98 for 94% of 24-hour flux measurements). This dissimilarity results partly because the fluxes were low
 348 enough to keep headspace concentrations well below equilibrium with the water column, and because on
 349 average, the gas transfer velocity deviated $\leq 10\%$ from its mean value over its diel cycle (Fig. 7d). Short-
 350 term measurements (upper dashed black line) may omit the need for headspace correction but can
 351 significantly overestimate the flux if—as in our study—initial (Bastviken et al., 2004). Because concentration
 352 measurements were not available for all chamber observations, we used multi-year mean values of $\Delta[\text{CH}_4]$



353 and k_{ch} to compute c_1 as a function of chamber deployment takes place during daytime and k or $\Delta[\text{CH}_4]$
 354 follow a diurnal pattern (Bastviken et al., 2004). For 24 hour chamber deployments, $c_1 = 1.21$.



355 **Figure 2** – Example of chamber headspace CH₄ concentrations versus deployment time. Measured
 356 concentrations (dots) are averages from 2015–2017 (0.1h) and 2011 (1h–24h); error bars represent the
 357 95% confidence intervals. Linear regressions (dashed black lines) show the rate increase over 1 hour (two
 358 measurements) and over 24 hours (five measurements). The solid red line represents chamber
 359 concentrations computed with Eq. 2 using multi-year mean values of $\Delta[\text{CH}_4]$ and k_{ch} (uncorrected for
 360 headspace accumulation). The rate increase associated with the mean 24h flux corrected for headspace
 361 accumulation is shown as a dashed red line (Eq. 1 with k_{ch} from Eq. 2, or Eq. 3 with $c_1 = 1.21$).
 362 Labels denote fluxes calculated from the linear regression slopes (Eq. 3, black) and from Eq. 2 (red).

363 2.9 Computing gas transfer velocities with the surface renewal model

364 We used the surface renewal model (Lamont and Scott, 1970)(Lamont and Scott, 1970) formulated for
365 small eddies at Reynolds numbers >500 (MacIntyre et al., 1995; Theofanous et al., 1976) to estimate k :

$$k_{mod} = \alpha(\epsilon\nu)^{\frac{1}{4}} Sc^{-\frac{1}{2}} \quad [4]$$

366 ~~where the hydrodynamic and thermodynamic forces driving gas transfer are expressed, respectively, as~~
367 ~~the dissipation of turbulent kinetic energy (TKE), ϵ [m^2s^{-3}], and the dimensionless Schmidt number Sc ,~~
368 ~~defined as the ratio of the kinematic viscosity ν [m^2s^{-1}] to the free solution diffusion coefficient D_0 [m^2s^{-1}]~~
369 ~~(Jähne et al., 1987; Wanninkhof, 2014). The scaling parameter α has a theoretical value of 0.37 (Katul et~~
370 ~~al., 2018), but is often estimated empirically (α') to calibrate the model (e.g. Wang et al., 2015). To allow~~
371 ~~for a qualitative comparison between model and chamber fluxes we regressed k_{ch} (floating chambers)~~
372 ~~onto $(\epsilon\nu)^{\frac{1}{4}} Sc^{-\frac{1}{2}}$ (surface renewal model, half-hourly values of k_{mod} averaged over each chamber~~
373 ~~deployment period), and determined $\alpha' = 0.24 \pm 0.04$ (mean \pm 95% CI, $n = 334$) (Fig. 3). When comparing~~
374 ~~k -values we normalized to a Schmidt number of 600 (CO_2 at 20 °C) (Wanninkhof, 1992): $k_{600} =$~~
375 ~~$(600/Sc)^{-0.5}k$. To enable comparison with published wind k relations we calculated the wind speed at~~
376 ~~10 m (U_{10}) from the anemometer datasets following Smith (1988), assuming a neutral atmosphere.~~

377
378 where the hydrodynamic and thermodynamic forces driving gas transfer are expressed, respectively, as
379 the TKE dissipation rate ϵ [m^2s^{-3}], and the dimensionless Schmidt number Sc , defined as the ratio of the
380 kinematic viscosity ν [m^2s^{-1}] to the free solution diffusion coefficient D_0 [m^2s^{-1}] (Jähne et al., 1987;
381 Wanninkhof, 2014). The scaling parameter α has a theoretical value of 0.37 (Katul et al., 2018), but is often
382 estimated empirically (α') to calibrate the model (e.g. Wang et al., 2015). To allow for a qualitative
383 comparison between model and chamber fluxes, we took ratios of k_{ch} (floating chambers) and $(\epsilon\nu)^{\frac{1}{4}} Sc^{-\frac{1}{2}}$
384 (surface renewal model, half-hourly values of k_{mod} averaged over each chamber deployment period), and
385 determined $\alpha' = 0.23 \pm 0.02$ for all lakes (mean \pm 95% CI, $n = 334$) (Fig. 3), and $\alpha' = 0.31 \pm 0.06$ ($n = 67$) for
386 Villasiön, $\alpha' = 0.25 \pm 0.03$ ($n = 136$) for Inre Harrsjön and $\alpha' = 0.17 \pm 0.02$ ($n = 131$) for Mellersta Harrsjön
387 (Supplementary Fig. 1). Calibrating the model in this way allowed us to assess whether chamber flux
388 relationships with wind speed and temperature were reproduced by the model. For similar comparative
389 purposes, k -values were normalized to a Schmidt number of 600 (CO_2 at 20 °C) (Wanninkhof, 1992): $k_{600} =$
390 $(600/Sc)^{-0.5}k$. The wind speed at 10 m (U_{10}) was computed from measured wind speed following Smith
391 (1988), assuming a neutral atmosphere.

392
393
394
395
396
397
398
399
400
401
402

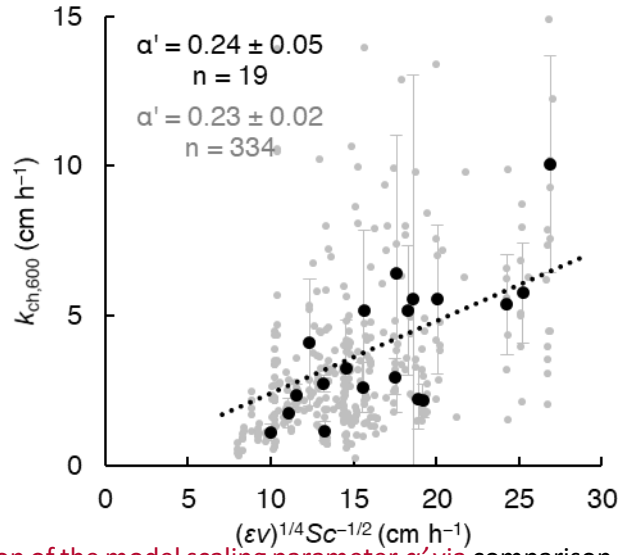


Figure 3 – Determination of the model scaling parameter α' via comparison between gas transfer velocities from floating chambers (Eq. 2) and the surface renewal model (Eq. 4 with $\alpha' = 1$ and $Sc = 600$, half-hourly values averaged over each chamber's 24 hour deployment period). Grey dots are for all three lakes. Dots represent individual chamber deployments (grey) and black dots represent multi-chamber means for each weekly deployment in 2016 and 2017, when concentration measurements were taken simultaneously with, and in close proximity to the chamber measurements. Intercepts (black). Mean ratios, and therefore α' , are represented by the slopes of the linear regressions (dotted lines) were fixed at 0. Error bars represent 95% confidence intervals of the means.

We used a parametrization by Tedford et al. (2014) based on Monin-Obukhov similarity theory to estimate the TKE dissipation rate at half-hourly time intervals:

We used a parametrization by Tedford et al. (2014) based on Monin-Obukhov similarity theory to estimate the TKE dissipation rate at half-hourly time intervals:

$$\varepsilon = \begin{cases} 0.56 u_{*w}^3 / \kappa z + 0.77 \beta & \text{if } \beta > 0 \\ 0.6 u_{*w}^3 / \kappa z & \text{if } \beta \leq 0 \end{cases} \varepsilon \quad [5]$$

$$= \begin{cases} 0.56 u_{*w}^3 / \kappa z + 0.77 \beta & \text{if } \beta > 0 \text{ (cooling)} \\ 0.6 u_{*w}^3 / \kappa z & \text{if } \beta \leq 0 \text{ (heating)} \end{cases}$$

where u_{*w} is the water friction velocity [$m s^{-1}$], κ is the von Kármán constant, z is the depth below the water surface (here set to 0.15 m, the depth for which Eq. 5 was calibrated). We determined u_{*w} from the air friction velocity u_{*a} assuming equal shear stresses (τ) on either side of the air-water interface; $\tau = \rho_a u_{*a}^2 = \rho_w u_{*w}^2$ (MacIntyre and Melack, 1995), and taking into account atmospheric stability (Imberger, 1985; MacIntyre et al., 2014; Tedford et al., 2014). β is the buoyancy flux [$m^2 s^{-3}$], which accounts for turbulence generated by convective mixing (Imberger, 1985):

where u_{*w} is the water friction velocity [$m s^{-1}$], κ is the von Kármán constant, z is depth below the water surface (0.15 m, the depth for which Eq. 5 was calibrated). We determined u_{*w} from the air friction velocity u_{*a} assuming equal shear stresses (τ) on both sides of the air-water interface; $\tau = \rho_a u_{*a}^2 = \rho_w u_{*w}^2$ and taking into account atmospheric stability (MacIntyre et al., 2014; Tedford et al., 2014). β is the buoyancy flux [$m^2 s^{-3}$], which accounts for turbulence generated by convection (Imberger, 1985):

$$\beta = \frac{\alpha_T g Q_{eff}}{\epsilon_{pw} \rho_w} = \alpha_T g Q_{eff} / c_{pw} \rho_w \quad [6]$$

440 where α_T is the thermal expansion coefficient [$\text{m}^3 \text{K}^{-1}$] (Kell, 1975), g is the standard gravity [m s^{-2}], ϵ_{pw}
 441 [$\text{J kg}^{-1} \text{K}^{-1}$] is the water specific heat and ρ_w [kg m^{-3}] is the water density, calculated from the water
 442 temperature and corrected for dissolved solids using conductivity measurements and a conversion factor
 443 of $0.57 \text{ g kg}^{-1} / \text{mS cm}^{-1}$. Q_{eff} [W m^{-2}] represents the net heat flux into the surface mixed layer and is the
 444 sum of net shortwave and long wave radiation and sensible and latent heat fluxes. We used Beer's Law
 445 to compute penetration of radiation into the water column across seven wavelength bands (Jellison and
 446 Melack, 1993). Attenuation of the visible portion of the spectrum was computed from the Secchi depth
 447 (Karlsson et al., 2010; Wik et al., 2018) with the inverse relationship from Idso and Gilbert (1974). We
 448 further computed outgoing component of the net longwave radiation (LW_{net}) using the Stefan-Boltzmann
 449 law: $LW_{out} = \sigma T^4$, where σ is the Stefan-Boltzmann constant ($5.67 \times 10^{-8} \text{ W m}^{-2} \text{ K}^{-4}$) and T is the surface
 450 water temperature in K. For periods where we did not have longwave radiation data we assumed $LW_{net} =$
 451 -50 W m^{-2} . Sensible and latent heat fluxes were computed with bulk aerodynamic formula described in
 452 MacIntyre et al. (2002). Both Q_{eff} and β are here defined as positive when the heat flux is directed out
 453 of the water, for example when the surface water cools.

454
 455 Direct measurements of turbulent dissipation rates in a small Arctic lake (1 m depth, 0.005 km^2) show
 456 that Equation 5 well characterizes near surface turbulence in small, sheltered water bodies similar to the
 457 lakes studied here (MacIntyre et al., 2018). Eq. 5 underestimates the dissipation suppressing effects of
 458 stratification of the upper water column at buoyancy frequencies ($N = \sqrt{g/\rho_w \times d\rho_w/dz}$) exceeding 25
 459 cycles per hour (MacIntyre et al., 2018). However, in the current dataset such periods of strong
 460 stratification ($N > 25$ cph) were observed $< 3\%$ of the time.

461 Here, α_T is the thermal expansion coefficient [$\text{m}^3 \text{K}^{-1}$] (Kell, 1975), g is the standard gravity [m s^{-2}], c_{pw} [J
 462 $\text{kg}^{-1} \text{K}^{-1}$] is the water specific heat and ρ_w [kg m^{-3}] is the water density. Q_{eff} [W m^{-2}] represents the net
 463 heat flux into the mixing layer and is the sum of net shortwave and long-wave radiation and sensible and
 464 latent heat fluxes. Penetration of radiation into the water column was evaluated across seven wavelength
 465 bands via Beer's Law (Jellison and Melack, 1993). An attenuation coefficient of 0.74 was computed for the
 466 visible portion of the spectrum from Secchi depth (2.3 m: Karlsson et al., 2010) following Idso and Gilbert
 467 (1974). Net longwave radiation ($LW_{net} = LW_{out} - LW_{in}$) was computed via measurements of LW_{in} (Table 1)
 468 and $LW_{out} = \sigma T^4$, where σ is the Stefan-Boltzmann constant ($5.67 \times 10^{-8} \text{ W m}^{-2} \text{ K}^{-4}$) and T is the surface
 469 water temperature in K. LW_{net} timeseries were gap-filled with ice-free mean values for each lake. Sensible
 470 and latent heat fluxes were computed with bulk aerodynamic formula (MacIntyre et al., 2002). Both Q_{eff}
 471 and β are here defined as positive when the heat flux is directed out of the water, for example when the
 472 surface water cools.

473
 474 Direct measurements of ϵ in an Arctic pond (1 m depth, 0.005 km^2 surface area) demonstrate that Equation
 475 5 can characterize near-surface turbulence in small, sheltered water bodies similar to the lakes studied
 476 here (MacIntyre et al., 2018). When the near surface was strongly stratified at instrument depth (buoyancy
 477 frequencies ($N = \sqrt{g/\rho_w \times d\rho_w/dz}$) > 25 cycles per hour (cph)), the required assumption of

478 homogeneous isotropic turbulence was not met and Equation 5 could not be evaluated. We observed
479 cases with $N > 25$ cph <3% of the time.

480

481 **2.10 Calculation of binned means**

482 We binned data to assess correlations between the flux and environmental covariates. Half-hourly values
483 of water temperature and wind speed were averaged over the deployment period of each chamber
484 (fluxes), and over 24 hours prior to the collection of each water sample (concentrations). ~~The 24 hour~~
485 ~~averaging period was chosen based on~~, reflecting the mean residence time of a CH_4 molecule in the lake
486 water column. ~~Parameters of interest~~ (Fluxes, concentrations and k -values) were then binned in 10 day,
487 1°C and 0.5 m s^{-1} bins to obtain relationships with time, water temperature and wind speed, respectively.
488 ~~For this calculation, lake-specific variables such as water temperature~~ The 10 day bins typically contained
489 at least one sampling day for each overlapping year, and enabled representative averaging across years.
490 Lake-dependent variables (e.g. flux) were normalized by lake to obtain a single timeseries (divided by the
491 lake mean, multiplied by the overall mean).

492

493 2.11 Calculation of the empirical activation energy

494 ~~Chamber and modelled fluxes as well as surface concentrations were fitted to an Arrhenius-type~~
495 ~~temperature function (e.g. Wik et al., 2014; Yvon-Durocher et al., 2014):~~

496 Chamber and modelled fluxes as well as concentrations were fitted to an Arrhenius-type temperature
497 function (e.g. Wik et al., 2014; Yvon-Durocher et al., 2014):

$$F = e^{-E_a'/k_B T + b} \quad [7]$$

498 where k_B is the Boltzmann constant (8.62×10^{-5} eV K⁻¹) and T is the water temperature in K. The empirical
499 activation energy (E_a' , in electron volts (eV), 1 eV = 96 kJ mol⁻¹) was computed with a linear regression of
500 natural logarithm of the fluxes and concentrations onto the inverse temperature (1/K), of which b is the
501 intercept.

502

503 2.12 Timescale analysis: power spectra and climacogram

504 We computed power spectra for near-continuous timeseries of the surface sediment, water- and air
505 temperature and the wind speed according to Welch's method (pwelch in MATLAB 2018a), which splits
506 the signal into overlapping sections and applies a cosine tapering window to each section (~~Hamming,~~
507 ~~1989).~~(Hamming, 1989). Data gaps were filled by linear interpolation. We removed the linear trend from
508 original timeseries to reduce red noise, and block-averaged spectra (8 segments with 50% overlap) to
509 suppress aliasing at higher frequencies. We normalized the ~~spectra~~spectral densities by multiplying by the
510 ~~natural~~ frequency and dividing by the variance of the original timeseries (~~Baldocchi et al., 2001~~)(Baldocchi
511 et al., 2001).

512

513 We evaluated our discontinuous (fluxes, concentrations) and continuous (meteorology) timeseries with a
514 climacogram, an intuitive way to visualize a continuum of variability (~~Dimitriadis and Koutsoyiannis,~~
515 ~~2015).~~(Dimitriadis and Koutsoyiannis, 2015). It displays the change of the standard deviation (σ) with
516 averaging timescale (t_{avg}) in double logarithmic space. Variables ~~of interest~~ were normalized by lake to
517 create a single time-series timeseries at half-hourly resolution (i.e. 48 entries for each 24-hour chamber
518 flux). To compute each standard deviation ($\sigma(t_{avg})$) data ~~was were~~ binned according to averaging timescale,
519 which ranged from 30 minutes to 1 year. Because of the discontinuous nature of the datasets, n bins were
520 distributed randomly across the time series. We chose $n = 100000$ to ensure that the 95% confidence
521 interval of the standard deviation at the smallest bin size was less than 1% of the value of σ (~~Sheskin,~~
522 ~~2007).~~(Sheskin, 2007). To allow for comparison between variables we normalized each σ -series by its
523 initial, smallest-bin value: $\sigma_{norm} = \sigma/\sigma_{init}$. For timescales < 1 week we used 1-hour chamber observations,
524 noting that sparse, daytime-only observations of concentrations and 1-hour fluxes may underestimate
525 short-term variability (σ_{init}). We use the climacogram ~~specifically~~ to test whether the variability of the
526 diffusive CH₄ flux is enveloped by hydrometeorological ~~contained within meteorological~~ variability, as for
527 terrestrial ecosystem processes (~~Pappas et al., 2017~~)(Pappas et al., 2017).

528

529 2.13 Statistics

530 We used Analysis of Variance (ANOVA) and the t-test to compare means of different groups. The use of
531 means, rather than medians was necessary because annual emissions can be determined by rare, high-

532 magnitude emission events. Parametric tests were justified because of the large number of samples in
533 each analysis, in accordance with the central limit theorem. Linear regressions were performed with the
534 ordinary least squares method (OLS): reported p -values refer to the significance of the regression slope.
535 Non-linear regressions were optimized with the Levenberg-Marquardt algorithm for non-linear least
536 squares with confidence intervals based on bootstrap replicates ($n = 1999$). Computations were done in
537 MATLAB 2018a and in PAST v3.25 (Paleontological Statistics software package) (~~Hammer et al.,~~
538 ~~2001~~)(Hammer et al., 2001).

539 3. Results

540 3.1 Measurements and models

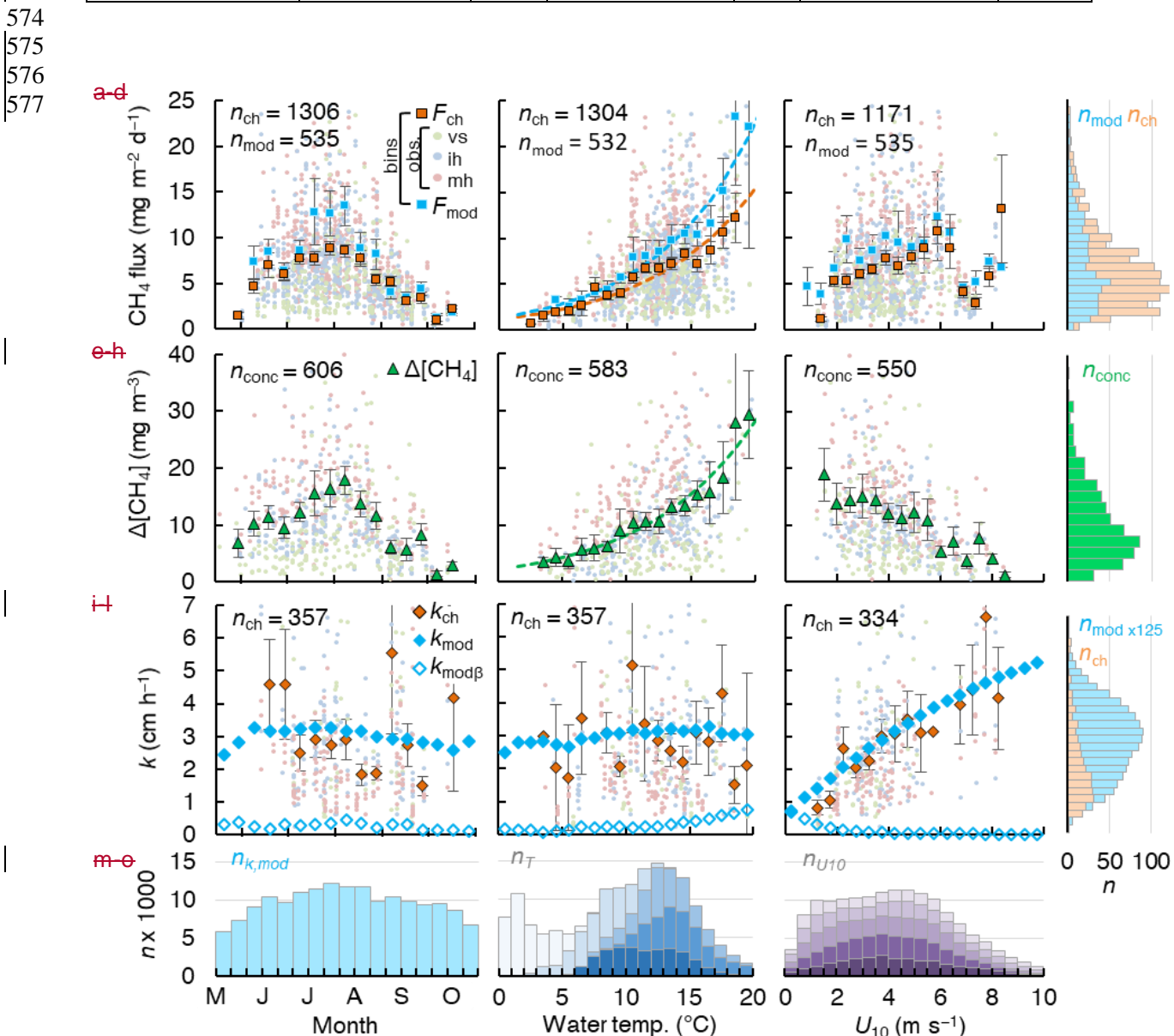
541 Chamber fluxes averaged $6.9 \text{ mg m}^{-2} \text{ d}^{-1}$ (range 0.2–32.2, $n = 1306$) and closely tracked the temporal
542 evolution of the surface water concentrations (mean 11.9 mg m^{-3} , range 0.3–120.8, $n = 606$), with the
543 higher values in each lake measured in the warmest months (July and August, Fig 4a,e). ~~As expected,~~
544 Diffusive fluxes increased with wind speed and water temperature (Fig 4b,c). Reduced emissions were
545 measured in the shoulder months (June and September) and were associated with lower water
546 temperatures. We also observed abrupt reductions of the flux at wind speeds lower than 2 m s^{-1} and higher
547 than 6.5 m s^{-1} . Surface water concentrations generally increased with temperature and peaked in the
548 summer months, but unlike the chamber fluxes they decreased with increasing wind speed (Fig. 4f,g).
549 Relationships with wind speed were approximately linear, while relationships with temperature fitted an
550 Arrhenius-type exponential function (Eq. 7). Activation energies were not significantly different ~~between~~
551 ~~the~~when using either surface water ~~and/or~~ sediment temperature ($E_a' = 0.90 \pm 0.14 \text{ eV}$, $R^2 = 0.93$, $E_a' = 1.00$
552 ± 0.17 , $R^2 = 0.93$, respectively, mean \pm 95% CI). The fluxes, concentrations, and the wind speed were non-
553 normally distributed (Fig. 4d,h,o). Surface water temperatures (0.1–0.5 m) were normally distributed
554 ~~for~~around the mean of each individual month of the ice-free season (Fig. 4n), but the composite
555 distribution was bimodal.

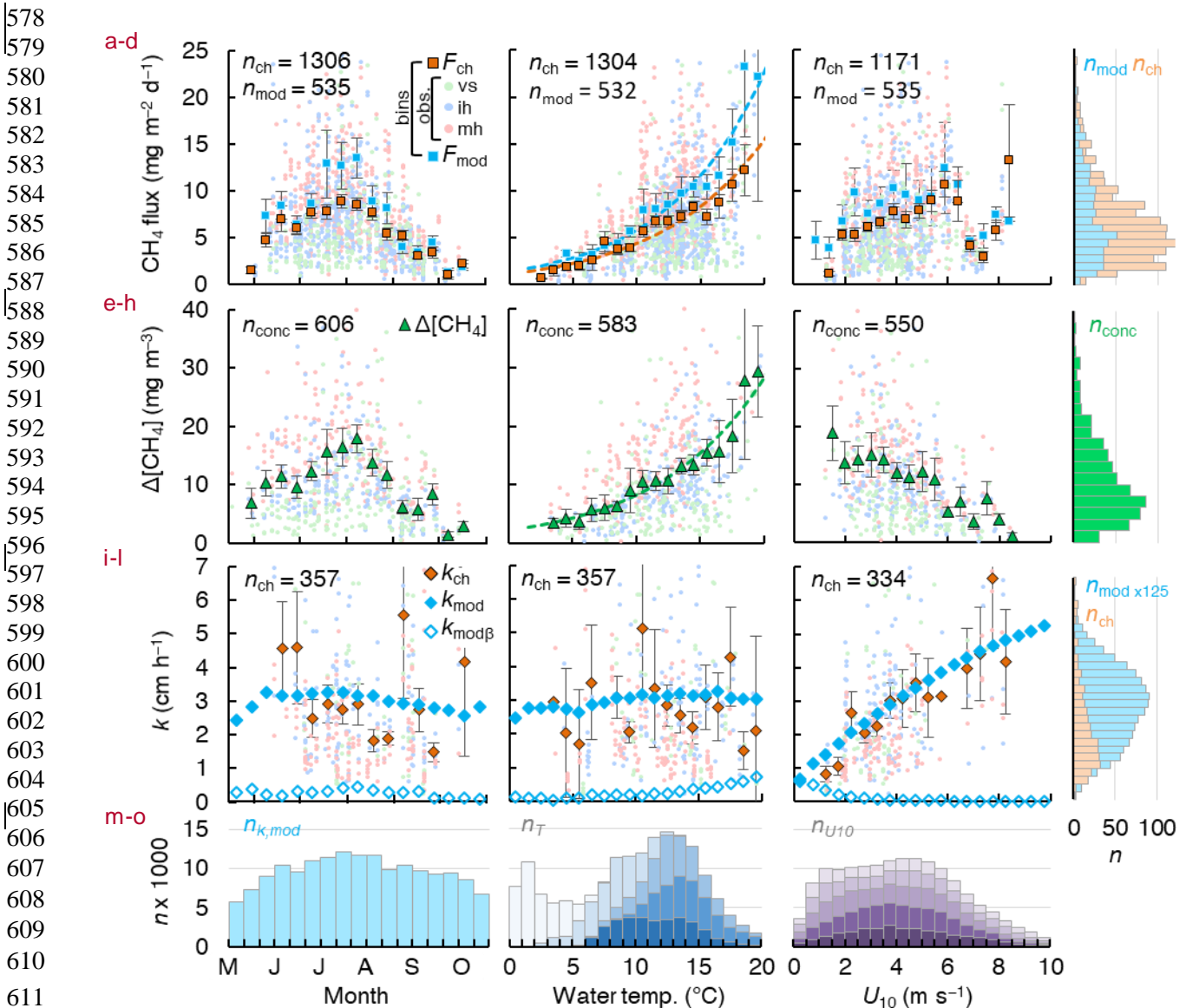
556
557 Fluxes computed with the surface renewal model (Eq. 1 using k_{mod}) closely resembled the chamber fluxes
558 (Eq. 3) in terms of temporal evolution (Fig. 4a) and correlation with environmental drivers (Fig. 4b,c).
559 ~~Despite the model's calibration with a subset of the chamber data,~~Mean model fluxes were slightly higher
560 than the chamber fluxes in ~~all lakes~~Villasjön and Inre Harrsjön, and slightly lower in Mellersta Harrsjön
561 (Table 2). Model fluxes were significantly different between littoral and pelagic zones in Inre and Mellersta
562 Harrsjön (paired t-tests, $p \leq 0.02$), reflecting spatial differences in the surface water concentration (Table
563 2). Similar to the chamber fluxes, the air-water concentration difference ($\Delta[\text{CH}_4]$) explained most of the
564 temporal variability of the modelled emissions; both k_{mod} (Eq. 4) and k_{ch} (Eq. 2) were functions of U_{10} (Fig.
565 4k) and did not display a distinctive seasonal pattern (Fig. 4i). Modelled fluxes ~~were lower~~decreased at
566 higher wind speeds when surface concentrations decreased, and displayed a cut-off at daily mean $U_{10} \geq$
567 6.5 m s^{-1} , similar to the chamber fluxes, but not at $U_{10} < 2.0 \text{ m s}^{-1}$. The temperature sensitivity of the
568 modelled fluxes ($E_a' = 0.97 \pm 0.12 \text{ eV}$, mean \pm 95% CI, $R^2 = 0.94$) did not differ significantly from that of the
569 chamber fluxes.

570

571 **Table 2** – CH₄ fluxes from floating chambers and the surface renewal model, and surface CH₄ concentrations. [Data](#)
 572 [from](#) 2014 was excluded from the model flux means because of a substantial bias in the timing of sample collection.
 573 [Model fluxes for each lake were computed with distinct scaling parameter values \(Supplementary Fig. 1\).](#)

Location	Chamber flux (mg m ⁻² d ⁻¹)		Modelled flux (mg m ⁻² d ⁻¹)		Surface concentration (mg m ⁻³)	
	mean ± 95% CI	<i>n</i>	mean ± 95% CI	<i>n</i>	mean ± 95% CI	<i>n</i>
Overall	6.9 ± 0.3	1306	7.6 ± 0.5	501	11.9 ± 0.9	606
Villasjön	5.2 ± 0.5	249	5.3 ± 7.0 <u>7 ± 0.9</u>	149	8.3 ± 1.1	183
Inre Harrsjön	6.6 ± 0.4	532	7.6 ± 0.6	176	10.2 ± 1.0	211
Shallow (<2 m)	6.0 ± 0.6	219	7.6 ± 0.4 <u>7.8 ± 0.9</u>	113	11.1 ± 1.3	133
Intermediate (2-4 m)	7.1 ± 0.6	212				
Deep (>4 m)	6.6 ± 0.8	101	6.4 ± 0.9	63	8.6 ± 1.4	78
Mellersta Harrsjön	8.0 ± 0.4	525	10.4 ± 0.9 <u>7.7 ± 0.9</u>	176	16.7 ± 2.0	212
Shallow (<2 m)	8.1 ± 0.6	272	11.1 ± 1.1 <u>8.3 ± 0.9</u>	113	18.2 ± 2.7	134
Intermediate (2-4 m)	7.8 ± 0.7	154				
Deep (>4 m)	8.0 ± 1.0	99	6.8 ± 0.9 <u>9.1 ± 1.2</u>	63	14.1 ± 2.7	78





612 **Figure 4** – Scatterplots of the CH₄ flux (a-c), CH₄ air-water concentration difference (e-g) and gas transfer
 613 velocity (i-k) versus time, surface water temperature and wind speed, as well as the histograms of the
 614 aforementioned variables- (d,h,l, m-o). In each scatter plot binned means of the flux (squares, a-c),
 615 concentrations (triangles, e-g) and gas transfer velocities (rhombuses, i-k) are represented by large
 616 symbols with error bars signifying 95% confidence intervals (error bars). Orange and light blue symbols
 617 reflect chamber-derived and model-derived binned values, respectively. Model k was computed with $\alpha' =$
 618 0.23. Bin sizes were 10 days, 1 °C and 0.5 m s⁻¹ for time, surface water temperature and U₁₀, respectively.
 619 Small green, blue and red dots represent individual measurements in Villasjön, Inre Harrsjön and Mellersta
 620 Harrsjön, respectively. Open rhombus symbols in panels i-k represent the buoyancy component of the gas
 621 transfer velocity, closed rhombus symbols include both the wind-driven and buoyancy-driven
 622 components. Dashed lines in panels b and f represent fitted Arrhenius functions (Eq. 7). Histograms of
 623 modelled (light blue) and measured (light orange) quantities (d,h,l) overlap. Histograms of the surface

624 water temperature (**m**) and U_{10} (**o**) are stacked by month, from June (darkest shade) to October (lightest
625 shade).

626 3.2 Meteorology and mixing regime

627 The water column of all three lakes was weakly stratified throughout the ice-free season, and the mean
628 diel mixing depths ($dp/dz < 0.03 \text{ kg m}^{-3} \text{ m}^{-1}$ (Rueda et al., 2007)) exceeded the lake mean depths (Table 3).
629 Figure 5 shows a timeseries of the mixing. Throughout the ice-free season the lakes were weakly stratified
630 (Table 3). Figure 5 shows a timeseries of the mixed layer depth and water temperature in the deeper lakes,
631 along with wind speed, air temperature and precipitation for the ice-free period of 2017. All lakes were
632 polymictic and mixed to the bottom several times during summer (Fig. 5 f-h). Water temperatures in the
633 surface mixed layer were lowest in Mellersta Harrsjön ($9.4 \pm 5.0 \text{ }^\circ\text{C}$), where the mooring was placed next
634 to the stream outlet (Fig. 1), and were higher in Inre Harrsjön ($9.9 \pm 5.5 \text{ }^\circ\text{C}$) and Villasjön ($10.2 \pm 5.3 \text{ }^\circ\text{C}$)
635 (ice-free seasons of 2009–2017, mean \pm SD). In early summer (June, July) deep mixing. The ice-free period
636 consisted of two phases. In the first, air and surface water temperatures were higher and the two deeper
637 lakes stratified. Wind speeds increased to mean values approaching 5 m s^{-1} for a few days at a time and
638 then decreased for a day or two. Deep mixing events followed surface cooling and heavy rainfall. Water
639 level maxima and surface temperature minima were observed 2-3 days after rainfall events, for example
640 between 15 and 18 July 2017 (Fig. 5e). In the second phase, wind speeds were persistently higher ($U_{10} > 5$
641 m s^{-1}), air and surface water temperatures declined and all lakes mixed to the bottom. Strong nocturnal
642 cooling on 16 August 2017 broke up stratification and the lakes remained well-mixed until ice-on (20
643 October). Increased wind speeds in September and October may have further enhanced mixing. Overall
644 (Throughout the ice-free seasons from 2009–2018), stratified periods ($z_{\text{mix}} \leq 1 \text{ m}$) lasted for 7 hours on
645 average and were common (2931% and 4445% of the time in Inre and Mellersta Harrsjön, respectively),
646 but were frequently interrupted/disrupted by deeper mixing events. Shallow mixing ($z_{\text{mix}} \leq z_{\text{mean}}$) occurred
647 on diel timescales. Deeper mixing occurred at longer intervals (days-weeks), and more frequently
648 toward the end of the ice-free season (Fig. 5g,h) in association with higher wind speeds.

649 Fluxes and near surface concentrations also varied within these periods, with concentrations and fluxes
650 higher in the warmer, stratified period and lower in the colder, mixed periods. In 2017, the highest
651 concentrations and fluxes occurred earlier in the season, with the initial high values in the two deeper
652 lakes indicative of residual CH_4 that had not evaded immediately after ice-off, around 1 June 2017 (Fig.
653 5c,d). As residual CH_4 was emitted, near surface concentrations declined, and then in the first half of the
654 stratified period (July 2017, Fig. 5d), particularly in Mellersta Harrsjön, increased with increased rainfall
655 and with temperature. During this period, k_{ch} and k_{mod} were similar. Decreases in k_{ch} occurred when air
656 temperatures increased above surface water temperatures in the day leading to a stable atmosphere and
657 when near surface temperatures were warmer, and depending upon the lake, stratified to the surface.
658 Thus, lower fluxes occurred during the second part of the stratified period (August 2017, Fig. 5c) when
659 surface concentrations increased during warming periods when winds were light, the atmosphere was
660 stable during the day, and the upper water column was strongly stratified. Fluxes and concentrations were
661 lower in the autumn mixed periods, by which time the lakes had degassed, and with the colder surface
662 sediment temperatures, rates of production had decreased.

663 The modelled gas transfer velocity generally followed the temporal pattern of the wind speed (Fig. 4b).
664 Due to model calibration, the chamber-derived modelled gas transfer velocities (Fig. 4b, orange
665 rhombuses/blue line) tracked those computed with the surface renewal model derived from chamber
666 observations (Fig. 4b, blue line/orange rhombuses). Discrepancies pointed to a mismatch between 24-hour
667 integrated chamber fluxes and surface concentrations measured at a single point in time. For example,
668 measuring a low surface concentration in the de-gassed water column after a windy period during which

669 the surface flux was high led to an overestimated k_{ch} on 21 September 2017. Contrastingly, k_{ch} was lower
670 than k_{mod} on 3 August 2017 due to elevated surface concentrations and a low chamber flux associated with
671 a warm and stratified period preceding water sampling.

672
673 The ~~mixed layer water~~ temperature of the surface mixed layer exceeded the air temperature by 1.6 °C on
674 average (Fig. 5a). ~~The bias was a function of temperatures~~5a), such that the atmospheric boundary layer
675 over the lakes was often unstable, particularly at night dropping below surface water temperatures, which
676 contributed to negative buoyancy fluxes during warm periods as well as during the many cold fronts. We
677 computed an unstable atmosphere over the lakes ($z/L_{MO,a} < 0$, where z is the measurement height and
678 $L_{MO,a}$ is the air-side Monin-Obukhov length; Foken 2006) ~76% of the time during ice-free seasons.
679 Atmospheric instability increases sensible and latent heat fluxes (Brutsaert, 1982), enhancing the cooling
680 rate. Thus, buoyancy fluxes were positive at night and during cold fronts throughout the ice-free season
681 (Fig 5b, Fig. 4i-k). We computed elevated contributions of theThe magnitude of buoyancy flux during
682 cooling periods tended to the TKE budget during the night and in the warmest monthsrange from 10^{-8} to
683 $10^{-7} \text{ m}^2 \text{ s}^{-3}$ in the stratified period and decreased as water temperatures cooled in autumn (Fig. 7), ~~but the~~
684 ~~overall influence of convection on near-surface turbulence~~4i,j). TKE dissipation rates at 0.15 m were high,
685 with values often between 10^{-6} and $10^{-5} \text{ m}^2 \text{ s}^{-3}$, although values did fall as low as $10^{-8} \text{ m}^2 \text{ s}^{-3}$ when winds
686 were light. Comparison of these two terms indicated that buoyancy flux during cooling was typically two
687 orders of magnitude less than ϵ and was only equal to it during the lightest winds (Fig. 4k). Consequently,
688 its contribution to the gas transfer coefficient was minor. (Fig. 7). Averaged over all ice-free seasons (2009–
689 2017) the buoyancy flux contributed only 8% to the TKE dissipation rate, but up to 90% during rare, very
690 calm periods ($U_{10} \leq 0.5 \text{ m s}^{-1}$, Fig. 4k) and up to 25% on during the warmest ~~days~~periods ($T_{surf} \geq 18 \text{ °C}$, Fig.
691 4j).

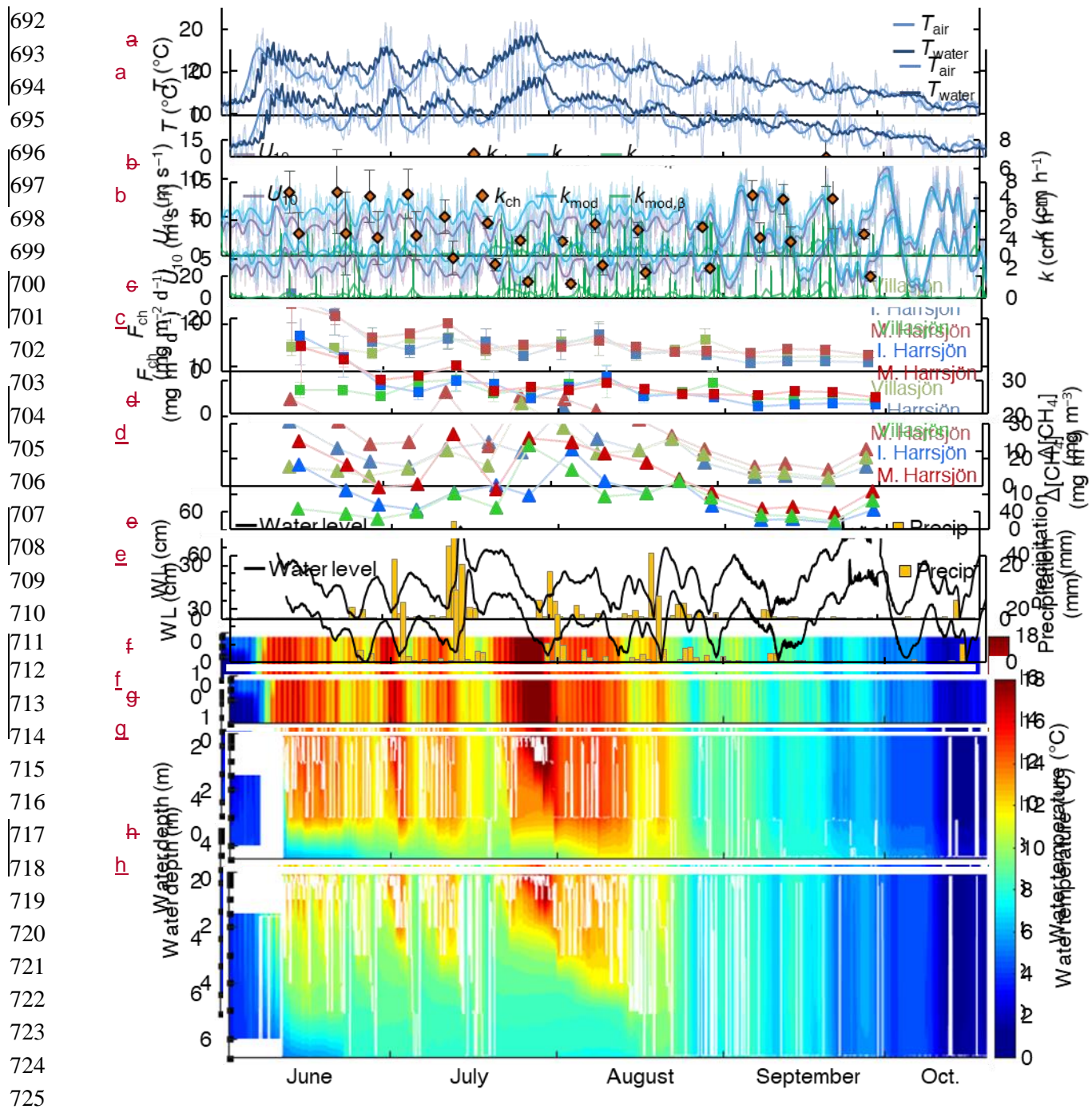


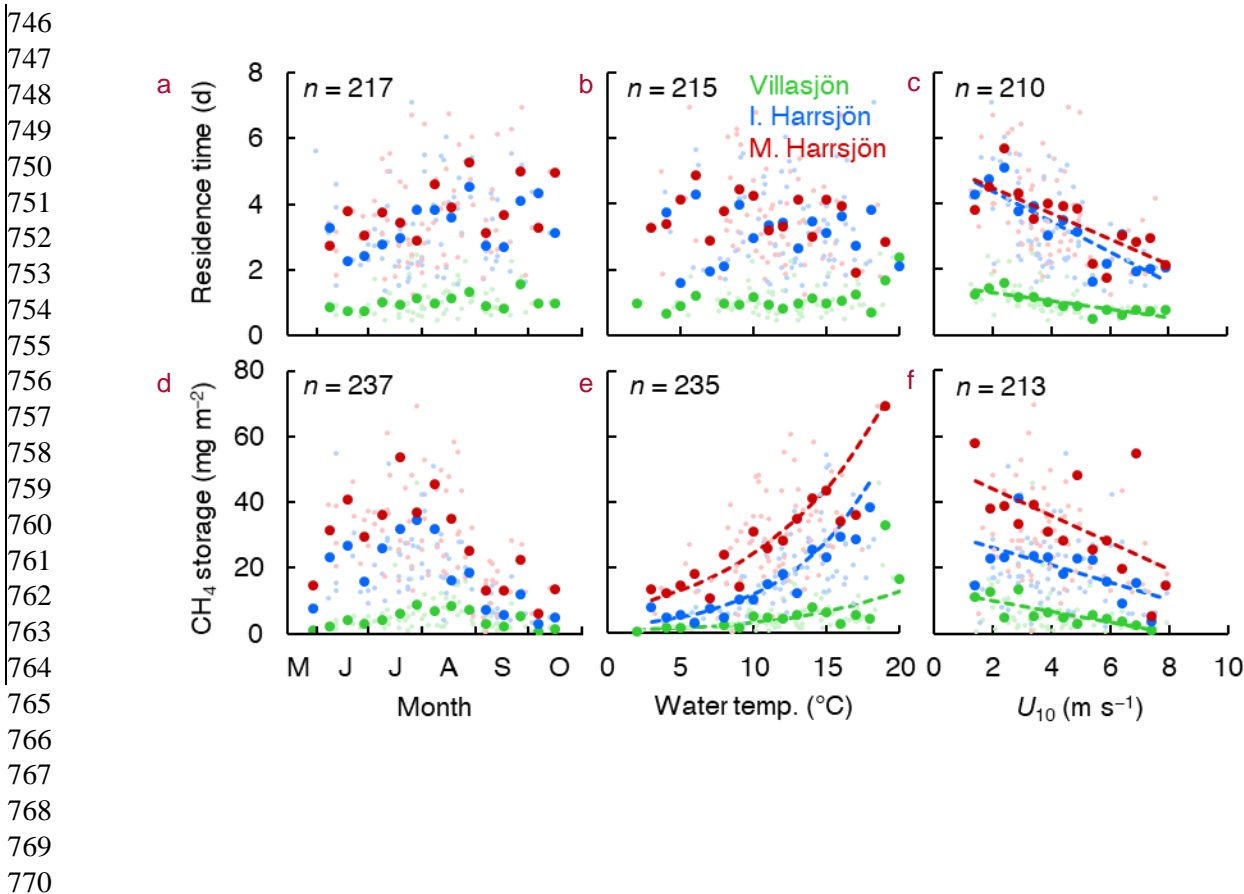
Figure 5 – Timeseries of air and surface mixed-layer water temperature (three-lake mean) (a), wind speed, gas transfer velocity from the surface renewal model (k_{mod} and its buoyancy component, $k_{mod,\beta}$) and from chamber observations (k_{ch}) (three-lake mean values, error bars represent 95% confidence intervals) (b), chamber CH_4 flux (c), air-water CH_4 concentration difference (d), precipitation and changes in water level in Mellersta Harrsjön (e) and the water temperature in Villarsjön (f), Inre Harrsjön (g) and Mellersta Harrsjön (h) during the ice-free season of 2017 (1 June to 20 October). The white lines in panels **e** and **f-h** represent the depth of the actively mixing surface mixed layer. Thin and thick curves in panels **a** and **b**

733 represent half-hourly and daily means, respectively. In panel **a** only the half-hourly timeseries of T_{water} was
734 plotted.

735 **Table 3** – Lake morphometry, mixing regime temperature of the surface mixing layer, buoyancy frequency and CH₄
 736 residence time. Mean values were calculated over the ice-free seasons of 2009–2017.

Lake	Area (ha)	Depth (m)		Mixed layer depth temp. (m(°C))		N (cycles h ⁻¹)		CH ₄ residence time (days)	
		mean	max	mean ± SD	n	mean ± SD	n	mean ± SD	n
Villasjön	17.0	0.7	1.3	0.7 ± 0.3 9.9 ± 5.5	664391 48976	5.7 ± 8.0	59552	1.0 ± 0.4	72
Inre Harrsjön	2.3	2.0	5.2	10.1 ± 5.2 ±1.6	583622 78752	5.2 ± 6.9	66757	3.4 ± 1.9	73
Mellersta Harrsjön	1.1	1.9	6.7	9.2 ± 24.9	624722 78014	5.3 ± 9.0	61268	3.7 ± 1.7	72

737
 738 **3.3 CH₄ storage and residence times**
 739 Residence times of stored CH₄ varied between 12 hours and 7 days and were inversely correlated with
 740 wind speed in all three lakes (OLS: R² ≥ 0.57, Fig. 6). The mean residence time was shortest in the shallowest
 741 lake, and was not significantly different between the two deeper lakes (paired t-test, p < 0.01, Table 3).
 742 We did not find a statistically significant linear correlation between the residence time and day of year or
 743 the water temperature. CH₄ storage was greatest in the deeper lakes and displayed patterns similar to the
 744 surface concentrations, increasing in the warmest months with water temperature and decreasing with
 745 wind speed.



771
772
773
774
775 **Figure 6** – Scatterplots of the CH₄ residence time **(a-c)** and storage **(d-f)** versus time, surface water
776 temperature and wind speed. Symbol colours represent the different lakes. Large symbols represent
777 binned means, small symbols represent individual estimates. Bin sizes were 10 days, 1 °C and 0.5 m s⁻¹ for
778 time, water temperature and U₁₀, respectively. ~~Linear relations of binned quantities and the wind speed~~
779 ~~were statistically significant (residence time: $p \leq 0.002$; Each storage: $p \leq 0.04$).~~ observation was paired
780 with T and U_{10} averaged over the 24h (Villasjön) and 72h (Inre and Mellersta Harrsjön) prior to water
781 sampling, reflecting average conditions during CH₄ residence times. The linear regressions of the residence
782 time onto time ~~of measurement~~**(a)** and ~~the surface water~~ temperature **(b)** were not statistically significant
783 ($p = 0.07$ – 0.10). Linear relations of binned quantities and U_{10} were statistically significant (c: $p \leq 0.002$; f: p
784 ≤ 0.04). Arrhenius-type functions (Eq. 7) adequately described the storage-temperature relation in each
785 lake (e: $R^2 \geq 0.70$, $p < 0.001$).

786 3.4 Variability

787 Chamber fluxes and surface water concentrations differed significantly between lakes (ANOVA, $p <$
788 0.001 , $n = 287$, $n = 365$). Both quantities were inversely correlated with lake surface area (Table 2). CH_4
789 concentrations in the stream feeding the Mire ($22.2 \pm 5.1 \text{ mg m}^{-3}$, $n = 29$, mean \pm 95% CI), were
790 significantly higher than those in the lakes (Table 2) (Lundin et al., 2013). Surface water concentrations
791 over the deep parts of the deeper lakes ($\geq 2 \text{ m}$ water depth) were lower than those in the shallows (< 2
792 m) by 21 to 26% for Inre and Mellersta Harrsjön, respectively. However, the diffusive CH_4 flux did not
793 differ significantly between depth zones in either Inre Harrsjön (ANOVA, $p = 0.27$, $n = 290$) or Mellersta
794 Harrsjön (ANOVA, $p = 0.90$, $n = 293$), or between zones of high and low CH_4 ebullition in Villasjön (paired
795 t -test, $p = 0.27$, $n = 89$). This is a contrast with ebullition, for which the highest fluxes were consistently
796 observed in the shallow lake and littoral areas of the deeper lakes (Jansen et al., 2019; Wik et al., 2013).

797
798 Chamber fluxes and surface water concentrations differed significantly between lakes (ANOVA, $p < 0.001$,
799 $n = 287$, $n = 365$) (Table 2). Both quantities were inversely correlated with lake surface area. CH_4
800 concentrations in the stream feeding the Mire ($22.2 \pm 5.1 \text{ mg m}^{-3}$, $n = 29$, mean \pm 95% CI), were significantly
801 higher than those in the lakes (Table 2). Surface water concentrations over the deep parts of the deeper
802 lakes ($\geq 2 \text{ m}$ water depth) were lower than those in the shallows ($< 2 \text{ m}$) by 21 to 26% for Inre and Mellersta
803 Harrsjön, respectively. However, the diffusive CH_4 flux did not differ significantly between depth zones in
804 either Inre Harrsjön (ANOVA, $p = 0.27$, $n = 290$) or Mellersta Harrsjön (ANOVA, $p = 0.90$, $n = 293$), or
805 between zones of high and low CH_4 ebullition in Villasjön (paired t -test, $p = 0.27$, $n = 89$). The similar fluxes
806 inshore and offshore present a contrast with ebullition, for which the highest fluxes were consistently
807 observed in the shallow lake and littoral areas of the deeper lakes (Jansen et al., 2019; Wik et al., 2013).

808
809 Relations between the flux and its drivers — temperature, wind speed and the surface concentration —
810 manifested on different timescales (Fig. 7). Over the ice-free season both the CH_4 fluxes and surface water
811 concentrations tracked changes in the water temperature. The wind speed (U_{10}) showed less variability
812 over seasonal (CV = 7%, $n = 17$) than over diel timescales (CV = 12%, $n = 24$) and displayed a clear diurnal
813 maximum. The surface water/sediment temperature varied primarily on a seasonal timescale (CV =
814 52%/45%, $n = 17$), and less on diel timescales (CV = 3%/2%, $n = 24$). Similar to the wind speed the gas
815 transfer velocity varied primarily on diel timescales (Fig. 7), albeit with a lower amplitude. This was in part
816 because $k_{mod} \propto u^{3/4}$ (Eq. 4.4), and because the drag coefficient, used to compute the water-side friction
817 velocity in Equation 5, increases at lower wind speeds and under an unstable atmosphere, which was
818 typically the case. The surface concentration correlated with wind speed and temperature (Fig. 4f,g), and
819 showed both seasonal and diel variability. On diel timescales $\Delta[\text{CH}_4]$ ~~appeared~~ and k_{mod} were out of phase
820 ~~with k_{mod} and; $\Delta[\text{CH}_4]$~~ peaked just before noon, when the gas transfer velocity reached its maximum value
821 (Fig. 7b,d). However, binned means of $\Delta[\text{CH}_4]$ the 1-hour chamber fluxes (F_{ch} (1h)) were not significantly
822 different at the 95% confidence level (error bars) and ~~the 1-hour chamber fluxes~~ did not show a clear diel
823 pattern (Fig. 7b). Temporal patterns of fluxes and concentrations were very similar between the lakes
824 (Supplementary Fig. 2 and 3).

825
 826
 827
 828
 829
 830
 831
 832
 833
 834
 835
 836
 837
 838
 839
 840
 841
 842
 843
 844
 845
 846
 847
 848

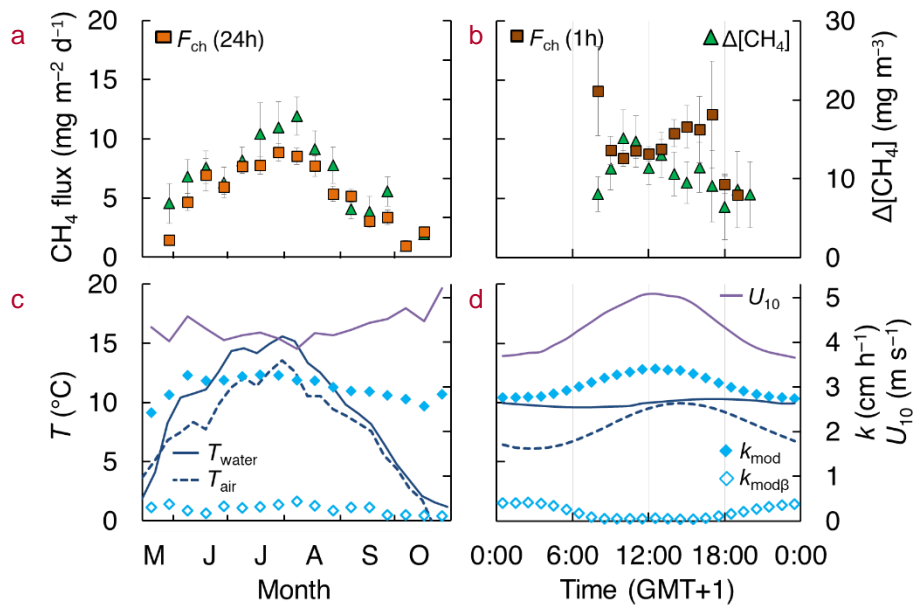


Figure 7 – Temporal patterns of CH₄ chamber fluxes, concentrations (a,b), gas transfer velocity, air and surface water temperature and wind speed (c,d). Bin sizes are 10 days (a,c) and 1 hour (b,d). Error bars represent 95% confidence intervals of the binned means. Temporal patterns in each individual lake are shown in Supplementary Figures 2 and 3.

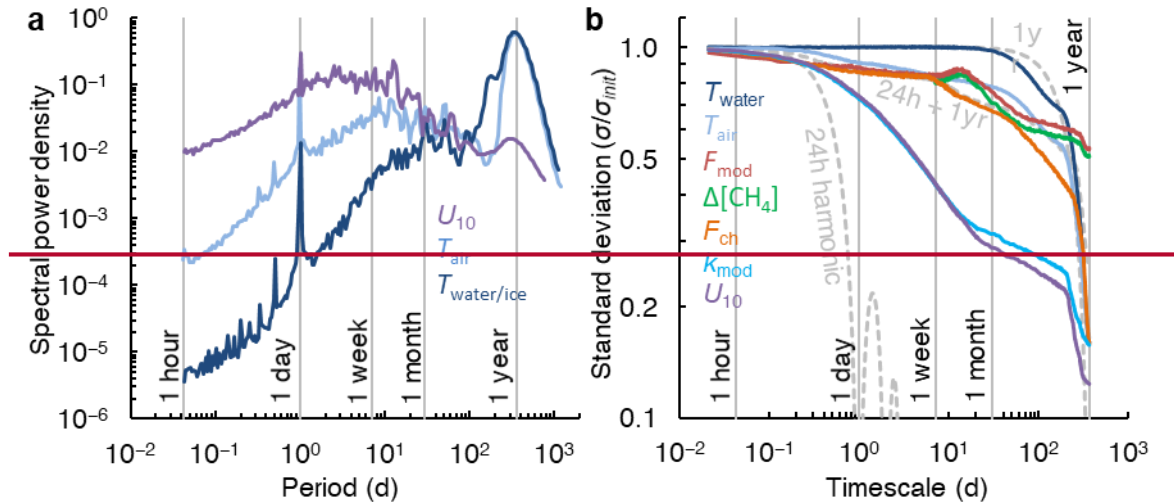
3.5 Timescale analysis

The spectral density plot (Fig. 8a) disentangles dominant timescales of variability of the drivers of the flux. The power spectra of wind speed and temperature peaked at periods of 1 day and 1 year, following well known diel and annual cycles of insolation and seasonal variations in climate (Baldocchi et al., 2001). For U_{10} , the overall spectral density maximum between 1 day and 1 week corresponds to synoptic-scale weather variability, such as the passage of fronts (MacIntyre et al., 2009). U_{10} and T_{air} also exhibit spectral density peaks at 1–3 weeks, which could be associated with persistent atmospheric blocking typical of the Scandinavian region (Tyrlis and Hoskins, 2008). While the temperature variability was concentrated at annual timescales, the wind speed varied primarily on timescales shorter than about a month.

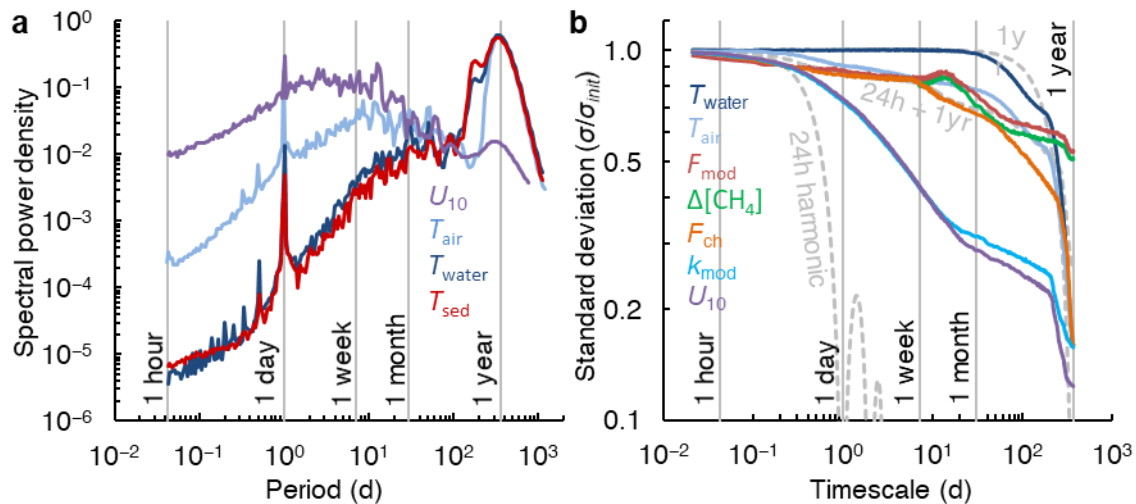
3.5 Timescale analysis

The spectral density plot (Fig. 8a) disentangles dominant timescales of variability of the drivers of the flux. The power spectra of wind speed and temperature peaked at periods of 1 day and 1 year, following well-known diel and annual cycles of insolation and seasonal variations in climate (Baldocchi et al., 2001). The diel spectral peak was subdued for the surface sediment temperature. For U_{10} , the overall spectral density maximum between 1 day and 1 week, and somewhat longer in spectra for the ice-free period only (Supplementary Fig. 4), corresponds to synoptic-scale weather variability, such as the passage of fronts (MacIntyre et al., 2009). U_{10} and T_{air} also exhibit spectral density peaks at 1–3 weeks, which could be associated with persistent atmospheric blocking typical of the Scandinavian region (Tyrlis and Hoskins, 2008). While the temperature variability was concentrated at annual timescales, the wind speed varied primarily on timescales shorter than about a month and often shorter than a week.

The climacogram (Fig. 8b) reveals that the variability of the chamber flux and the gas transfer velocity was enveloped by that of the water temperature and the wind speed, as was the surface concentration difference for timescales < 5 months. The distribution of variability over the different timescales is similar to that shown in the spectral density plot (Fig. 8a). The standard deviation of the water temperature did not change from its initial value ($\sigma/\sigma_{init} = 1$) until timescales of about 1 month, following the 1 year harmonic. In contrast, most of the variability of the wind speed was concentrated at time scales shorter than 1 month. The variability of the chamber and modelled fluxes first tracked that of the wind speed, but for timescales longer than about 1 month the decrease in variability resembled that of water temperature. The variability of the modelled fluxes followed that of the surface concentration difference rather than the gas transfer velocity. However, the coarse sampling resolution of the fluxes and concentrations may have led to an underestimation of both the variability at <1-week timescales (Fig. 7b) and the value of σ_{init} . Finally, the climacogram shows that k_{mod} retains about 72% of its variability at 24-hour timescales, which justifies our averaging over chamber deployment periods for comparison with k_{ch} and the computation of the model scaling parameter α' (Fig. 3).



885



886

887 **Figure 8** – Timescale analysis of the diffusive CH_4 flux and its drivers. **a**: Normalized spectral density of
 888 whole-year near-continuous timeseries of the air temperature (T_{air}), temperature of the
 889 temperature and ice (0.1–0.5 m, $T_{water/ice}$), temperature of the surface sediment in Mellersta Harrsjön (T_{sed})
 890 and the wind speed (U_{10}). **b**: Climacogram of the measured and modelled CH_4 flux (F_{ch} , F_{mod}), the air and
 891 surface water temperature (T_{air} , T_{water}), water-air concentration difference ($\Delta[\text{CH}_4]$), modelled gas transfer
 892 velocity (k_{mod}) and the wind speed (U_{10}) during the ice-free seasons of 2009–2017. Dashed, light-grey
 893 curves represent (combinations of) trigonometric functions of mean 0 and amplitude 1 with a specified
 894 period. 24h and 1yr harmonic functions were continuous over the dataset period while the 24h + 1yr
 895 harmonic was limited to periods when chamber flux data were available.

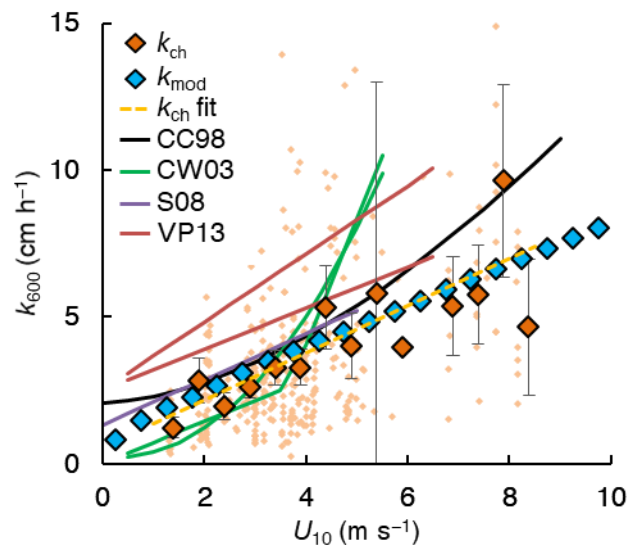
896 Panel a is based on continuous timeseries that include the ice-cover seasons: Supplementary Figure 4
897 shows spectral density plots for individual ice-free seasons.

898 4. Discussion

899 4.1 Magnitudes of fluxes and gas transfer velocities

900 Overall, diffusive CH₄ emissions from the Stordalen Mire lakes ($6.9 \pm 0.3 \text{ mg m}^{-2} \text{ d}^{-1}$, mean \pm 95% CI) were
901 lower than the average of postglacial lakes north of 50°N, but within the interquartile range (mean 12.5,
902 IQR 3.0–17.9 $\text{mg m}^{-2} \text{ d}^{-1}$, Wik et al., 2016b). Emissions are also at the lower end of the range for northern
903 lakes of similar size (0.01–0.2 km^2) (1–100 $\text{mg m}^{-2} \text{ d}^{-1}$, Wik et al., 2016b). As emissions of the Stordalen
904 Mire lakes do not appear to be limited by substrate quality or quantity (Wik et al., 2018), but strongly
905 depend on temperature (Fig. 4b), the difference is likely because a majority of flux measurements from
906 other postglacial lakes were conducted in the warmer, subarctic boreal zone. Boreal lake CH₄ emissions
907 are generally higher for lakes of similar size: 20–40 $\text{mg m}^{-2} \text{ d}^{-1}$ (binned means), $n = 91$ (Rasilo et al., 2015);
908 $\sim 12 \text{ mg m}^{-2} \text{ d}^{-1}$, $n = 72$ (Juutinen et al., 2009).

909
910 The gas transfer velocity in the Stordalen Mire lakes was similar to that predicted from wind-based models
911 of Cole and Caraco (1998) and Crusius and Wanninkhof (2003) at low wind speeds (Fig. 9). Both were based
912 on tracer experiments with sampling over several days, and thus, like our approach, are integrative
913 measures. The slope of the linear wind- k_{ch} relation (OLS: 0.81 ± 0.21 , slope \pm 95% CI, $R^2 = 0.20$ and $p < 0.01$
914 for the individual k_{ch} estimates (small orange rhombuses in Fig. 9)) was similar to that reported by Soumis
915 et al. (2008) (0.78 for a 0.06 km^2 lake), who also used a mass balance approach, and Vachon and Prairie
916 (2013) (0.70–1.16 for lakes 0.01–0.15 km^2). Part of the difference with the models of Vachon and Prairie
917 (2013), Cole and Caraco (1998) and Soumis et al. (2008) was caused by the offset at 0 wind speed, which
918 may stem from a larger contribution of the buoyancy flux in their lakes than we computed for our lakes
919 with the surface renewal model (Crill et al., 1988; Read et al., 2012) or from remnant wind shear turbulence
920 (MacIntyre et al., 2018). While fetch limitation can reduce gas transfer at high wind speeds in small lakes
921 (Vachon and Prairie, 2013; Wanninkhof, 1992), and the lakes studied here are at the low end of the size
922 spectrum of water bodies in which the gas transfer models in Fig. 9 were developed (Table S1), there are
923 a number of other explanations for the low values we obtained. We further discuss these in section 4.5
924 after evaluating drivers of fluxes.



936 **Figure 9** – Normalized gas transfer velocities (k_{600}) versus the wind speed at 10 m (U_{10}). Binned values
 937 (large rhombuses, k_{ch} and k_{mod} , bin size = 0.5 m s^{-1}) and individual observations (small rhombuses, k_{ch}) from
 938 floating chambers (k_{ch}) and the surface renewal model (k_{mod} with $\alpha' = 0.23$). Error bars represent 95%
 939 confidence intervals of the binned means. Solid lines represent models from the literature: Cole and
 940 Caraco (1998) (CC98), Crusius and Wanninkhof (2003) (bilinear and power law models) (CW03), Soumis et
 941 al. (2008) (S08) and Vachon and Prairie (2013) (VP13) for lake surface areas of 0.01 and 0.15 km^2 .
 942 Supplementary Table 1 lists the model equations and calibration ranges. A power-law regression model is
 943 shown for the individual k_{ch} datapoints ($n = 334$): $k_{600} = 0.77 \times U_{10}^{1.02} + 0.62$ (dashed yellow line).

4.2 Drivers of flux

Methane emitted from lakes in wetland environments can be produced in situ, or be transported in from the surrounding landscape (Paytan et al., 2015). The distinction is important because some controls on terrestrial methane production, such as water table depth (Brown et al., 2014), are irrelevant in lakes. In the Stordalen Mire lakes, the Arrhenius-type relation of CH₄ fluxes and concentrations (Fig. 4b,f) together with short CH₄ residence times (Fig. 6) suggest that efficient redistribution of dissolved CH₄ strongly coupled emissions to sediment methane production. High CH₄ concentrations in the stream (section 3.4) further suggest that external inputs of CH₄ — produced in the fens and transported into the stream with surface runoff, or produced in stream sediments — may have elevated emissions in Mellersta Harrsjön (Lundin et al., 2013). However, although the Mire exports substantial quantities of DOC and presumably CH₄ from the water-logged fens to the lakes (Olefeldt and Roulet, 2012), after rainy periods we observed either a decrease in Δ[CH₄] (13–19 July 2017, Fig. 5) or no significant change (3–6 July and 21–27 August 2017, Fig. 5). It remains unclear whether such reduced storage resulted from lower methanogenesis rates associated with the temperature drop after rainfall, convection-induced degassing, or lake water displacement or dilution by surface runoff.

Turbulent transfer was dominated by wind shear in the Stordalen Mire lakes, and we computed a minor contribution (~8%) of the buoyancy-controlled fraction of k . Our result differs from that in Read et al. (2012) who found that buoyancy flux dominated turbulence production in temperate lakes 0.1 km² in size and smaller. For the Stordalen lakes we computed higher ice-free season mean values of u_{*w} , as well as lower values of the water-side vertical friction velocity, $w_{*w} = (\beta z_{mix})^{1/3}$, (1.2–1.8 mm s⁻¹) than they report (2.0–7.5 mm s⁻¹, $n = 40$ lakes). The difference here results from high wind speeds and often colder surface waters compared to many temperate lakes. Therefore, values of sensible and latent heat fluxes are lower in our lakes than in lakes in warmer regions. Many small lakes have low wind speeds particularly at night. Consequently, the temperate lakes surveyed in Read et al. (2012), will have a larger contribution of buoyancy flux to the gas transfer coefficient at night (MacIntyre and Melack, 2009). The contribution of convection also depends on the wind-sheltering properties of the landscape surrounding the lake (Kankaala et al., 2013; Markfort et al., 2010). Depending on the turbulence environment, the buoyancy flux is thus weighed differently in parameterizations of ϵ (Heiskanen et al., 2014; Tedford et al., 2014) and in wind-based models (offsets at $U_{10} = 0$ in Fig. 9), contributing to significant differences between model realizations of k (Dugan et al., 2016; Erkkilä et al., 2018; Schilder et al., 2016).

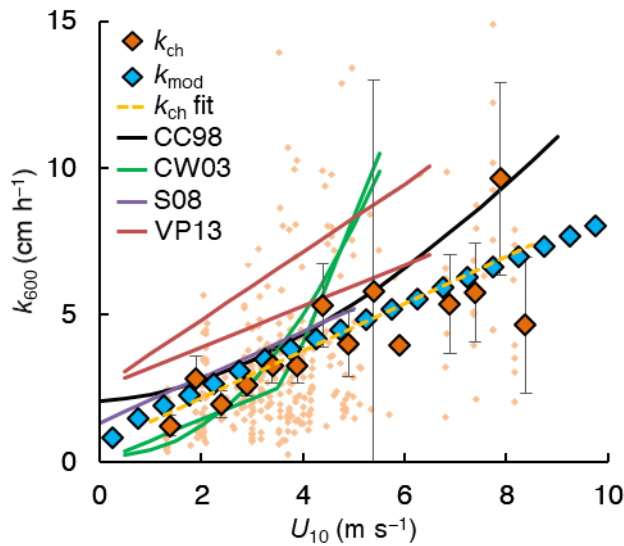
The distinct spectral peaks of temperature and U_{10} (Fig. 8) indicate that flux dependencies on these parameters (Fig. 4b,c) acted on different timescales. **4.1 Magnitude**

Overall, diffusive emissions were lower than the average of postglacial lakes north of 50°N, but within the interquartile range (12.5, 3.0–17.9 mg m⁻² d⁻¹, Wik et al., 2016b). Emissions are also on the lower end of the range for northern lakes of similar size (0.01–0.2 km²) (1–100 mg m⁻² d⁻¹, Wik et al., 2016b). As emissions of the Stordalen lakes do not appear to be limited by substrate quality or quantity (Wik et al., 2018) this difference has implications for the choice of models or proxies of the flux in predictive analyses. For lakes that mix frequently and a climatology similar to that of the Stordalen Mire (Malmer et al., 2005), temperature-based proxies (e.g. Thornton et al., 2015) would resolve most of the variability of the ice-free diffusive CH₄ flux at timescales longer than a month. Advanced gas transfer models that account for

986 atmospheric stability and rapid variations in wind shear, such as we have used here, allowed us to resolve
987 variability in flux at timescales shorter than about a month. Our results are representative of small, wind-
988 exposed lakes in cold environments, where, as a result of considerable wind driven mixing, fluxes are lower
989 than would be predicted in lakes where buoyancy fluxes during heating and cooling are higher.
990 ~~, but strongly depend on temperature (Fig. 4b), the difference is likely because a majority of flux~~
991 ~~measurements from other postglacial lakes were conducted in the warmer, subarctic boreal zone. Boreal~~
992 ~~lake CH₄ emissions are generally higher for lakes of similar size: 20–40 mg m⁻² d⁻¹ (binned means), n = 91~~
993 ~~(Rasilo et al., 2015); ~12 mg m⁻² d⁻¹, n = 72 (Juutinen et al., 2009).~~

994
995 The gas transfer velocity in the Stordalen lakes was similar to Cole and Caraco (1998) and Crusius and
996 Wanninkhof (2003) at low wind speeds, both of which were based on tracer experiments with sampling
997 over several days, and thus, like our approach, are integrative measures (Fig. 9). At higher winds we
998 obtain lower k values by nearly a factor of 2 (Table S1). The slope of the linear wind- k_{CH_4} relation (OLS:
999 0.81 ± 0.21 , slope \pm 95% CI, dashed yellow line in Fig. 9) was similar to that reported by Soumis et al.
1000 (2008) (0.78 for a 0.06 km² lake), who also used a mass balance approach, and Vachon and Prairie (2013)
1001 (0.70–1.16 for lakes 0.01–0.15 km²). Part of the difference with literature models was caused by the
1002 offset at 0 wind speed, which may stem from a larger contribution of the buoyancy flux (Crill et al., 1988;
1003 Read et al., 2012) or from remnant wind shear turbulence (MacIntyre et al., 2018). Another explanation
1004 may be the damping of turbulence by near surface stratification (MacIntyre et al., 2010, 2018), ~~however,~~
1005 ~~such stratification was intermittent in our study (Fig. 5f–h).~~ It may also result from our typically having a
1006 stable atmosphere in the day for much of the summer which reduces momentum transfer to the water
1007 surface. While our calculations take atmospheric stability into account, work on modelling momentum
1008 flux and related drag coefficients under stable atmospheres is ongoing and may lead to lower dissipation
1009 rates than we compute (Grachev et al., 2013). Due to the large spread of the chamber derived gas
1010 transfer velocities (small rhombuses, Fig. 9) a power-law exponent to U_{10} (1.0 ± 0.8 ; exponent and 95% CI)
1011 and thus the nature of the wind- k relation could not be determined with confidence.

1012
 1013
 1014
 1015
 1016
 1017
 1018
 1019
 1020
 1021
 1022
 1023
 1024
 1025
 1026
 1027
 1028
 1029
 1030
 1031



~~Figure 9 Normalized gas transfer velocities (k_{600}) versus the wind speed at 10 m (U_{10}). Binned values (large rhombuses) and individual observations (small rhombuses) from floating chambers (k_{ch}) and the surface renewal model (k_{mod} with $\alpha' = 0.24$). Error bars represent 95% confidence intervals of the binned means. Solid lines represent models from the literature: Cole and Caraco (1998), Crusius and Wanninkhof (2003) (bilinear and power law models), Soumis et al. (2008) and Vachon and Prairie (2013) for lake surface areas of 0.01 and 0.15 km². Supplementary Table 1 lists the model equations and calibration ranges. A linear regression model is shown for the k_{ch} data (dashed yellow line): $k_{600} = 0.8_{-0.6}^{+1.0} \times U_{10} + 0.6_{-0.2}^{+1.3}$ (sub- and superscripts denote 95% confidence intervals), with $R^2 = 0.20$ for individual chamber values (small orange rhombuses) and $R^2 = 0.64$ for the binned means (large orange rhombuses).~~

4.2 Drivers of the flux

the Arrhenius-type relation of CH_4 fluxes and concentrations (Fig. 4b,f) together with short CH_4 residence times (Fig. 6) suggest that emissions from the Stordalen lakes were strongly coupled to sediment production through efficient redistribution of dissolved CH_4 . High CH_4 concentrations in the stream suggest that terrestrial inputs of CH_4 may have elevated emissions in Mellersta Harrsjön (Lundin et al., 2013; Paytan et al., 2015). Similarly, terrestrial inputs of nutrients may have indirectly enhanced emissions in the littoral zones by supporting production of autochthonous organic substrates (Davidson et al., 2018; Rantala et al., 2016). However, although the Mire exports substantial quantities of DOC and presumably CH_4 from the water-logged fens to the lakes (Olefeldt and Roulet, 2012), after cold and rainy periods we observed either a decrease in $\Delta[\text{CH}_4]$ (13–19 July 2017, Fig. 5) or no significant change (3–6 July and 21–27 August 2017, Fig. 5). It remains unclear whether such reduced storage resulted from lower methanogenesis rates, convection-induced degassing or lake water displacement by surface runoff.

Turbulent transfer was dominated by wind shear in the Stordalen lakes. We computed a minor contribution ($\sim 8\%$) of the buoyancy-controlled fraction of k ($k_{600,\beta} = 0.3 \text{ cm h}^{-1}$) (ice-free season mean, 2009–2017). Our results differ from that in Read et al. (2012) who expect a dominant role of convection to k in small lakes. The difference here results from low values of sensible and latent heat fluxes due to colder temperatures during summer such that net long-wave radiation was often less than 50 W m^{-2} . Lakes in warmer regions with lower humidity and clearer skies and low wind speeds particularly at night will have a larger contribution of buoyancy flux to the gas transfer coefficient (MacIntyre and Melack, 2009). The contribution of convection also depends on the wind-sheltering properties of the landscape surrounding the lake (Kankaala et al., 2013; Markfort et al., 2010). Depending on the turbulence environment the buoyancy flux is thus weighed differently in parameterizations of ϵ (Heiskanen et al., 2014; Tedford et al., 2014) and in wind-based models (offsets at $U_{10} = 0$ in Fig. 9), contributing to significant differences between model realizations of k (Dugan et al., 2016; Erkkilä et al., 2018; Schilder et al., 2016). We expect our results to be representative of small, wind-exposed lakes in cold environments.

4.3 Storage and stability

The robust temperature-sensitivity of lake methane emissions (Fig. 4b,f) (Wik et al., 2014; Yvon-Durocher et al., 2014) is driven by biotic and abiotic mechanisms. Lake mixing regime can modulate flux-temperature relationshipsrelations by periodically decoupling production from emission rates (e.g. Yvon-Durocher et al., 2014). Enhanced(Engle and Melack, 2000). Here, enhanced CH_4 accumulation during periods of stratification may have contributed to concentration and storage maxima in July and August (Fig. 4e, 6d). However, as the CH_4 residence time was invariant over the season and with temperature (Fig. 6a,b), the storage-temperature relation (Fig. 6e) likely reflects rate changes in sediment methanogenesis rather than inhibited mixing. For example, the highest CH_4 concentrations in our dataset ($59.1 \pm 26.4 \text{ mg m}^{-3}$, $n = 37$) were measured during a period with exceptionally high surface water temperatures ($T_{\text{water}} = 18.5 \pm 3.6 \text{ }^\circ\text{C}$) that lasted from 23 June to 30 July 2014. Emissions during this period comprised 29%–56% (depending on lake) of the 2014 ice-free diffusive flux, while the peak quantity of accumulated CH_4 wascomprised <5%. Two mechanisms may explain the lack of CH_4 accumulation. First, stratification was frequently disrupted

1074 by vertical mixing (Fig. 5g-h) and concurrent hypolimnetic CH₄ concentrations were not significantly
1075 different from (Inre Harrsjön, 2010–2017, paired t-test, $p = 0.12$, $n = 32$) or lower than (Mellersta Harrsjön,
1076 2010–2017, paired t-test, $p < 0.01$, $n = 35$) those in the surface mixed layer. Second, stratification often
1077 was not strong enough to affect gas transfer velocities (~~$N > 25$ during $< 17\%$ of this period~~). Even when
1078 assuming ϵ was suppressed by an order of magnitude for $N > 25$ and by two orders of magnitude for $N > 40$
1079 (~~MacIntyre et al., 2018~~)(MacIntyre et al., 2018), k_{mod} was only slightly lower (2.8 cm h^{-1}) than the multi-
1080 year mean (3.0 cm h^{-1}). Thus, in weakly stratified, ~~polymictic~~ lakes with strong wind mixing, the
1081 temperature sensitivity of diffusive CH₄ emissions may be observed without significant modulation by
1082 stratification.

1083
1084 ~~The water-air concentration difference~~ Degassing (Fig. 4c,g) prevented an unlimited increase of the
1085 emission rate with the gas transfer velocity. In this way, $\Delta[\text{CH}_4]$ acted as a negative feedback that
1086 maintained a quasi-steady state between CH₄ production and removal processes throughout the ice-free
1087 season. In other words, higher temperatures led to elevated CH₄ concentrations (Fig. 4f) which in turn
1088 increased emission rates (Eq. 1, Fig. 4b). However, in contrast to the temperature-binned fluxes, when
1089 binned by wind speed high emission rates were associated with low concentrations (Fig. 4c,g). In this way
1090 the $\Delta[\text{CH}_4]$ feedback limited the increase of the emission rate with the gas transfer velocity. In all three
1091 lakes CH₄ residence times were inversely proportional to the wind speed (Fig. 6c), indicating an imbalance
1092 between production and removal processes. We hypothesize that the imbalance exists because the
1093 variability of wind speed peaked on shorter timescales than that of the water temperature (Fig. 8a).
1094 Changes in wind shear periodically pushed the system out of production-emission equilibrium, allowing
1095 for transient degassing and accumulation of dissolved CH₄. The temporal variability of dissolved gas
1096 concentrations is likely higher in shallow wind-exposed systems with limited buffer capacity (~~Natchimuthu~~
1097 ~~et al., 2016, 2017~~)(Natchimuthu et al., 2016, 2017), and should be taken into account when applying gas
1098 transfer models to small lakes and ponds.

1099
1100 Rapid degassing occurred at $U_{10} \geq 6.5 \text{ m s}^{-1}$ (Fig. 4c, ~~mean wind speed during chamber deployments~~).
1101 Gas fluxes at high wind speeds may have been enhanced by the kinetic action of breaking waves (~~Ferray~~
1102 ~~et al., 1996~~)(Ferray et al., 1996) or through microbubble-mediated transfer. Wave breaking was observed
1103 on the Stordalen lakes at wind speeds $\geq 7 \text{ m s}^{-1}$. Microbubbles of atmospheric gas (diameter $< 1 \text{ mm}$) can
1104 form due to photosynthesis, rain or wave breaking (~~Woolf and Thorpe, 1991~~)(Woolf and Thorpe, 1991)
1105 and remain entrained for several days (~~Turner, 1961~~)(Turner, 1961). Due to their relatively large surface
1106 area they quickly equilibrate with sparingly soluble gases in the water column, providing an efficient
1107 emission pathway to the atmosphere when the bubbles rise to the surface (~~Merlivat and Memery,~~
1108 ~~1983~~)(Merlivat and Memery, 1983). In inland waters microbubble emissions of CH₄ have only been
1109 indirectly inferred from differences in CO₂ and CH₄ gas transfer velocities (McGinnis et al., 2015; Prairie
1110 and del Giorgio, 2013), and more work is needed to evaluate their significance in relatively sheltered
1111 systems.

1112 1113 **4.4 Timescales of variability**

1114 Overall, the short-term variability of the flux due to wind speed ($1.1\text{--}13.2 \text{ mg m}^{-2} \text{ d}^{-1}$) was similar to the
1115 long-term variability due to temperature ($0.7\text{--}12.2 \text{ mg m}^{-2} \text{ d}^{-1}$) (ranges of the binned means, Fig. 4b-c).

1116 The diel patterns in the mixed layer depth (Fig. 5) and the gas transfer velocity (Fig. 7d) and daytime
1117 variation of the surface concentration (Fig. 7b) were indicative of daily storage-and-release cycles,
1118 resulting in a model flux difference of about 5 mg m⁻² d⁻¹ between morning and afternoon; about half the
1119 mean seasonal range (Fig. 7a). Diel variability of lake methane fluxes has been observed at Villasjön (eddy
1120 covariance, Jammet et al., 2017) and elsewhere (Bastviken et al., 2004, 2010; Crill et al., 1988; Erkkilä et
1121 al., 2018; Eugster et al., 2011; Hamilton et al., 1994; Podgrajsek et al., 2014). Similarly, diel patterns in the
1122 gas transfer velocity have been observed with the eddy covariance technique (Podgrajsek et al., 2015) and
1123 in model studies (Erkkilä et al., 2018). Apparent offsets between the diurnal peaks of the flux, surface
1124 concentrations and drivers (Fig 7b,d) have been noted previously (Koebsch et al., 2015), but have yet to
1125 be explained. Continuous eddy covariance measurements in lakes where the dominant emission pathway
1126 is turbulence-driven diffusion could help characterize flux variability on short timescales (e.g. Bartosiewicz
1127 et al., 2015).

1128
1129 The CH₄ residence times (1–3 days) were not much longer than the diel timescale of vertical mixing (Fig.
1130 5g,h). As a result, horizontal concentration gradients developed in the deeper lakes (Table 2). The 23 ±
1131 11% concentration difference between depth zones in the deeper lakes (mean ± 95%) fits transport model
1132 predictions of DelSontro et al. (2017) for small lakes (< 1 km²) that highlight the role of outgassing and
1133 oxidation during transport from production zones in the shallow littoral zones or the deeper sediments
1134 (Hofmann, 2013). Concentration gradients may also have been caused by physical processes, such as
1135 upwelling due to thermocline tilting (Heiskanen et al., 2014). Higher resolution measurements, for
1136 example with automated equilibration systems (Erkkilä et al., 2018; Natchimuthu et al., 2016), are needed
1137 to assess how much of the spatial and diel patterns of the CH₄ concentration can be explained by physical
1138 drivers such as gas transfer and mixed layer deepening (Eugster et al., 2003; Vachon et al., 2019), or by
1139 biological processes such as methanogenesis and microbial oxidation (Ford et al., 2002).

1140
1141 Gas transfer models can only deliver accurate fluxes if they are combined with measurements that capture
1142 the full spatiotemporal variability of the surface concentration (Erkkilä et al., 2018; Hofmann, 2013;
1143 Natchimuthu et al., 2016; Schilder et al., 2016). The short CH₄ residence times and diel pattern of Δ[CH₄]
1144 suggest that weekly sampling did not capture the full temporal variability of the surface concentrations.
1145 Especially after episodes of high wind speeds and lake degassing (Fig. 4c,g), concentrations may not have
1146 been representative of the 24-hour chamber deployment period.

1147 Overall, the short-term variability of the flux due to wind speed was similar to the long-term variability due
1148 to temperature (ranges of the binned means, Fig. 4a-c). The diel patterns in the mixing depth (Fig. 4.5-5)
1149 and the gas transfer velocity (Fig. 7d) and daytime variation of the surface concentration (Fig. 7b) were
1150 indicative of daily storage and release cycles, resulting in a model flux difference of about $5 \text{ mg m}^{-2} \text{ d}^{-1}$
1151 between morning and afternoon; about half the mean seasonal range (Fig. 7a). Diel variability of lake
1152 methane fluxes has been observed at Villasjön (eddy covariance, Jammet et al., 2017) and elsewhere
1153 (Bastviken et al., 2004, 2010; Crill et al., 1988; Erkkilä et al., 2018; Eugster et al., 2011; Hamilton et al.,
1154 1994; Podgrajsek et al., 2014b). Similarly, diel patterns in the gas transfer velocity have been observed
1155 with the eddy covariance technique (Podgrajsek et al., 2015) and in model studies (Erkkilä et al., 2018).
1156 Apparent offsets between the diurnal peaks of the flux, surface concentrations and drivers (Fig 7b,d) have
1157 been noted previously (Koebsch et al., 2015), but have yet to be explained. Continuous eddy covariance
1158 measurements in lakes where the dominant emission pathway is turbulence driven diffusion could help
1159 characterize flux variability on short timescales (e.g. Bartosiewicz et al., 2015).

1160
1161 The CH_4 residence times (1–3 days) were not much longer than the diel timescale of vertical mixing (Fig.
1162 5g,h). As a result, horizontal concentration gradients developed in the deeper lakes (Table 2). The $23 \pm$
1163 11% concentration difference between depth zones in the deeper lakes (mean \pm 95%) fits transport
1164 model predictions of DelSontro et al. (2017) for small lakes ($< 1 \text{ km}^2$) that highlight the role of outgassing
1165 and oxidation during transport from production zones in the shallow littoral zones or the deeper
1166 sediments (Hofmann, 2013). Concentration gradients may also have been caused by physical processes,
1167 such as upwelling due to thermocline tilting (Heiskanen et al., 2014). Higher resolution measurements,
1168 for example with automated equilibration systems (Erkkilä et al., 2018; Natchimuthu et al., 2016), are
1169 needed to assess how much of the spatial and diel patterns of the CH_4 concentration can be explained by
1170 physical drivers such as gas transfer and mixed layer deepening (Eugster et al., 2003; Vachon et al.,
1171 2019), or by biological processes such as methanogenesis and microbial oxidation (Ford et al., 2002).

1172
1173 The distinct spectral peaks of U_{10} and temperature (Fig. 8) suggest that flux dependencies on these
1174 parameters (Fig. 4b,c) acted on different timescales. This has implications for the choice of models or
1175 proxies of the flux in predictive analyses. For polymictic lakes and a climatology similar to that of the
1176 Stordalen Mire (Malmer et al., 2005), temperature based proxies (e.g. Thornton et al., 2015) would resolve
1177 most of the variability of the ice-free diffusive CH_4 flux at timescales longer than a month. Advanced gas
1178 transfer models that account for atmospheric stability and rapid variations in wind shear are necessary to
1179 resolve the flux variability at timescales shorter than about a month. However, gas transfer models can
1180 only deliver accurate fluxes if they are combined with measurements that capture the full spatiotemporal
1181 variability of the surface concentration (Erkkilä et al., 2018; Hofmann, 2013; Natchimuthu et al., 2016;
1182 Schilder et al., 2016). The short CH_4 residence times and diel pattern of $\Delta[\text{CH}_4]$ suggest that weekly
1183 sampling did not capture the full temporal variability of the surface concentrations. Especially after
1184 episodes of high wind speeds and lake degassing (Fig. 4c,g), concentrations may not have been
1185 representative of the 24-hour chamber deployment period.

4.6 Model-chamber comparison

It is fundamental to our understanding of controls on fluxes to determine why empirically derived values of the model scaling parameter α' are relatively low in this study (0.17–0.31) compared to the theoretical value of $\sqrt{2/15} \cong 0.37$ (Katul et al., 2018), and why they were different in the three lakes. Differences in α' resulted from k_{ch} , with mean (\pm 95% CI) values estimated at 3.5 ± 0.7 ($n = 74$), 3.1 ± 0.4 ($n = 131$) and 2.5 ± 0.6 ($n = 142$) cm h^{-1} in Villasjön, Inre Harrsjön and Mellersta Harrsjön, respectively, while k_{mod} did not differ significantly between lakes (ANOVA, $p < 0.001$). Synthesis studies show that scaling parameter values can vary between 0.1 and 0.7 over the range of moderate to high dissipation rates computed for the Stordalen Mire lakes (Eq. 5: $\epsilon = 10^{-7}$ – 10^{-5} $\text{m}^2 \text{s}^{-3}$) (Esters et al., 2017; Wang et al., 2015 and references therein). In such cases ϵ has been measured directly with acoustic Doppler- or particle image velocimetry and compared with independent estimates of k using chambers (Gålfalk et al., 2013; Tokoro et al., 2008; Vachon et al., 2010; Wang et al., 2015), eddy covariance observations (Heiskanen et al., 2014) or the gradient flux technique (Zappa et al., 2007) and a sparingly soluble tracer, such as CO_2 or SF_6 . Measured and modelled lake CO_2 fluxes agree reasonably well if Eq. 4 and Eq. 5 are used with a multi-study mean α' of 0.5 (Bartosiewicz et al., 2015; Czikowsky et al., 2018; Erkkilä et al., 2018; Mammarella et al., 2015), but the agreement is less clear for CH_4 fluxes (Bartosiewicz et al., 2015). The observed variability in α' could be explained by chemical or biological factors that limit surface exchange, or by the variable contributions of wind sheltering, atmospheric stability, and within lake stratification and mixing. Here, the low α' value may imply an underestimation of k derived from chamber observations or an overestimation of dissipation rates used in the modelling of gas transfer velocities.

An underestimation of chamber-derived gas transfer velocities may have resulted from an overestimation of C_{aq} in Equation 1. In most freshwater systems a significant fraction of CH_4 is removed through microbial oxidation (Bastviken et al., 2002). This additional removal process invalidates the implicit assumption in Eq. 1 and 2 that all dissolved CH_4 that we measure in the surface water is emitted to the atmosphere. Omitting oxidation would bias $\Delta[\text{CH}_4]$ high, and k_{ch} low. The Stordalen Mire lakes remained oxygenated throughout the ice-free season and CH_4 stable isotopes indicate that between 24% (Villasjön) and 60% (Inre and Mellersta Harrsjön) of CH_4 in the water column was continually oxidized (Jansen et al., 2019). This may explain not only the low scaling parameter value compared to those found with other tracers, but also why α' was higher in Villasjön (0.31, $n = 67$) than in the deeper lakes (0.17–0.25, $n = 267$) (Supplementary Fig. 1). However, more work is needed to establish how the oxidation effect partitioned between CH_4 reservoirs in the water column, where it would affect surface emissions, and the sediment.

An increase in surface concentrations which typically occurs at night would not have been manifest (Crill et al., 1988; Czikowsky et al., 2018) because there was, apart from the period just after ice-off in 2017, no significant CH_4 accumulation below the mixing layer throughout the ice-free seasons. Indeed, CH_4 concentrations within the 0.1–1 m surface layer of the deeper lakes (Table 2) were not significantly different from those at greater depth (Inre Harrsjön: 12.2 ± 2.7 mg m^{-3} , $n = 292$; Mellersta Harrsjön: 17.7 ± 4.9 mg m^{-3} , $n = 405$; means \pm 95% CI).

An overestimation of gas transfer velocities computed with the surface renewal model may result if actual dissipation rates are lower than we compute. Such occurs under high wind shear when more of the introduced turbulent kinetic energy is used for mixing the water column and deepening the mixing layer,

1228 and less is dissipated (Ivey and Imberger, 1991; Jonas et al., 2003). When this occurs, the coefficient on
1229 u_*w^3 in Eq. 5 may have a lower value (Tedford et al., 2014), which translates to a reduced estimate of ϵ and
1230 increased α' values. A similar decrease of ϵ can be assumed during heating, when strong stratification ($N >$
1231 25 cph) dampens turbulent dissipation (MacIntyre et al., 2010, 2018), however, such stratification was
1232 intermittent in our study (Fig. 5f-h). Comparing gas transfer velocities from the floating chambers and the
1233 surface renewal model we find a scaling parameter value (α' in Eq. 4) of approximately 0.24 (Fig. 3). Its
1234 theoretical value (α) is $\sqrt{2/15} \cong 0.37$ (Katul et al., 2018) but empirically derived values (α') can vary
1235 between 0.1 and 0.7 over the range of moderate to high dissipation rates computed for the Stordalen
1236 lakes (Eq. 5: $\epsilon = 10^{-7} - 10^{-5} \text{ m}^2 \text{ s}^{-3}$) (Esters et al., 2017; Wang et al., 2015 and references therein), when ϵ is
1237 measured directly with acoustic Doppler- or particle image velocimetry and compared with independent
1238 estimates of k using chambers (Gålfalk et al., 2013; Tokoro et al., 2008; Vachon et al., 2010; Wang et al.,
1239 2015), eddy covariance observations (Heiskanen et al., 2014) or the gradient flux technique (Zappa et al.,
1240 2007) and a sparingly soluble tracer, such as CO_2 or SF_6 . Recent studies report a reasonable agreement
1241 between measured and modeled lake CO_2 fluxes if Eq.

1242
1243 Reduced gas transfer velocities and between-lake differences in k_{ch} could also be due to differences in
1244 atmospheric forcing. First, the wind speed may have been lower over the lakes than on the Mire due to
1245 the slight elevation (<1 m) of the surrounding peatland hummocks (Markfort et al., 2010). The wind-
1246 sheltering effect of tall shrubs (*Betula nana* L, Malmer et al., 2005) on the shores of the deeper lakes (Fig.
1247 1) was readily noticed during sample collection, particularly in Mellersta Harrsjön. Second, atmospheric
1248 stability was different over the three lakes. The atmosphere was stable ($z/L_{MO,0} > 0$) over Mellersta
1249 Harrsjön, Inre Harrsjön, and Villasjön during 29%, 21% and 22% of the ice free periods (2009–2017),
1250 respectively, with drag coefficients $\sim 16\%$ lower than their neutral value during these times. The effect was
1251 more pronounced when winds were light during daytime heating, with somewhat higher frequency during
1252 autumn. Colder incoming stream water flowing into Mellersta Harrsjön may have contributed to lower
1253 surface water temperatures in this lake (Table 3), with the discrepancy more noticeable as lake level rose
1254 (Fig. 5e-h). More frequent periods with a stable atmosphere above Mellersta Harrsjön reduced sensible
1255 and latent heat fluxes and are a likely cause of the increased stratification of the surface layer: water at
1256 0.1 m was sometimes 0.5 °C to 2 °C warmer than at 0.3 m in Mellersta Harrsjön (5% of the time during ice-
1257 free seasons) when temperatures were isothermal in the upper 0.5 m in Villasjön and Inre Harrsjön.
1258 Greater near-surface stratification coupled with lower winds than measured on the Mire would have led
1259 to the lower values of k and α' obtained in this lake. While this analysis points to the challenges in modelling
1260 fluxes when meteorological instrumentation is not situated on the lakes, it also suggests that a solution is
1261 to use lower values of α' when modelling k for sheltered water bodies.

1262
1263 In summary, the model scaling parameter α' computed in this study are lower than the theoretical value
1264 of 0.37 and the 0.5 recently obtained in eddy covariance studies in which fluxes were measured with CO_2
1265 and modelled. The discrepancy may be explained by surface CH_4 concentrations decreasing due to
1266 microbial oxidation over the same timescale as our chamber measurements. Alternate explanations take
1267 into account the magnitude of wind shear and degree of sheltering. Differences in α' between lakes
1268 indicate the care required in modelling emissions from sheltered lakes; the overall cooler surface water
1269 temperatures in the lake with greater stream inflows points to a new control on emissions. That is, when

1270 stream inflows lead to surface water temperatures cooler than air temperature in sheltered lakes, a stable
1271 atmosphere results which leads to a reduced momentum flux, lower emissions, and a longer time over
1272 which methane oxidation can occur. The cooling effect may be especially pronounced in northern
1273 landscapes underlain by permafrost, where the temperature of meltwater streams and subsurface flow in
1274 the active layer remains low throughout the year. Thus, these comparisons of modelled and measured
1275 fluxes point to new areas of research.

~~4 and Eq. 5 are used with a multi-study mean α' of 0.5 (Bartosiewicz et al., 2015; Czikowsky et al., 2018; Erkkilä et al., 2018; Mammarella et al., 2015). While there is evidence for similar agreement for CH₄ with $\alpha' = 0.5$ (Erkkilä et al., 2018), this approach may exceed chamber-derived emissions by a factor of 2 (Bartosiewicz et al., 2015) — i.e. closer to our scaling parameter value of 0.24.~~

~~Because the physical drivers of gas exchange have been accounted for in the formulation of k_{mod} , chemical or biological factors that do not affect turbulence in the actively mixed layer but can limit surface exchange could be responsible for the observed variability in α' . In most freshwater systems a significant fraction of CH₄ is removed through microbial oxidation at the sediment surface and in the water column (Bastviken et al., 2002). The Stordalen lakes remained oxygenated throughout the ice-free season and CH₄ stable isotopes indicate that between 24% (Villasjön) and 60% (Inre and Mellersta Harrsjön) of CH₄ in the water column was oxidized (Jansen et al., 2019). This may explain not only the low scaling parameter value compared to those found with other tracers, but also why α' was higher in Villasjön (0.31, $n = 67$) than in the deeper lakes (0.17–0.25, $n = 267$). However, more work is needed to establish how the oxidation effect partitioned between CH₄ reservoirs in the water column, where it would affect surface emissions, and the sediment. Other biogenic factors may also have impacted gas transfer, such as organic surface slicks in the 10–100 μm diffusive sublayer (Tokoro et al., 2008). Additionally, the wind speed may have been lower over the lakes than on the Mire due to the slight elevation (<1 m) of the surrounding peatland hummocks and the wind-sheltering effect of tall shrubs (*Betula nana* L, Malmer et al., 2005) on the shores of the deeper lakes (Fig. 1) (Markfort et al., 2010).~~

4.7 Omitted fluxes?

~~We investigated whether our chamber measurements may have missed high-quantity release from storage (Podgrajsek et al., 2014a). In stratified lakes mixed layer deepening can bring up accumulated gas, resulting in elevated surface fluxes, for example due to night time convection (Eugster et al., 2003), during autumn overturns (Encinas Fernández et al., 2014; Juutinen et al., 2009; Laurion et al., 2010; López Bellido et al., 2009) or rain events (Bartosiewicz et al., 2015; Ojala et al., 2011). Here however, >80% of the lakes' volume mixed on diel timescales and we did not observe substantial CH₄ accumulation over summer. Indeed, CH₄ concentrations within the 0.1–1 m surface layer of the deeper lakes (Table 2) were not significantly different from those at greater depth (Inre Harrsjön: $12.2 \pm 2.7 \text{ mg m}^{-3}$, $n = 292$; Mellersta Harrsjön: $17.7 \pm 4.9 \text{ mg m}^{-3}$, $n = 405$; means \pm 95% CI). It is therefore unlikely that our chamber fluxes omitted emissions from hypolimnetic storage.~~

5. Summary and conclusions

In this study we combined a unique, multi-year dataset with a modelling approach to better understand environmental controls on turbulence-driven diffusion-limited CH₄ emissions from small, shallow lakes. Floating chambers estimated the seasonal mean flux at $6.9 \text{ mg m}^{-2} \text{ d}^{-1}$ and illustrated how the flux depended on temperature and wind speed. Wind shear controlled the gas transfer velocity while thermal convection and release from storage were minor drivers of the flux. CH₄ fluxes and surface concentrations fitted an Arrhenius-type temperature function ($E_a' = 0.88\text{--}0.97 \text{ eV}$), suggesting that emissions were strongly coupled to rates of methanogenesis in the sediment. However, temperature was only an accurate proxy of the flux on averaging timescales longer than a month. On shorter timescales wind-induced variability in the gas transfer velocity, mixed mixing layer depth, and storage decoupled production from

1318 emission rates. Transient stratification changes in the lake mixing regime allowed for periodic CH₄
1319 accumulation and resulted in an inverse relationship between wind speed and surface concentrations. In
1320 this way, the air-water concentration difference acted as a negative feedback to emissions and prevented
1321 complete degassing of the lakes, except at high wind speeds ($U_{10} \geq 6.5 \text{ m s}^{-1}$).
1322

1323 Freshwater flux studies are increasingly focused on understanding mechanisms and developing proxies for
1324 use in upscaling efforts and process-based models. ~~Our results show that the timescale of driver variability
1325 can inform the frequency of field measurements to yield representative datasets. Observations that
1326 capture the spatiotemporal variability of dissolved gas concentrations could help realize the potential of
1327 advanced gas transfer models to disentangle biogeochemical and physical flux drivers at half-hourly to
1328 interannual timescales. Linking model and field measurement approaches could uncover non-linear
1329 feedbacks, such as shallow lake degassing at high wind speeds, quantify biases associated with
1330 measurement timing and location, and constrain the applicability timescale of novel emission
1331 proxies. Simple temperature- or wind-based proxies can yield accurate flux estimates, but model
1332 parameters, such as E_g' and α' , must be calibrated to local conditions to reflect relevant biotic and abiotic
1333 processes at appropriate timescales. Our study highlights the importance of non-linear feedbacks, such as
1334 shallow lake degassing at high wind speeds, as well as microbial removal processes and the need to
1335 consider the timescale over which fluxes occur relative to the timescale over which CH₄ can be oxidized.
1336 Such biological removal processes may violate the fundamental assumption of gas transfer models that all
1337 gas measured in the surface mixing layer is emitted to the atmosphere. Advanced gas transfer models can
1338 only improve the accuracy of flux estimates if they are paired with observations that capture the
1339 meteorological conditions over the lake and the spatiotemporal variability of dissolved gas concentrations.
1340 Therefore, field measurements remain necessary to inform, calibrate and validate models. Our results
1341 indicate that the timescale of driver variability can inform the frequency of field measurements necessary
1342 to yield representative datasets for novel proxy development.~~

1343 **6. Data availability**

1344 Data are available at www.bolin.su.se/data/. ~~Surface renewal model code is available by contacting SM.~~

1345

1346 **7. Author contributions**

1347 JJ, MW and PC designed the study. Fieldwork and laboratory measurements were ~~guided~~conducted by JJ,
1348 JS and MW. SM ~~and AC~~ developed the surface renewal model code ~~-,~~ with contributions from AC. JJ
1349 performed the analyses and prepared the manuscript with contributions from BT, PC and SM.

1350

1351 **8. Competing interests**

1352 The authors declare that they have no conflict of interest.

1353

1354 **9. Acknowledgements**

1355 This work was funded by the Swedish Research Council (VR) with grants to P. Crill (#2007-4547 and #2013-
1356 5562) and by the U.S. National Science Foundation with Arctic Natural Sciences Grants #1204267 and
1357 #1737411 to S. MacIntyre. The collection of ICOS data was funded by the Swedish Research Council
1358 (#2015-06020). We thank the McGill University researchers (David Olefeldt, Silvie Harder and Nigel Roulet)
1359 for the data they provided from the carbon flux tower that was supported by the Natural Science and
1360 Engineering Research Council of Canada (~~#NSERC~~ RGPIN-2017-04059). We are grateful to D. Bastviken for
1361 validating our implementation of the chamber headspace equilibration model. We thank the staff at the
1362 Abisko Scientific Research Station (ANS) for logistic and technical support. Noah Jansen created the
1363 schematic of the floating chamber pair. We thank Carmody McCalley, Christoffer Hemmingsson, Emily
1364 Pickering-Pedersen, Erik Wik, Hanna Axén, Hedvig Öste, Jacqueline Amante, Jenny Gåling, Jóhannes West,
1365 Kaitlyn Steele, Kim Jäderstrand, Lina Hansson, Lise Johnsson, Livija Ginters, Mathilda Nyzell, Niklas Rakos,
1366 Oscar Bergkvist, Robert Holden, Tyler Logan and Ulf Swendsén for their help in the field.

1367

1368 **10. References**

- 1369 Baldocchi, D., Falge, E. and Wilson, K.: A spectral analysis of biosphere–atmosphere trace gas flux
1370 densities and meteorological variables across hour to multi-year time scales, *Agric. For. Meteorol.*,
1371 107(1), 1–27, doi:10.1016/S0168-1923(00)00228-8, 2001.
- 1372 Bartosiewicz, M., Laurion, I. and MacIntyre, S.: Greenhouse gas emission and storage in a small shallow
1373 lake, *Hydrobiologia*, 757(1), 101–115, doi:10.1007/s10750-015-2240-2, 2015.
- 1374 Bastviken, D., Ejlertsson, J. and Tranvik, L.: Measurement of Methane Oxidation in Lakes: A Comparison
1375 of Methods, *Environ. Sci. Technol.*, 36(15), 3354–3361, doi:10.1021/es010311p, 2002.
- 1376 Bastviken, D., Cole, J., Pace, M. and Tranvik, L.: Methane emissions from lakes: Dependence of lake
1377 characteristics, two regional assessments, and a global estimate, *Global Biogeochem. Cycles*, 18(4),
1378 doi:10.1029/2004GB002238, 2004.
- 1379 Bastviken, D., Santoro, A. L., Marotta, H., Pinho, L. Q., Calheiros, D. F., Crill, P. and Enrich-Prast, A.:
1380 Methane Emissions from Pantanal, South America, during the Low Water Season: Toward More
1381 Comprehensive Sampling, *Environ. Sci. Technol.*, 44(14), 5450–5455, doi:10.1021/es1005048, 2010.
- 1382 Bastviken, D., Tranvik, L. J., Downing, J. A., Crill, P. M. and Enrich-Prast, A.: Freshwater Methane
1383 Emissions Offset the Continental Carbon Sink, *Science (80-.)*, 331(6013), 50–50,
1384 doi:10.1126/science.1196808, 2011.
- 1385 Borrel, G., Jézéquel, D., Biderre-Petit, C., Morel-Desrosiers, N., Morel, J.-P., Peyret, P., Fonty, G. and
1386 Lehours, A.-C.: Production and consumption of methane in freshwater lake ecosystems, *Res. Microbiol.*,
1387 162(9), 832–847, doi:10.1016/j.resmic.2011.06.004, 2011.
- 1388 [Brown, M. G., Humphreys, E. R., Moore, T. R., Roulet, N. T. and Lafleur, P. M.: Evidence for a](#)
1389 [nonmonotonic relationship between ecosystem-scale peatland methane emissions and water table](#)
1390 [depth, *J. Geophys. Res. Biogeosciences*, 119\(5\), 826–835, doi:10.1002/2013JG002576, 2014.](#)
- 1391 [Brutsaert, W.: *Evaporation into the Atmosphere*, Springer Netherlands, Dordrecht., 1982.](#)
- 1392 [Chen, C.-T. and Millero, F. J.: The use and misuse of pure water PVT properties for lake waters, *Nature*,](#)
1393 [266\(5604\), 707–708, doi:10.1038/266707a0, 1977.](#)
- 1394 Cole, J. J. and Caraco, N. F.: Atmospheric exchange of carbon dioxide in a low-wind oligotrophic lake
1395 measured by the addition of SF_6 , *Limnol. Oceanogr.*, 43(4), 647–656, doi:10.4319/lo.1998.43.4.0647,
1396 1998.
- 1397 Cole, J. J., Prairie, Y. T., Caraco, N. F., McDowell, W. H., Tranvik, L. J., Striegl, R. G., Duarte, C. M.,
1398 Kortelainen, P., Downing, J. A., Middelburg, J. J. and Melack, J.: Plumbing the Global Carbon Cycle:
1399 Integrating Inland Waters into the Terrestrial Carbon Budget, *Ecosystems*, 10(1), 172–185,
1400 doi:10.1007/s10021-006-9013-8, 2007.
- 1401 Crill, P. M., Bartlett, K. B., Wilson, J. O., Sebacher, D. I., Harriss, R. C., Melack, J. M., MacIntyre, S., Lesack,
1402 L. and Smith-Morrill, L.: Tropospheric methane from an Amazonian floodplain lake, *J. Geophys. Res.*,
1403 93(D2), 1564, doi:10.1029/JD093iD02p01564, 1988.
- 1404 Crusius, J. and Wanninkhof, R.: Gas transfer velocities measured at low wind speed over a lake, *Limnol.*
1405 *Oceanogr.*, 48(3), 1010–1017, doi:10.4319/lo.2003.48.3.1010, 2003.
- 1406 Csanady, G. T.: *Air-Sea Interaction - Laws and Mechanisms*, Cambridge University Press., 2001.

- 1407 Czikowsky, M. J., MacIntyre, S., Tedford, E. W., Vidal, J. and Miller, S. D.: Effects of Wind and Buoyancy on
1408 Carbon Dioxide Distribution and Air-Water Flux of a Stratified Temperate Lake, *J. Geophys. Res.*
1409 *Biogeosciences*, 123(8), 2305–2322, doi:10.1029/2017JG004209, 2018.
- 1410 Davidson, T. A., Audet, J., Jeppesen, E., Landkildehus, F., Lauridsen, T. L., Søndergaard, M. and Syväranta,
1411 J.: Synergy between nutrients and warming enhances methane ebullition from experimental lakes, *Nat.*
1412 *Clim. Chang.*, 8(2), 156–160, doi:10.1038/s41558-017-0063-z, 2018.
- 1413 DelSontro, T., Boutet, L., St-Pierre, A., del Giorgio, P. A. and Prairie, Y. T.: Methane ebullition and
1414 diffusion from northern ponds and lakes regulated by the interaction between temperature and system
1415 productivity, *Limnol. Oceanogr.*, 61(S1), S62–S77, doi:10.1002/lno.10335, 2016.
- 1416 DelSontro, T., del Giorgio, P. A. and Prairie, Y. T.: No Longer a Paradox: The Interaction Between Physical
1417 Transport and Biological Processes Explains the Spatial Distribution of Surface Water Methane Within
1418 and Across Lakes, *Ecosystems*, ~~4–15~~21(6), 1073–1087, doi:10.1007/s10021-017-0205-1, 2017.
- 1419 DelSontro, T., Beaulieu, J. J. and Downing, J. A.: Greenhouse gas emissions from lakes and
1420 impoundments: Upscaling in the face of global change, *Limnol. Oceanogr. Lett.*, doi:10.1002/lol2.10073,
1421 2018.
- 1422 Dimitriadis, P. and Koutsoyiannis, D.: Climacogram versus autocovariance and power spectrum in
1423 stochastic modelling for Markovian and Hurst–Kolmogorov processes, *Stoch. Environ. Res. Risk Assess.*,
1424 29(6), 1649–1669, doi:10.1007/s00477-015-1023-7, 2015.
- 1425 Duc, N. T., Crill, P. and Bastviken, D.: Implications of temperature and sediment characteristics on
1426 methane formation and oxidation in lake sediments, *Biogeochemistry*, 100(1–3), 185–196,
1427 doi:10.1007/s10533-010-9415-8, 2010.
- 1428 Dugan, H. A., Woolway, R. I., Santoso, A. B., Cormann, J. R., Jaimes, A., Nodine, E. R., Patil, V. P., Zwart, J.
1429 A., Brentrup, J. A., Hetherington, A. L., Oliver, S. K., Read, J. S., Winters, K. M., Hanson, P. C., Read, E. K.,
1430 Winslow, L. A. and Weathers, K. C.: Consequences of gas flux model choice on the interpretation of
1431 metabolic balance across 15 lakes, *Int. Waters*, 6(4), 581–592, doi:10.1080/IW-6.4.836, 2016.
- 1432 Encinas Fernández, J., Peeters, F. and Hofmann, H.: Importance of the Autumn Overturn and Anoxic
1433 Conditions in the Hypolimnion for the Annual Methane Emissions from a Temperate Lake, *Environ. Sci.*
1434 *Technol.*, 48(13), 7297–7304, doi:10.1021/es4056164, 2014.
- 1435 Engle, D. and Melack, J. M.: Methane emissions from an Amazon floodplain lake: Enhanced release
1436 during episodic mixing and during falling water, *Biogeochemistry*, 51(1), 71–90,
1437 doi:10.1023/A:1006389124823, 2000.
- 1438 Erkkilä, K.-M., Ojala, A., Bastviken, D., Biermann, T., Heiskanen, J. J., Lindroth, A., Peltola, O., Rantakari,
1439 M., Vesala, T. and Mammarella, I.: Methane and carbon dioxide fluxes over a lake: comparison between
1440 eddy covariance, floating chambers and boundary layer method, *Biogeosciences*, 15(2), 429–445,
1441 doi:10.5194/bg-15-429-2018, 2018.
- 1442 Esters, L., Landwehr, S., Sutherland, G., Bell, T. G., Christensen, K. H., Saltzman, E. S., Miller, S. D. and
1443 Ward, B.: Parameterizing air-sea gas transfer velocity with dissipation, *J. Geophys. Res. Ocean.*, 122(4),
1444 3041–3056, doi:10.1002/2016JC012088, 2017.
- 1445 Eugster, W., Kling, G., Jonas, T., McFadden, J. P., Wüest, A., MacIntyre, S. and Chapin III, F. S.: CO₂
1446 exchange between air and water in an Arctic Alaskan and midlatitude Swiss lake: Importance of
1447 convective mixing, *J. Geophys. Res. Atmos.*, 108(D12), doi:10.1029/2002JD002653, 2003.

- 1448 Eugster, W., DelSontro, T. and Sobek, S.: Eddy covariance flux measurements confirm extreme CH₄
 1449 emissions from a Swiss hydropower reservoir and resolve their short-term variability, *Biogeosciences*,
 1450 8(9), 2815–2831, doi:10.5194/bg-8-2815-2011, 2011.
- 1451 Fang, X. and Stefan, H. G.: Dynamics of heat exchange between sediment and water in a lake, *Water*
 1452 *Resour. Res.*, 32(6), 1719–1727, doi:10.1029/96WR00274, 1996.
- 1453 ~~Foken, T.: 50 Years of the Monin–Obukhov Similarity Theory, *Boundary-Layer Meteorol.*, 119(3), 431–~~
 1454 ~~447, doi:10.1007/s10546-006-9048-6, 2006.~~
- 1455 Ford, P. W., Boon, P. I. and Lee, K.: Methane and oxygen dynamics in a shallow floodplain lake: The
 1456 significance of periodic stratification, *Hydrobiologia*, 485, 97–110, doi:10.1023/A:102137953, 2002.
- 1457 Gålfalk, M., Bastviken, D., Fredriksson, S. and Arneborg, L.: Determination of the piston velocity for
 1458 water-air interfaces using flux chambers, acoustic Doppler velocimetry, and IR imaging of the water
 1459 surface, *J. Geophys. Res. Biogeosciences*, 118(2), 770–782, doi:10.1002/jgrg.20064, 2013.
- 1460 ~~Grachev, A. A., Andreas, E. L., Fairall, C. W., Guest, P. S. and Persson, P. O. G.: The Critical Richardson~~
 1461 ~~Number and Limits of Applicability of Local Similarity Theory in the Stable Boundary Layer, *Boundary-*~~
 1462 ~~*Layer Meteorol.*, 147(1), 51–82, doi:10.1007/s10546-012-9771-0, 2013.~~
- 1463 Hamilton, J. D., Kelly, C. a, Rudd, J. W. M., Hesslein, R. H. and Roulet, N. T.: Flux to the atmosphere of CH₄
 1464 and CO₂ from wetland ponds on the Hudson Bay lowlands (HBLs), *J. Geophys. Res.*, 99(D1), 1495,
 1465 doi:10.1029/93JD03020, 1994.
- 1466 Hammer, Ø., Harper, D. A. T. and Ryan, P. D.: Past: Paleontological statistics software package for
 1467 education and data analysis, *Palaeontol. Electron.*, 4(1) [online] Available from:
 1468 <https://folk.uio.no/ohammer/past/>, 2001.
- 1469 Hamming, R. W.: *Digital Filters*, Dover publications, Dover, New York., 1989.
- 1470 Heiskanen, J. J., Mammarella, I., Haapanala, S., Pumpanen, J., Vesala, T., MacIntyre, S. and Ojala, A.:
 1471 Effects of cooling and internal wave motions on gas transfer coefficients in a boreal lake, *Tellus B Chem.*
 1472 *Phys. Meteorol.*, 66(1), 22827, doi:10.3402/tellusb.v66.22827, 2014.
- 1473 Hofmann, H.: Spatiotemporal distribution patterns of dissolved methane in lakes: How accurate are the
 1474 current estimations of the diffusive flux path?, *Geophys. Res. Lett.*, 40(11), 2779–2784,
 1475 doi:10.1002/grl.50453, 2013.
- 1476 Holgerson, M. A. and Raymond, P. A.: Large contribution to inland water CO₂ and CH₄ emissions from
 1477 very small ponds, *Nat. Geosci.*, 9(3), 222–226, doi:10.1038/ngeo2654, 2016.
- 1478 Idso, S. B. and Gilbert, R. G.: On the Universality of the Poole and Atkins Secchi Disk-Light Extinction
 1479 Equation, *J. Appl. Ecol.*, 11(1), 399, doi:10.2307/2402029, 1974.
- 1480 Imberger, J.: The diurnal mixed layer, *Limnol. Oceanogr.*, 30(4), 737–770, doi:10.4319/lo.1985.30.4.0737,
 1481 1985.
- 1482 ~~Ivey, G. N. and Imberger, J.: On the Nature of Turbulence in a Stratified Fluid. Part I: The Energetics of~~
 1483 ~~Mixing, *J. Phys. Oceanogr.*, 21(5), 650–658, doi:10.1175/1520-0485(1991)021<0650:OTNOTI>2.0.CO;2,~~
 1484 ~~1991.~~
- 1485 Jähne, B., Heinz, G. and Dietrich, W.: Measurement of the diffusion coefficients of sparingly soluble gases
 1486 in water, *J. Geophys. Res.*, 92(C10), 10767, doi:10.1029/JC092iC10p10767, 1987.

- 1487 Jammet, M., Crill, P., Dengel, S. and Friborg, T.: Large methane emissions from a subarctic lake during
 1488 spring thaw: Mechanisms and landscape significance, *J. Geophys. Res. Biogeosciences*, 120(11), 2289–
 1489 2305, doi:10.1002/2015JG003137, 2015.
- 1490 Jammet, M., Dengel, S., Kettner, E., Parmentier, F.-J. W., Wik, M., Crill, P. and Friborg, T.: Year-round CH₄
 1491 and CO₂ flux dynamics in two contrasting freshwater ecosystems of the subarctic, *Biogeosciences*,
 1492 14(22), 5189–5216, doi:10.5194/bg-14-5189-2017, 2017.
- 1493 Jansen, J., Thornton, B. F., Jammet, M. M., Wik, M., Cortés, A., Friborg, T., MacIntyre, S. and Crill, P. M.:
 1494 Climate-Sensitive Controls on Large Spring Emissions of CH₄ and CO₂ From Northern Lakes, *J. Geophys.*
 1495 *Res. Biogeosciences*, 2019JG005094, doi:10.1029/2019JG005094, 2019.
- 1496 Jellison, R. and Melack, J. M.: Meromixis in hypersaline Mono Lake, California. 1. Stratification and
 1497 vertical mixing during the onset, persistence, and breakdown of meromixis, *Limnol. Oceanogr.*, 38(5),
 1498 1008–1019, doi:10.4319/lo.1993.38.5.1008, 1993.
- 1499 [Jonas, T., Stips, A., Eugster, W. and Wüest, A.: Observations of a quasi shear-free lacustrine convective](#)
 1500 [boundary layer: Stratification and its implications on turbulence, *J. Geophys. Res. C Ocean.*, 108\(10\), 26–](#)
 1501 [1, doi:10.1029/2002jc001440, 2003.](#)
- 1502 Juutinen, S., Rantakari, M., Kortelainen, P., Huttunen, J. T., Larmola, T., Alm, J., Silvola, J. and
 1503 Martikainen, P. J.: Methane dynamics in different boreal lake types, *Biogeosciences*, 6(2), 209–223,
 1504 doi:10.5194/bg-6-209-2009, 2009.
- 1505 Kankaala, P., Huotari, J., Tulonen, T. and Ojala, A.: Lake-size dependent physical forcing drives carbon
 1506 dioxide and methane effluxes from lakes in a boreal landscape, *Limnol. Oceanogr.*, 58(6), 1915–1930,
 1507 doi:10.4319/lo.2013.58.6.1915, 2013.
- 1508 Karlsson, J., Christensen, T. R., Crill, P., Förster, J., Hammarlund, D., Jackowicz-Korczynski, M., Kokfelt, U.,
 1509 Roehm, C. and Rosén, P.: Quantifying the relative importance of lake emissions in the carbon budget of a
 1510 subarctic catchment, *J. Geophys. Res.*, 115(G3), G03006, doi:10.1029/2010JG001305, 2010.
- 1511 Katul, G., Mammarella, I., Grönholm, T. and Vesala, T.: A Structure Function Model Recovers the Many
 1512 Formulations for Air-Water Gas Transfer Velocity, *Water Resour. Res.*, 54(9), 5905–5920,
 1513 doi:10.1029/2018WR022731, 2018.
- 1514 Kell, G. S.: Density, thermal expansivity, and compressibility of liquid water from 0.deg. to 150.deg..
 1515 Correlations and tables for atmospheric pressure and saturation reviewed and expressed on 1968
 1516 temperature scale, *J. Chem. Eng. Data*, 20(1), 97–105, doi:10.1021/je60064a005, 1975.
- 1517 Koebisch, F., Jurasinski, G., Koch, M., Hofmann, J. and Glatzel, S.: Controls for multi-scale temporal
 1518 variation in ecosystem methane exchange during the growing season of a permanently inundated fen,
 1519 *Agric. For. Meteorol.*, 204, 94–105, doi:10.1016/j.agrformet.2015.02.002, 2015.
- 1520 Kokfelt, U., Reuss, N., Struyf, E., Sonesson, M., Rundgren, M., Skog, G., Rosén, P. and Hammarlund, D.:
 1521 Wetland development, permafrost history and nutrient cycling inferred from late Holocene peat and lake
 1522 sediment records in subarctic Sweden, *J. Paleolimnol.*, 44(1), 327–342, doi:10.1007/s10933-010-9406-8,
 1523 2010.
- 1524 Lamont, J. C. and Scott, D. S.: An eddy cell model of mass transfer into the surface of a turbulent liquid,
 1525 *AIChE J.*, 16(4), 513–519, doi:10.1002/aic.690160403, 1970.
- 1526 [Laurion, I., Vincent, W. F., MacIntyre, S., Retamal, L., Dupont, C., Francus, P. and Pienitz, R.: Variability in](#)

- 1527 ~~greenhouse gas emissions from permafrost thaw ponds, *Limnol. Oceanogr.*, 55(1), 115–133,~~
1528 ~~doi:10.4319/lo.2010.55.1.0115, 2010.~~
- 1529 Liss, P. S. and Slater, P. G.: Flux of Gases across the Air-Sea Interface, *Nature*, 247(5438), 181–184,
1530 doi:10.1038/247181a0, 1974.
- 1531 Lofton, D. D., Whalen, S. C. and Hershey, A. E.: Effect of temperature on methane dynamics and
1532 evaluation of methane oxidation kinetics in shallow Arctic Alaskan lakes, *Hydrobiologia*, 721(1), 209–222,
1533 doi:10.1007/s10750-013-1663-x, 2014.
- 1534 Loken, L. C., Crawford, J. T., Schramm, P. J., Stadler, P., Desai, A. R. and Stanley, E. H.: Large spatial and
1535 temporal variability of carbon dioxide and methane in a eutrophic lake, *J. Geophys. Res. Biogeosciences*,
1536 2019JG005186, doi:10.1029/2019JG005186, 2019.
- 1537 López Bellido, J., Tulonen, T., Kankaala, P. and Ojala, A.: CO₂ and CH₄ fluxes during spring and autumn
1538 mixing periods in a boreal lake (Pääjärvi, southern Finland), *J. Geophys. Res.*, 114(G4), G04007,
1539 doi:10.1029/2009JG000923, 2009.
- 1540 Lundin, E. J., Giesler, R., Persson, A., Thompson, M. S. and Karlsson, J.: Integrating carbon emissions from
1541 lakes and streams in a subarctic catchment, *J. Geophys. Res. Biogeosciences*, 118(3), 1200–1207,
1542 doi:10.1002/jgrg.20092, 2013.
- 1543 Lundin, E. J., Klaminder, J., Giesler, R., Persson, A., Olefeldt, D., Heliasz, M., Christensen, T. R. and
1544 Karlsson, J.: Is the subarctic landscape still a carbon sink? Evidence from a detailed catchment balance,
1545 *Geophys. Res. Lett.*, 43(5), 1988–1995, doi:10.1002/2015GL066970, 2016.
- 1546 ~~MacIntyre, S. and Melack, J. M.: *Vertical and Horizontal Transport in Lakes: Linking Littoral, Benthic, and*
1547 *Pelagic Habitats, J. North Am. Benthol. Soc.*, 14(4), 599–615, doi:10.2307/1467544, 1995.~~
- 1548 ~~MacIntyre, S. and Melack, J. M.: Mixing Dynamics in Lakes Across Climatic Zones, in *Encyclopedia of*
1549 *Inland Waters*, pp. 603–612, Elsevier., 2009.~~
- 1550 MacIntyre, S., Wanninkhof, R. and Chanton, J. P.: Trace gas exchange across the air–water interface in
1551 freshwater and coastal marine environments, in *Biogenic trace gases: Measuring emissions from soil and*
1552 *water*, pp. 52–97., 1995.
- 1553 MacIntyre, S., Romero, J. R. and Kling, G. W.: Spatial-temporal variability in surface layer deepening and
1554 lateral advection in an embayment of Lake Victoria, East Africa, *Limnol. Oceanogr.*, 47(3), 656–671,
1555 doi:10.4319/lo.2002.47.3.0656, 2002.
- 1556 MacIntyre, S., Fram, J. P., Kushner, P. J., Bettez, N. D., O’Brien, W. J., Hobbie, J. E. and Kling, G. W.:
1557 Climate-related variations in mixing dynamics in an Alaskan arctic lake, *Limnol. Oceanogr.*, 54(6part2),
1558 2401–2417, doi:10.4319/lo.2009.54.6_part_2.2401, 2009.
- 1559 MacIntyre, S., Jonsson, A., Jansson, M., Aberg, J., Turney, D. E. and Miller, S. D.: Buoyancy flux,
1560 turbulence, and the gas transfer coefficient in a stratified lake, *Geophys. Res. Lett.*, 37(24),
1561 doi:10.1029/2010GL044164, 2010.
- 1562 MacIntyre, S., Romero, J. R., Silsbe, G. M. and Emery, B. M.: Stratification and horizontal exchange in
1563 Lake Victoria, East Africa, *Limnol. Oceanogr.*, 59(6), 1805–1838, doi:10.4319/lo.2014.59.6.1805, 2014.
- 1564 MacIntyre, S., Crowe, A. T., Cortés, A. and Arneborg, L.: Turbulence in a small arctic pond, *Limnol.*
1565 *Oceanogr.*, 63(6), 2337–2358, doi:10.1002/lno.10941, 2018.

- 1566 Malmer, N., Johansson, T., Olsrud, M. and Christensen, T. R.: Vegetation, climatic changes and net
1567 carbon sequestration in a North-Scandinavian subarctic mire over 30 years, *Glob. Chang. Biol.*, 11, 1895–
1568 1909, doi:10.1111/j.1365-2486.2005.01042.x, 2005.
- 1569 Mammarella, I., Nordbo, A., Rannik, Ü., Haapanala, S., Levula, J., Laakso, H., Ojala, A., Peltola, O.,
1570 Heiskanen, J., Pumpanen, J. and Vesala, T.: Carbon dioxide and energy fluxes over a small boreal lake in
1571 Southern Finland, *J. Geophys. Res. Biogeosciences*, 120(7), 1296–1314, doi:10.1002/2014JG002873,
1572 2015.
- 1573 Markfort, C. D., Perez, A. L. S., Thill, J. W., Jaster, D. A., Porté-Agel, F. and Stefan, H. G.: Wind sheltering of
1574 a lake by a tree canopy or bluff topography, *Water Resour. Res.*, 46(3), 1–13,
1575 doi:10.1029/2009WR007759, 2010.
- 1576 Matthews, C. J. D., St.Louis, V. L. and Hesslein, R. H.: Comparison of Three Techniques Used To Measure
1577 Diffusive Gas Exchange from Sheltered Aquatic Surfaces, *Environ. Sci. Technol.*, 37(4), 772–780,
1578 doi:10.1021/es0205838, 2003.
- 1579 McCalley, C. K., Woodcroft, B. J., Hodgkins, S. B., Wehr, R. A., Kim, E.-H., Mondav, R., Crill, P. M., Chanton,
1580 J. P., Rich, V. I., Tyson, G. W. and Saleska, S. R.: Methane dynamics regulated by microbial community
1581 response to permafrost thaw, *Nature*, 514(7523), 478–481, doi:10.1038/nature13798, 2014.
- 1582 McGinnis, D. F., Kirillin, G., Tang, K. W., Flury, S., Bodmer, P., Engelhardt, C., Casper, P. and Grossart, H.-
1583 P.: Enhancing surface methane fluxes from an oligotrophic lake: exploring the microbubble hypothesis.,
1584 *Environ. Sci. Technol.*, 49(2), 873–80, doi:10.1021/es503385d, 2015.
- 1585 Merlivat, L. and Memery, L.: Gas exchange across an air-water interface: Experimental results and
1586 modeling of bubble contribution to transfer, *J. Geophys. Res.*, 88(C1), 707,
1587 doi:10.1029/JC088iC01p00707, 1983.
- 1588 Miettinen, H., Pumpanen, J., Heiskanen, J. J., Aaltonen, H., Mammarella, I., Ojala, A., Levula, J. and
1589 Rantakari, M.: Towards a more comprehensive understanding of lacustrine greenhouse gas dynamics —
1590 two- year measurements of concentrations and fluxes of CO₂, CH₄ and N₂O in a typical boreal ~~lake,~~
1591 *Boreal Environ. Res.*, 6095(December), 75–89, 2015.
- 1592 ~~Murase, J., Sakai, Y., Sugimoto, A., Okubo, K. and Sakamoto, M.: Sources of dissolved methane in Lake~~
1593 ~~Biwa, *Limnology*, 4(2), 91–99, doi:10.1007/s10201-003-0095-0, 2003.~~
- 1594 ~~Miljödata-MVM. Swedish University of Agricultural Sciences (SLU). National data host for lakes and~~
1595 ~~watercourses, and national data host for agricultural land, <http://miljodata.slu.se/mvm/> [07-10-2017].~~
- 1596 Natchimuthu, S., Sundgren, I., Gålfalk, M., Klemedtsson, L., Crill, P., Danielsson, Å. and Bastviken, D.:
1597 Spatio-temporal variability of lake ~~CH₄CH₄~~ fluxes and its influence on annual whole lake emission
1598 estimates, *Limnol. Oceanogr.*, 61(S1), S13–S26, doi:10.1002/lno.10222, 2016.
- 1599 Natchimuthu, S., Sundgren, I., Gålfalk, M., Klemedtsson, L. and Bastviken, D.: Spatiotemporal variability
1600 of lake ~~pCO₂pCO₂~~ and ~~CO₂CO₂~~ fluxes in a hemiboreal catchment, *J. Geophys. Res. Biogeosciences*,
1601 122(1), 30–49, doi:10.1002/2016JG003449, 2017.
- 1602 ~~Ojala, A., Bellido, J. L., Tulonen, T., Kankaala, P. and Huotari, J.: Carbon gas fluxes from a brown water~~
1603 ~~and a clear water lake in the boreal zone during a summer with extreme rain events, *Limnol. Oceanogr.*,~~
1604 ~~56(1), 61–76, doi:10.4319/lno.2011.56.1.0061, 2011.~~
- 1605 Olefeldt, D. and Roulet, N. T.: Effects of permafrost and hydrology on the composition and transport of

1606 dissolved organic carbon in a subarctic peatland complex, *J. Geophys. Res. Biogeosciences*, 117(G1), 1–
1607 15, doi:10.1029/2011JG001819, 2012.

1608 Olefeldt, D., Roulet, N. T., Bergeron, O., Crill, P., Bäckstrand, K. and Christensen, T. R.: Net carbon
1609 accumulation of a high-latitude permafrost palsa mire similar to permafrost-free peatlands, *Geophys.*
1610 *Res. Lett.*, 39(3), ~~n/a-n/a~~, doi:10.1029/2011GL050355, 2012.

1611 Pappas, C., Mahecha, M. D., Frank, D. C., Babst, F. and Koutsoyiannis, D.: Ecosystem functioning is
1612 enveloped by hydrometeorological variability, *Nat. Ecol. Evol.*, 1(9), 1263–1270, doi:10.1038/s41559-
1613 017-0277-5, 2017.

1614 Paytan, A., Lecher, A. L., Dimova, N., Sparrow, K. J., Kodovska, F. G.-T., Murray, J., Tulaczyk, S. and
1615 Kessler, J. D.: Methane transport from the active layer to lakes in the Arctic using Toolik Lake, Alaska, as a
1616 case study, *Proc. Natl. Acad. Sci.*, 112(12), 201417392, doi:10.1073/pnas.1417392112, 2015.

1617 ~~Podgrajsek, E., Sahlée, E., Bastviken, D., Holst, J., Lindroth, A., Tranvik, L. and Rutgersson, A.: Comparison~~
1618 ~~of floating chamber and eddy covariance measurements of lake greenhouse gas fluxes, *Biogeosciences*,~~
1619 ~~11(15), 4225–4233, doi:10.5194/bg-11-4225-2014, 2014a.~~

1620 ~~Podgrajsek, E., Sahlée, E.~~ and Rutgersson, A.: Diurnal cycle of lake methane flux, *J. Geophys. Res.*
1621 *Biogeosciences*, 119(3), 236–248, doi:10.1002/2013JG002327, ~~2014b~~2014.

1622 Podgrajsek, E., Sahlée, E. and Rutgersson, A.: Diel cycle of lake-air CO₂ flux from a shallow lake and the
1623 impact of waterside convection on the transfer velocity, *J. Geophys. Res. Biogeosciences*, 120(1), 29–38,
1624 doi:10.1002/2014JG002781, 2015.

1625 ~~Podgrajsek, E., Sahlée, E., Bastviken, D., Natchimuthu, S., Kljun, N., Chmiel, H. E., Klemetsson, L. and~~
1626 ~~Rutgersson, A.: Methane fluxes from a small boreal lake measured with the eddy covariance method,~~
1627 ~~*Limnol. Oceanogr.*, 61(S1), S41–S50, doi:10.1002/lno.10245, 2016.~~

1628 Poindexter, C. M., Baldocchi, D. D., Matthes, J. H., Knox, S. H. and Variano, E. A.: The contribution of an
1629 overlooked transport process to a wetland's methane emissions, *Geophys. Res. Lett.*, 43(12), 6276–6284,
1630 doi:10.1002/2016GL068782, 2016.

1631 Prairie, Y. and del Giorgio, P.: A new pathway of freshwater methane emissions and the putative
1632 importance of microbubbles, *Int. Waters*, 3(3), 311–320, doi:10.5268/IW-3.3.542, 2013.

1633 ~~Rantala, M. V., Nevalainen, L., Rautio, M., Galkin, A. and Luoto, T. P.: Sources and controls of organic~~
1634 ~~carbon in lakes across the subarctic treeline, *Biogeochemistry*, 129(1–2), 235–253, doi:10.1007/s10533-~~
1635 ~~016-0229-1, 2016.~~

1636 Rasilo, T., Prairie, Y. T. and del Giorgio, P. A.: Large-scale patterns in summer diffusive CH₄ fluxes across
1637 boreal lakes, and contribution to diffusive C emissions, *Glob. Chang. Biol.*, 21(3), 1124–1139,
1638 doi:10.1111/gcb.12741, 2015.

1639 Read, J. S., Hamilton, D. P., Desai, A. R., Rose, K. C., MacIntyre, S., Lenters, J. D., Smyth, R. L., Hanson, P.
1640 C., Cole, J. J., Staehr, P. A., Rusak, J. A., Pierson, D. C., Brookes, J. D., Laas, A. and Wu, C. H.: Lake-size
1641 dependency of wind shear and convection as controls on gas exchange, *Geophys. Res. Lett.*, 39(9),
1642 doi:10.1029/2012GL051886, 2012.

1643 Ribas-Ribas, M., Kilcher, L. F. and Wurl, O.: *Sniffle*: a step forward to measure *in situ* CO₂ fluxes with the
1644 floating chamber technique, *Elem Sci Anth*, 6(1), 14, doi:10.1525/elementa.275, 2018.

1645 Rueda, F., Moreno-Ostos, E. and Cruz-Pizarro, L.: Spatial and temporal scales of transport during the

- 1646 cooling phase of the ice-free period in a small high-mountain lake, *Aquat. Sci.*, 69(1), 115–128,
1647 doi:10.1007/s00027-006-0823-8, 2007.
- 1648 Schilder, J., Bastviken, D., van Hardenbroek, M., ~~Kankaala, P., Rinta, P., Stötter, T. and Heiri, O.: Spatial~~
1649 ~~heterogeneity and lake morphology affect diffusive greenhouse gas emission estimates of lakes,~~
1650 ~~Geophys. Res. Lett., 40(21), 5752–5756, doi:10.1002/2013GL057669, 2013.~~
- 1651 ~~Schilder, J., Bastviken, D., van Hardenbroek, M.~~ and Heiri, O.: Spatiotemporal patterns in methane flux
1652 and gas transfer velocity at low wind speeds: Implications for upscaling studies on small lakes, *J.*
1653 *Geophys. Res. Biogeosciences*, 121(6), 1456–1467, doi:10.1002/2016JG003346, 2016.
- 1654 Sepulveda-Jauregui, A., Walter Anthony, K. M., Martinez-Cruz, K., Greene, S. and Thalasso, F.: Methane
1655 and carbon dioxide emissions from 40 lakes along a north–south latitudinal transect in Alaska,
1656 *Biogeosciences*, 12(11), 3197–3223, doi:10.5194/bg-12-3197-2015, 2015.
- 1657 Sheskin, D. J.: *Handbook of Parametric and Nonparametric Statistical Procedures*, 4th ed., Chapman &
1658 Hall/CRC., 2007.
- 1659 Smith, S. D.: Coefficients for sea surface wind stress, heat flux, and wind profiles as a function of wind
1660 speed and temperature, *J. Geophys. Res.*, 93(C12), 15467, doi:10.1029/JC093iC12p15467, 1988.
- 1661 Soumis, N., Canuel, R. and Lucotte, M.: Evaluation of Two Current Approaches for the Measurement of
1662 Carbon Dioxide Diffusive Fluxes from Lentic Ecosystems, *Environ. Sci. Technol.*, 42(8), 2964–2969,
1663 doi:10.1021/es702361s, 2008.
- 1664 Tan, Z. and Zhuang, Q.: Methane emissions from pan-Arctic lakes during the 21st century: An analysis
1665 with process-based models of lake evolution and biogeochemistry, *J. Geophys. Res. Biogeosciences*,
1666 120(12), 2641–2653, doi:10.1002/2015JG003184, 2015.
- 1667 Tedford, E. W., MacIntyre, S., Miller, S. D. and Czikowsky, M. J.: Similarity scaling of turbulence in a
1668 temperate lake during fall cooling, *J. Geophys. Res. Ocean.*, 119(8), 4689–4713,
1669 doi:10.1002/2014JC010135, 2014.
- 1670 ~~Tennekes, H. and Lumley, L. J.: *A First Course In Turbulence*, The MIT Press, Cambridge, MA., 1972.~~
- 1671 Terray, E. A., Donelan, M. A., Agrawal, Y. C., Drennan, W. M., Kahma, K. K., Williams, A. J., Hwang, P. A.
1672 and Kitaigorodskii, S. A.: Estimates of Kinetic Energy Dissipation under Breaking Waves, *J. Phys.*
1673 *Oceanogr.*, 26(5), 792–807, doi:10.1175/1520-0485(1996)026<0792:EOKEDU>2.0.CO;2, 1996.
- 1674 Theofanous, T. G., Houze, R. N. and Brumfield, L. K.: Turbulent mass transfer at free, gas-liquid interfaces,
1675 with applications to open-channel, bubble and jet flows, *Int. J. Heat Mass Transf.*, 19(6), 613–624,
1676 doi:10.1016/0017-9310(76)90044-2, 1976.
- 1677 Thornton, B. F., Wik, M. and Crill, P. M.: Climate-forced changes in available energy and methane
1678 bubbling from subarctic lakes, *Geophys. Res. Lett.*, 42(6), 1936–1942, doi:10.1002/2015GL063189, 2015.
- 1679 Tokoro, T., Kayanne, H., Watanabe, A., Nadaoka, K., Tamura, H., Nozaki, K., Kato, K. and Negishi, A.: High
1680 gas-transfer velocity in coastal regions with high energy-dissipation rates, *J. Geophys. Res.*, 113(C11),
1681 C11006, doi:10.1029/2007JC004528, 2008.
- 1682 Turner, W. R.: Microbubble Persistence in Fresh Water, *J. Acoust. Soc. Am.*, 33(9), 1223–1233,
1683 doi:10.1121/1.1908960, 1961.
- 1684 Tveit, A. T., Urich, T., Frenzel, P. and Svenning, M. M.: Metabolic and trophic interactions modulate

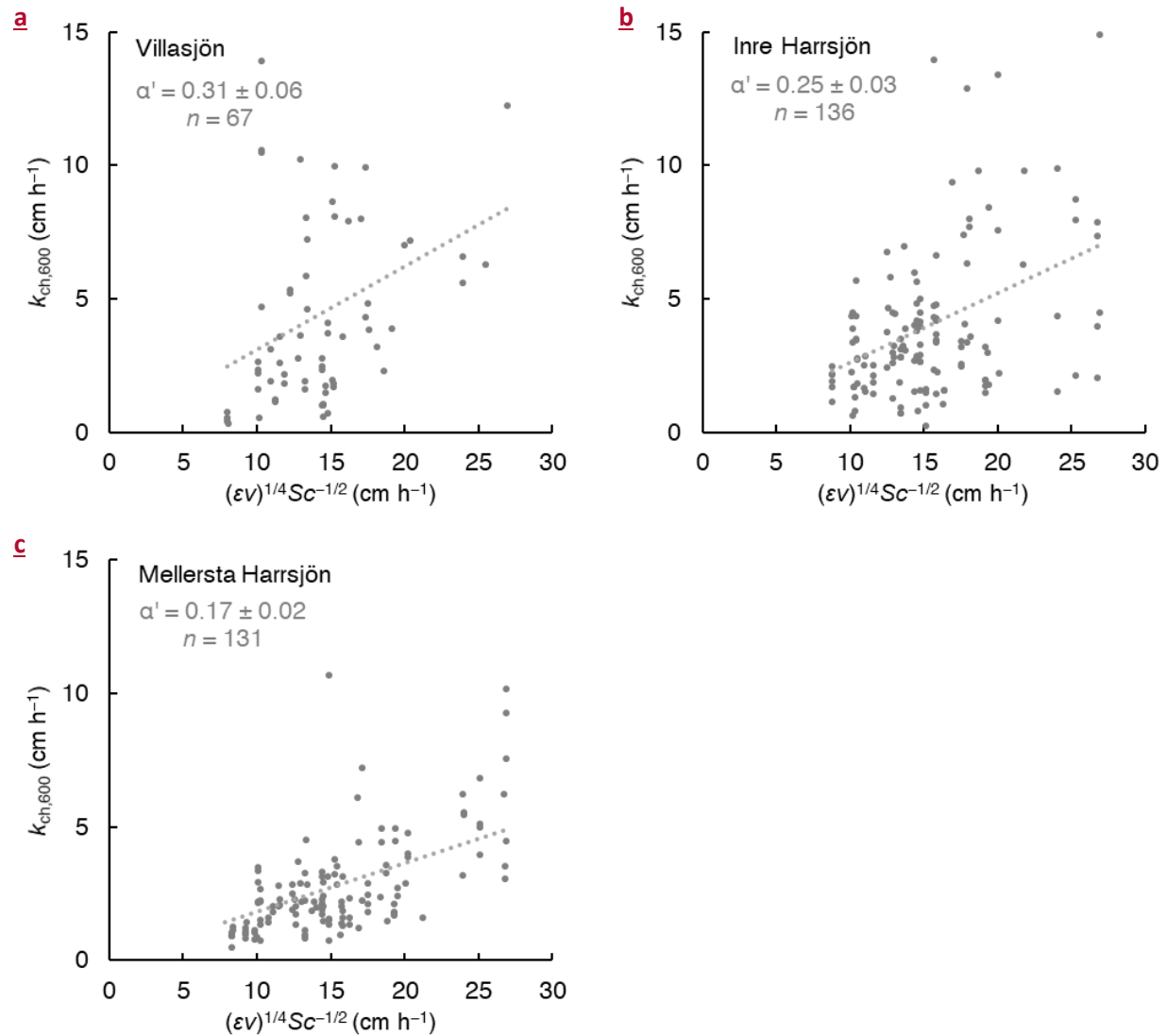
- 1685 methane production by Arctic peat microbiota in response to warming, *Proc. Natl. Acad. Sci.*, 112(19),
1686 E2507–E2516, doi:10.1073/pnas.1420797112, 2015.
- 1687 Tyrllis, E. and Hoskins, B. J.: Aspects of a Northern Hemisphere Atmospheric Blocking Climatology, *J.*
1688 *Atmos. Sci.*, 65(5), 1638–1652, doi:10.1175/2007JAS2337.1, 2008.
- 1689 Vachon, D. and Prairie, Y. T.: The ecosystem size and shape dependence of gas transfer velocity versus
1690 wind speed relationships in lakes, edited by R. Smith, *Can. J. Fish. Aquat. Sci.*, 70(12), 1757–1764,
1691 doi:10.1139/cjfas-2013-0241, 2013.
- 1692 Vachon, D., Prairie, Y. T. and Cole, J. J.: The relationship between near-surface turbulence and gas
1693 transfer velocity in freshwater systems and its implications for floating chamber measurements of gas
1694 exchange, *Limnol. Oceanogr.*, 55(4), 1723–1732, doi:10.4319/lo.2010.55.4.1723, 2010.
- 1695 Vachon, D., Langenegger, T., Donis, D. and McGinnis, D. F.: Influence of water column stratification and
1696 mixing patterns on the fate of methane produced in deep sediments of a small eutrophic lake, *Limnol.*
1697 *Oceanogr.*, Ino.11172, doi:10.1002/Ino.11172, 2019.
- 1698 Wang, B., Liao, Q., Fillingham, J. H. and Bootsma, H. A.: On the coefficients of small eddy and surface
1699 divergence models for the air-water gas transfer velocity, *J. Geophys. Res. Ocean.*, 120(3), 2129–2146,
1700 doi:10.1002/2014JC010253, 2015.
- 1701 Wanninkhof, R.: Relationship between wind speed and gas exchange over the ocean, *J. Geophys. Res.*,
1702 97(C5), 7373, doi:10.1029/92JC00188, 1992.
- 1703 Wanninkhof, R.: Relationship between wind speed and gas exchange over the ocean revisited, *Limnol.*
1704 *Oceanogr. Methods*, 12(6), 351–362, doi:10.4319/lom.2014.12.351, 2014.
- 1705 Weyhenmeyer, G. A., Kosten, S., Wallin, M. B., Tranvik, L. J., Jeppesen, E. and Roland, F.: Significant
1706 fraction of CO₂ emissions from boreal lakes derived from hydrologic inorganic carbon inputs, *Nat.*
1707 *Geosci.*, 8(12), 933–936, doi:10.1038/ngeo2582, 2015.
- 1708 Wiesenburg, D. A. and Guinasso, N. L.: Equilibrium solubilities of methane, carbon monoxide, and
1709 hydrogen in water and sea water, *J. Chem. Eng. Data*, 24(4), 356–360, doi:10.1021/je60083a006, 1979.
- 1710 Wik, M., Crill, P. M., Bastviken, D., Danielsson, Å. and Norbäck, E.: Bubbles trapped in arctic lake ice:
1711 Potential implications for methane emissions, *J. Geophys. Res.*, 116(G3), G03044,
1712 doi:10.1029/2011JG001761, 2011.
- 1713 Wik, M., Crill, P. M., Varner, R. K. and Bastviken, D.: Multiyear measurements of ebullitive methane flux
1714 from three subarctic lakes, *J. Geophys. Res. Biogeosciences*, 118(3), 1307–1321, doi:10.1002/jgrg.20103,
1715 2013.
- 1716 Wik, M., Thornton, B. F., Bastviken, D., MacIntyre, S., Varner, R. K. and Crill, P. M.: Energy input is primary
1717 controller of methane bubbling in subarctic lakes, *Geophys. Res. Lett.*, 41(2), 555–560,
1718 doi:10.1002/2013GL058510, 2014.
- 1719 Wik, M., Thornton, B. F., Bastviken, D., Uhlbäck, J. and Crill, P. M.: Biased sampling of methane release
1720 from northern lakes: A problem for extrapolation, *Geophys. Res. Lett.*, 43(3), 1256–1262,
1721 doi:10.1002/2015GL066501, 2016a.
- 1722 Wik, M., Varner, R. K., Walter Anthony, K. M., MacIntyre, S. and Bastviken, D.: Climate-sensitive northern
1723 lakes and ponds are critical components of methane release, *Nat. Geosci.*, 9(2), 99–105,
1724 doi:10.1038/ngeo2578, 2016b.

- 1725 Wik, M., Johnson, J. E., Crill, P. M., DeStasio, J. P., Erickson, L., Halloran, M. J., Fahnestock, M. F.,
1726 Crawford, M. K., Phillips, S. C. and Varner, R. K.: Sediment Characteristics and Methane Ebullition in
1727 Three Subarctic Lakes, *J. Geophys. Res. Biogeosciences*, 123(8), 2399–2411, doi:10.1029/2017JG004298,
1728 2018.
- 1729 Woolf, D. K. and Thorpe, S. A.: Bubbles and the air-sea exchange of gases in near-saturation conditions, *J.*
1730 *Mar. Res.*, 49(3), 435–466, doi:10.1357/002224091784995765, 1991.
- 1731 Yvon-Durocher, G., Allen, A. P., Bastviken, D., Conrad, R., Gudas, C., St-Pierre, A., Thanh-Duc, N. and del
1732 Giorgio, P. A.: Methane fluxes show consistent temperature dependence across microbial to ecosystem
1733 scales, *Nature*, 507(7493), 488–491, doi:10.1038/nature13164, 2014.
- 1734 Yvon-Durocher, G., Hulatt, C. J., Woodward, G. and Trimmer, M.: Long-term warming amplifies shifts in
1735 the carbon cycle of experimental ponds, *Nat. Clim. Chang.*, 7(3), 209–213, doi:10.1038/nclimate3229,
1736 2017.
- 1737 Zappa, C. J., McGillis, W. R., Raymond, P. A., Edson, J. B., Hintsa, E. J., Zemmelen, H. J., Dacey, J. W. H.
1738 and Ho, D. T.: Environmental turbulent mixing controls on air-water gas exchange in marine and aquatic
1739 systems, *Geophys. Res. Lett.*, 34(10), L10601, doi:10.1029/2006GL028790, 2007.
- 1740 Zimov, S. A., Voropaev, Y. V., Semiletov, I. P., Davidov, S. P., Prosiannikov, S. F., Chapin, M. C., Chapin III,
1741 F. S., Trumbore, S. and Tyler, S.: North Siberian Lakes: A Methane Source Fueled by Pleistocene Carbon,
1742 *Science (80-.)*, 277(5327), 800–802, doi:10.1126/science.277.5327.800, 1997.
- 1743

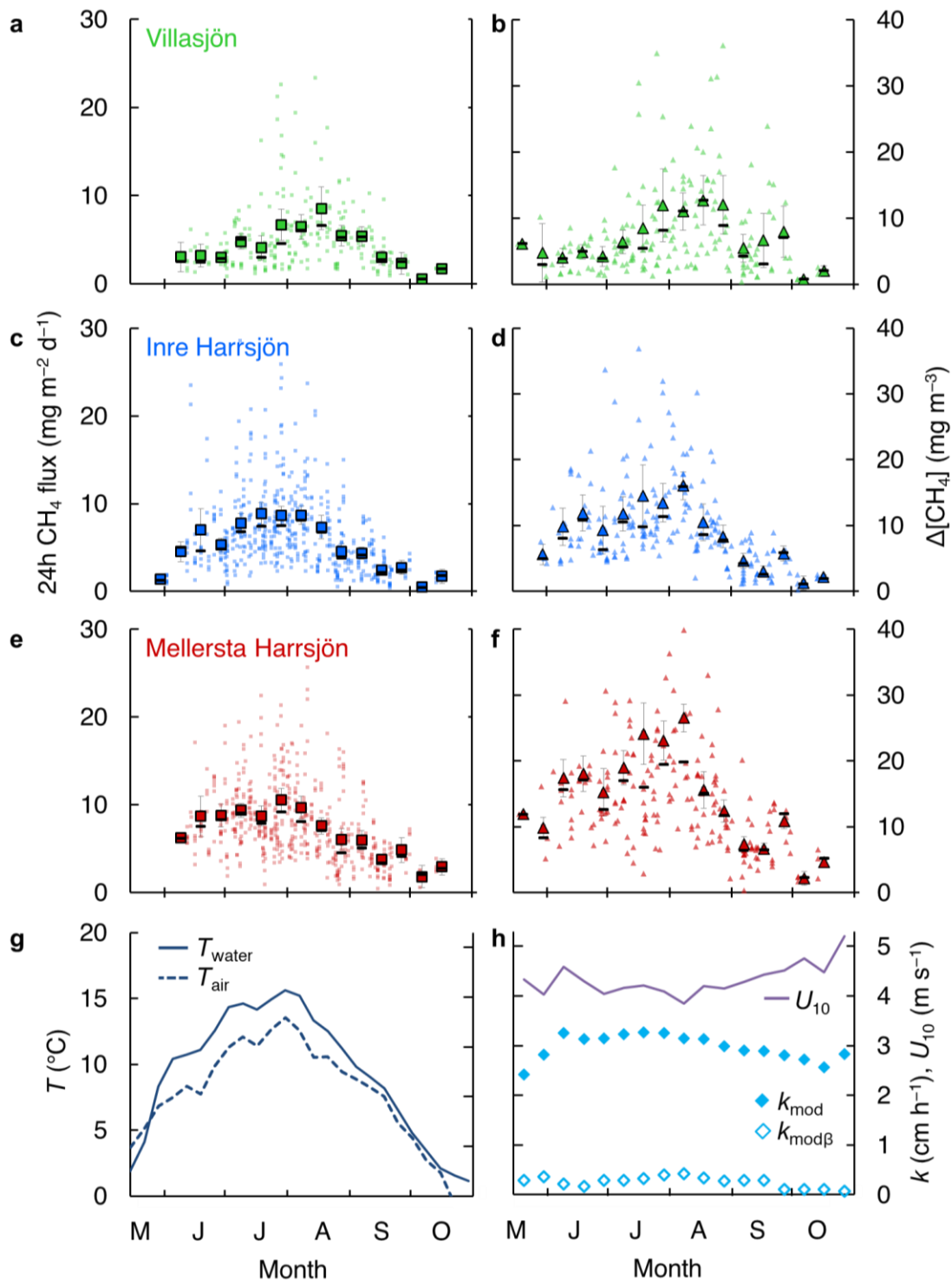
Supplementary material

Supplementary Table 1 – Different relations of k with the wind speed at 10 m (U_{10}) and lake surface area (SA). Validity ranges of U_{10} were based on the data range used to construct each model. For comparison, gas transfer velocities were computed from the multi-year ice-free mean wind speed on the Stordalen Mire and normalized to a Schmidt number of 600 (CO_2 at 20 °C).

Model	Method	Lake surface area (km^2)	U_{10} validity range (m s^{-1})	k_{600} at $U_{10} = 4.3 \text{ m s}^{-1}$ (cm h^{-1})	Reference
$k_{600} = 0.77 \times U_{10}^{1.02} + 0.62$	FC	0.01–0.17	1–9	4.0	This work
$k_{600} = 0.45 \times U_{10}^{1.6}$	Tracers	0.13–500	1–8	4.6	MacIntyre et al., 1995
$k_{600} = 0.215 \times U_{10}^{1.7} + 2.07$	SF_6	0.15	0–9	4.6	Cole and Caraco, 1998
$k_{600} = 4.33 \times U_{10} - 13.3$	SF_6	0.13	1–5.5	5.3	Crusius and Wanninkhof, 2003
$k_{600} = 0.228 \times U_{10}^{2.2} + 0.168$	SF_6	0.13	1–5.5	5.8	Crusius and Wanninkhof, 2003
$k_{600} = 0.78 \times U_{10} + 1.31$	FC	0.06	0–5	4.7	Soumis et al., 2008
$k_{600} = 1.48 \times U_{10} + 1.48 \times U_{10} \times \log_{10}(\text{SA}) + 2.51$	FC	0.01–0.15	1–6.5	5.5–7.5	Vachon and Prairie, 2013

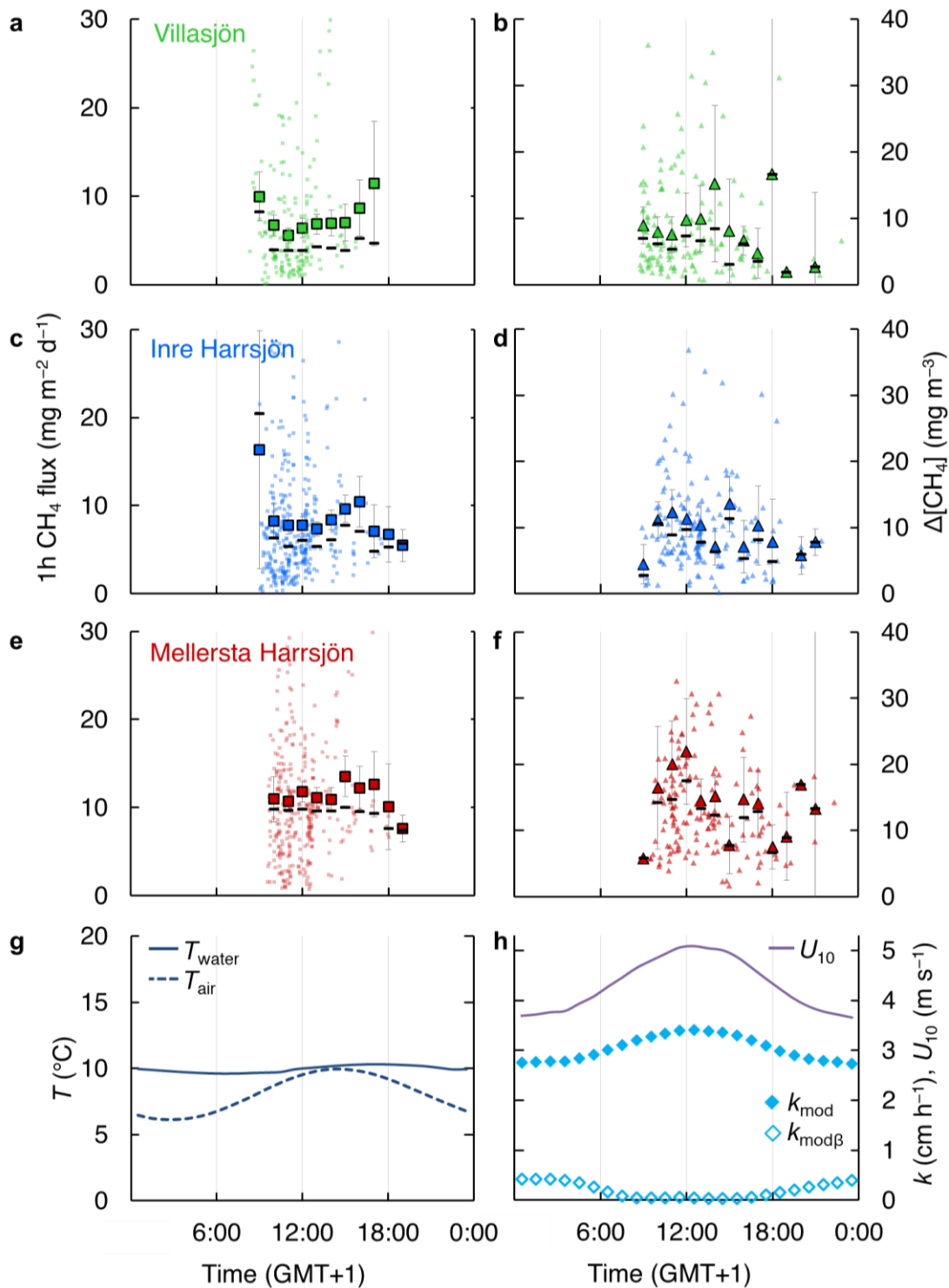


Supplementary Figure 1 – Based on Figure 3 (main text), but for individual lakes: Villasjön (a), Inre Harrsjön (b) and Mellersta Harrsjön (c). Comparison between gas transfer velocities from floating chambers (Eq. 2, main text) and the surface renewal model (Eq. 4, main text, with $\alpha' = 1$ and $Sc = 600$, half-hourly values averaged over each chamber deployment period). Mean ratios, and therefore α' , are represented by the slopes of the dotted lines. Error estimates represent the 95% confidence intervals of the mean ratios.



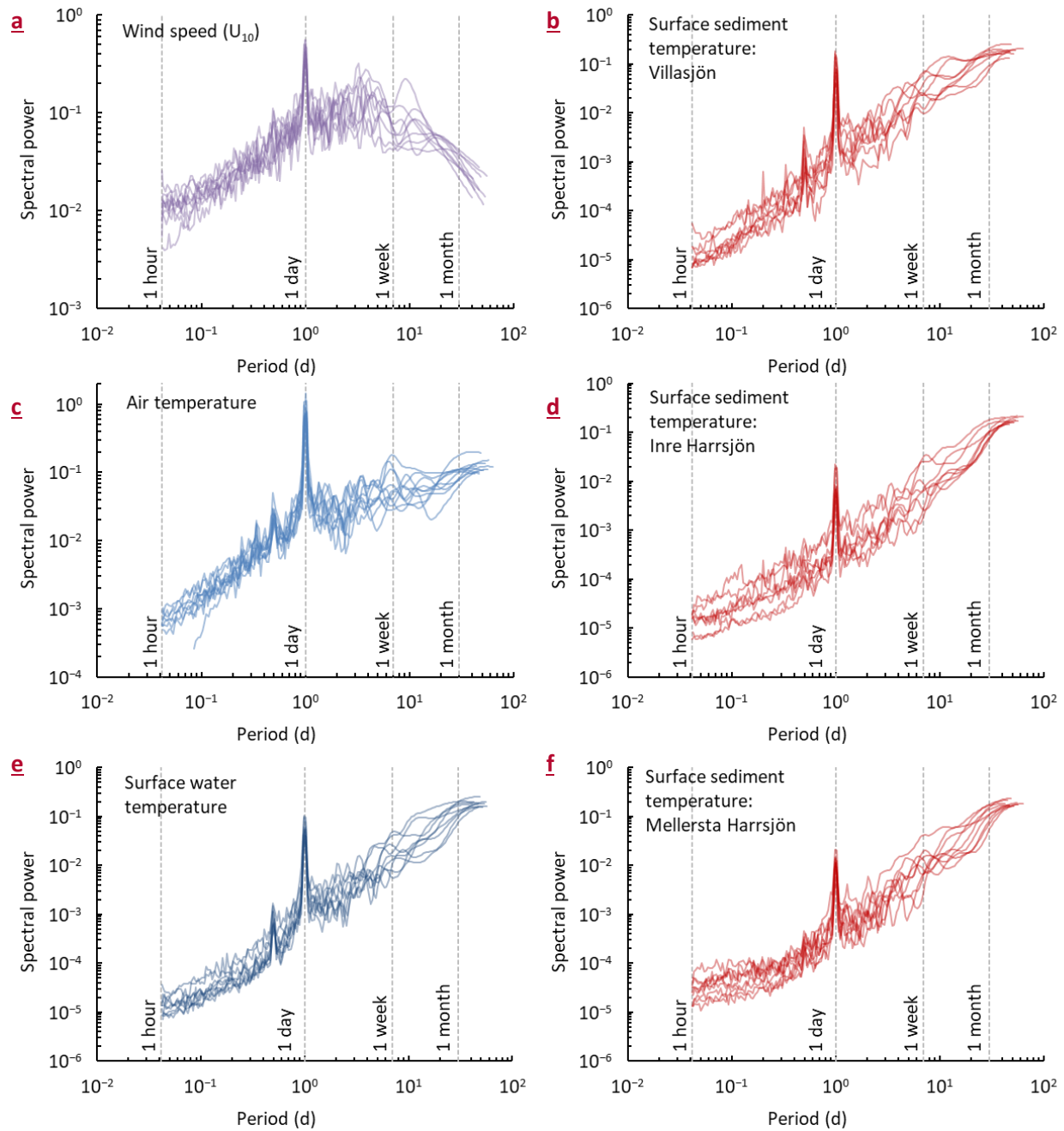
Supplementary Figure 2 – Based on Figure 7a and 7c (main text), but for individual lakes: Villasjön (a,b), Inre Harrsjön (c,d) and Mellersta Harrsjön (e,f). Temporal variation of the 24-hour chamber fluxes (a,c,e), air-water concentration difference (b,d,f), air and water temperature (g) and modelled gas transfer velocity and measured wind speed (h). In panels a-f, large squares and triangles represent binned means

with 95% confidence interval error bars, horizontal bars represent binned medians and small symbols show individual measurements. Variables were binned in 10-day bins.



Supplementary Figure 3 – Based on Figure 7b and 7d (main text), but for individual lakes: Villasjön (a,b), Inre Harrsjön (c,d) and Mellersta Harrsjön (e,f). Temporal variation of the 1-hour chamber fluxes (a,c,e), air-water concentration difference (b,d,f), air and water temperature (g) and modelled gas transfer velocity and measured wind speed (h). In panels a-f, large squares and triangles represent binned means

with 95% confidence interval error bars, horizontal bars represent binned medians and small symbols show individual measurements. Variables were binned in 1-hour bins.



Supplementary Figure 4 – Based on Figure 8a (main text), but for the ice-free seasons of individual measurement years. Normalized spectral densities of wind speed (a), air temperature (c), surface water temperature (e) and surface sediment temperature in Villasjön (b), Inre Harrsjön (d) and Mellersta Harrsjön (f).

Supplementary References

Cole, J. J. and Caraco, N. F.: Atmospheric exchange of carbon dioxide in a low-wind oligotrophic lake measured by the addition of ~~SF~~⁶~~SF~~₆, *Limnol. Oceanogr.*, 43(4), 647–656, doi:10.4319/lo.1998.43.4.0647, 1998.

Crusius, J. and Wanninkhof, R.: Gas transfer velocities measured at low wind speed over a lake, *Limnol. Oceanogr.*, 48(3), 1010–1017, doi:10.4319/lo.2003.48.3.1010, 2003.

MacIntyre, S., Wanninkhof, R. and Chanton, J. P.: Trace gas exchange across the air–water interface in freshwater and coastal marine environments, in *Biogenic trace gases: Measuring emissions from soil and water*, pp. 52–97., 1995.

Soumis, N., Canuel, R. and Lucotte, M.: Evaluation of Two Current Approaches for the Measurement of Carbon Dioxide Diffusive Fluxes from Lentic Ecosystems, *Environ. Sci. Technol.*, 42(8), 2964–2969, doi:10.1021/es702361s, 2008.

Vachon, D. and Prairie, Y. T.: The ecosystem size and shape dependence of gas transfer velocity versus wind speed relationships in lakes, edited by R. Smith, *Can. J. Fish. Aquat. Sci.*, 70(12), 1757–1764, doi:10.1139/cjfas-2013-0241, 2013.